DECENTRALISED VIBRATION CONTROL

LAI WEE LEONG

NATIONAL UNIVERSITY OF SINGAPORE

2003

DECENTRALISED VIBRATION CONTROL

LAI WEE LEONG
(B.Eng.(Hons), NUS)

A THESIS SUBMITTED

FOR THE DEGREE OF MASTER OF ENGINEERING

DEPARTMENT OF CIVIL ENGINEERING

NATIONAL UNIVERSITY OF SINGAPORE

2003

ACKNOWLEDGEMENTS

I wish to express my heartfelt gratefulness towards Associate Professors K.K. Ang and S.T. Quek. Their patient, invaluable and insightful guidance is crucial for the successful completion of this study.

I am indebted to my family. I am also grateful to the National University of Singapore for providing this precious opportunity to do research and take courses that form the fundamentals for this study. I appreciate the IT resources as well as the Internet search engine, Google.com, without which research would become difficult.

Lai Wee Leong

TABLE OF CONTENTS

SUMMARY

This thesis presents the realisation of decentralised robust reliable controller that uses local information for independent local control of subsystems, each with sensors and actuators, in order to achieve pre-defined specifications for robust stability, robust reliable structural seismic response mitigation performance and control optimisation for uncertain faulty multi degree of freedom (MDOF) systems. Using state-space Riccati-based approach for linear systems, the decentralised controls use controller with flexible tuning parameters to explicitly account for system variations in the masses, damping and stiffnesses as well as device malfunctions of sensors and actuators.

Following global state-decentralisation into inter-connected local subsystems, decentralised control consists of state feedback control to regulate the local 'uncoupled' subsystem and a saturation control to account for the coupling terms (or inter-connections) and excitations with noise-corrupted partial state measurements. Step-by-step procedures are presented to design and implement the decentralised robust reliable control strategy to reach the seismic mitigation specifications. Simulation results for linear nominal and uncertain faulty MDOF systems under seismic excitations show that decentralised robust reliable saturation controls generally perform better than central linear quadratic regulator (LQR), central robust reliable optimal controls, as well as decentralised nominal saturation controls. Robust reliable controls perform consistently better than nominal controls for both nominal and uncertain systems under both central and decentralised control systems.

NOMENCLATURE

A	Nominal global ROM state-space system matrix
ΔA	Global ROM state-space system uncertainty
α_i	User-defined positive robust degree relative asymptotic stability of subsystem i
Δ_a	The additive uncertainty accounting for the difference between the nominal system G_0 and the actual system G
A_{ci}	Closed-loop controlled system matrix of subsystem i
A_f	Closed-loop LTR error system matrix
A_{ii}	Nominal subsystem matrix of subsystem i
ΔA_{ii}	Uncertain subsystem matrix of subsystem i
A_{ij}	Nominal subsystem inter-coupling matrix between subsystems i and j
ΔA_{ij}	Uncertain subsystem inter-coupling matrix between subsystems i and j
A_m	Input-matched component of A such that $\Delta A = BA_m$
B	Global ROM state-space nominal control location matrix
ΔB	Global ROM state-space uncertain control location matrix
B_{ci}	Closed-loop augmented disturbance input location matrix of subsystem i
B_f	Closed-loop LTR error noise input matrix
B_Ω	Control location matrix corresponding to predefined redundant actuators susceptible to failures

$B_{\bar{\Omega}}$	Control location matrix corresponding to fail-safe actuators for stabilisability
B_{ω}	Actual control location matrix corresponding to actual failures such that $B_{\bar{\omega}} : B_{\bar{\Omega}} \leq B_{\bar{\omega}} \leq B$
$B_{\bar{\omega}}$	Actual control location matrix corresponding to actual working actuators such that $B_{\omega} : 0 \leq B_{\omega} \leq B_{\Omega}$
b_i	Nominal subsystem control input matrix of subsystem i
Δb_i	Uncertain subsystem control input matrix of subsystem i
β_i	Robust control gain tuning scalar of subsystem i such that $0 < \beta_i \leq 1$
C	Nominal system measurement and regulated output matrix
ΔC	System measurement uncertainty corresponding to sensor failures
C_{ci}	Closed-loop measurement and regulated output matrix of subsystem i
C_{ii}	Nominal measurement and regulated output matrix of subsystem i
ΔC_{ii}	Uncertain measurement and regulated output matrix of subsystem i
C_{ij}	Nominal measurement and regulated output inter-coupling matrix between subsystems i and j
ΔC_{ij}	Uncertain measurement and regulated output inter-coupling matrix between subsystems i and j
C_{fi}	CSS subsystem controller transfer function from $y_i(t)$ to $u_{1i}(t)$
C_r	Global nominal reduced-order damping matrix
ΔC_r	Global uncertain reduced-order damping matrix
C_s	Global linear viscous symmetric s.p.d. damping matrix
ΔC_s	Global uncertain damping matrix

C_s^- , C_s^+	The lower and upper bounds to the global damping matrix
C_Ω	LTR input matrix corresponding to the set of sensors susceptible to failures by zeroing out appropriate rows
$C_{\overline{\Omega}}$	LTR input matrix corresponding to the set of sensors robust to failures
χ_{0i} , χ_{ij}	Non-negative constants for the bounds of nonlinear stiffness component and inter-coupling of subsystem i
ΔD	Control measurement uncertainty corresponding to actuator failures
D_c	Constant pre-multiplying matrix of ΔC_s decomposition
D_i	Constant pre-multiplying matrix of system uncertainty decomposition of subsystem i
D_k	Constant pre-multiplying matrix of ΔK_s decomposition
δ	User-defined robust prescribed H_∞–norm disturbance rejection positive constant for the worst-case system
δ_{1i} , δ_{2i}	Positive upper bound to the lumped subsystem disturbances of subsystem i for the nominal and worst-case layers respectively
δ_c	Positive H_2–norm constant for sensor measurement uncertainty
δ_h	Positive H_2–norm constant seismic influence uncertainty
E_c	Constant post-multiplying matrix of ΔC_s decomposition
E_i	Constant post-multiplying matrix of system uncertainty decomposition of subsystem i
E_k	Constant post-multiplying matrix of ΔK_s decomposition

E_{r1I}, E_{r2i}	LTR recovery error for subsystem i for the nominal and worst-case layers respectively
e	LTR observation error $e(t) = x(t) - v(t)$
e_{1I}, e_{2i}	Lumped subsystem coupling, nonlinearity and excitation vectors of subsystem i for the nominal and worst-case layers respectively
ε_i	Positive robust controller tuning scalar of subsystem i
ε_{1i}	Positive tuning scalar of subsystem i for system uncertainties
ε_{2i}	Positive tuning scalar of subsystem i for sensor uncertainties
ε_{3i}	Positive robust controller tuning scalar of subsystem i
ε_{4i}	Positive tuning scalar of inequality
$\overline{F}$	Nominal component of closed-loop LTR error noise input matrix
$\Delta\overline{F}$	Uncertain component of closed-loop LTR error noise input matrix
F_c	Global control force distribution matrix; Time-varying matrix of ΔC_s decomposition
ΔF_c	Global uncertain control force distribution matrix
F_c^-, F_c^+	Lower and upper bounds to global control force distribution matrix
F_i	Time-varying matrix component of system uncertainty decomposition s.t. $F_i(t)^T F_i(t) \le I$
F_k	Time-varying matrix of ΔK_s decomposition
f	FDI fault vector due to fluctuating partial (incipient or soft) or total (hard) component failure
f_i	FDI fault signal of ith device failure
ϕ_i	Adaptive parameter error of subsystem i

G_0, G	The transfer functions from U to Y of the global nominal and actual systems respectively
H	Nominal disturbance input matrix
ΔH	Disturbance input uncertainty
h_i	Nominal subsystem excitation input matrix of subsystem i
η	Independent white noise of sensor measurements
η_i	Independent white noise of sensor measurements of subsystem i
$\overline{\eta}_i$, $\overline{\eta}_{2i}$	Independent white noise of sensor measurements of subsystem i for LTR design for the nominal and worst-case layers respectively
J_{1i}, J_{2i}	H_2 energy-weighted optimisation performance indices for subsystem i in the nominal and worst-case layers respectively
J_{tr}	The threshold value above which a fault would be considered detected
J_{tri}	The threshold value above which fault $f_i(t)$ would be considered isolated
K_c	Static robust state feedback control matrix
K_f	LTR optimal observer gain
K_n	Global nonlinear n-vector stiffness force that is assumed to be a function of V
K_r	Global nominal reduced-order stiffness matrix
ΔK_r	Global uncertain reduced-order stiffness matrix
K_s	Global nominal linear spring stiffness s.p.d. matrix
ΔK_s	Global uncertain stiffness matrix
K_s^-, K_s^+	The lower and upper bounds to the global stiffness matrix

k_{1i}	Static LQR full state feedback control gain of nominal subsystem i
k_{2i}	Static robust reliable full state feedback control gain of worst-case subsystem i
k_{f1i}, k_{f2i}	Static LTR gains for subsystem i for the nominal and worst-case layers respectively
L_{ci}	Achieved robust reliable LQR open-loop transfer function of the subsystem i at the input point
L_{fi}	Achieved LTR open-loop transfer function of the subsystem i at the input point
L_{1i}, $\hat{L}_{1i}$, $\bar{L}_{1i}$	The decentralised nominal open-loop controller transfer functions of subsystem i from -y_i to u_{1i}, $\hat{u}_{1i}$ and $\bar{u}_{1i}$ respectively
L_{2i}, $\hat{L}_{2i}$, $\bar{L}_{2i}$	The decentralised nominal open-loop controller transfer functions of subsystem i from -y_i to u_{2i}, $\hat{u}_{2i}$ and $\bar{u}_{2i}$ respectively
l	Earthquake influence vector consisting of ones
l_c	Global actuation force per unit voltage transformation matrix
Δl_c	Global uncertain actuation force-voltage transformation matrix
M	Domain matrix such that $B_\omega = B_{\bar{\omega}} M$
M_r	Global nominal reduced-order mass matrix
M_s	Global nominal mass matrix
m	Nos. of groups of actuators used for global aseismic control
μ_{1i}, μ_{2i}	Augmented saturation control of subsystem i for the nominal and worst-case layers respectively
N_s	Nos. of coupled subsystems

n	Nos. of unconstrained degrees of freedom
P_{1i}, P_{2i}	Symmetric positive definite (s.p.d.) matrix solutions to algrebraic Riccati equations of subsystem i in the nominal and worst-case layers
$\widetilde{P}_{1i}$, $\widetilde{P}_{2i}$	S.p.d. solution Lyapunov equation for saturation control of subsystem i for the nominal and worst-case layers respectively
P_f	Positive-definite solution to dual Riccati equation for LTR observer gain
p_c	Global actuation force distribution vector
Q_i	Stabilising inner robust reliable loop controller of LDGIMC from Youla parameterisation
Q_{1i}, $\widetilde{Q}_{1i}$	Semi-positive-definite control weighting matrices of nominal subsystem i for LQR control and saturation control respectively
Q_{2i}, $\overline{Q}_{2i}$, $\widetilde{Q}_{2i}$	Semi-positive-definite control weighting matrices of worst-case subsystem i for robust reliable control, saturation control and H_2-optimal control respectively
$\hat{Q}_{2i}$	Positive-definite matrix of robust closed-loop Lyapunov equation for subsystem i
q	ROM global displacement vector; total number of considered faults
R_{1i}, R_{2i}	Symmetric positive-definite energy-weights for subsystem i for the nominal and worst-case layers respectively
$\widetilde{R}_{2i}$	Positive-definite H_2 control weighting matrix of subsystem i
R_a	Actuator fault distribution matrix
R_f	Power of measurement noises
R_s	Sensor fault distribution matrix

r	Fault residual vector; nos. of degrees of freedom of global ROM
r_i	Fault residual vector of ith device failure
T	Hamiltonian nominal kinetic energy scalar
ΔT	Hamiltonian uncertain kinetic energy scalar
T_{Ai}	Augmented matrix of pre-multiplying matrices of general uncertainties of subsystem i
T_{mA}	Augmented matrix of pre-multiplying matrices of matched uncertainties
$T_{z_i w_{Fi}}$	Transfer function or frequency response function from augmented disturbances to regulated output for subsystem i
U	Global ROM control voltage vector; Hamiltonian nominal potential energy scalar
ΔU	Hamiltonian uncertain potential energy scalar
U^-, U^+	The lower and upper bounds to the global control vector
U_{Ai}	Augmented matrix of post-multiplying matrices of general uncertainties of subsystem i
U_{mA}	Augmented matrix of post-multiplying matrices of matched uncertainties
$\tilde{U}_{1i}$, $\tilde{V}_{1i}$	The left coprime matrices of L_{1i}
u	Control voltage vector
$\hat{u}$	Augmented control vector for fault compensation such that $\hat{u}(t) = -Mu_F(t)$
u_{Fi}	Actuator failure signal of subsystem i

u_{1i}, u_{2i}	Decentralised control vectors of subsystem i for nominal layer 1 and worst-case layer 2
$\hat{u}_{1i}$	LQR optimal regulation control for the nominal subsystem i
$\hat{u}_{2i}$	Robust reliable control for the worst-case subsystem i
$\overline{u}_{1i}$, $\overline{u}_{2i}$	Augmented saturation control of the subsystem i for nominal layer 1 and worst-case layer 2
υ	Any positive scalar for validity of inequality
V	A function of the system responses with bounded coefficients
v_i	CSS-LTR control state of subsystem i
W	Hamiltonian work done by nominal external sources
ΔW	Hamiltonian work done by uncertain external sources
w_i	Disturbance vector; independent white noise of subsystem i
w_{Fi}	Augmented subsystem i excitation vector
Ω	The set of predefined or redundant actuators susceptible to failures
$\overline{\Omega}$	The set of fail-safe actuators needed to maintain stabilisability
X	Global state vector augmenting ROM relative displacement and velocity vectors
X_n	Global ROM nonlinear stiffness component
x	System state vector augmenting system relative displacement and velocity vectors
$\tilde{x}$	Auxiliary system state for determining H-norm optimal LTR observer gain
x_i	Subsystem state vector of subsystem i
x_{ni}	Subsystem nonlinear stiffness component of subsystem i

$\ddot{x}_g$	Arbitrary 1-D horizontal ground acceleration
ξ	Global relative displacement vector w.r.t. the ground; positive scalar
$\dot{\xi}$	Global relative velocity vector
$\ddot{\xi}$	Global relative acceleration vector
Y	Global ROM measurement output vector
Ψ	Load-dependent Ritz transformation matrix
Ψ_u	Load-dependent Ritz transformation matrix of the uncertain FOM
y	Sensor measurement output vector
y_i	Noise-corrupted subsystem measurement output of subsystem i
Z	Global ROM controlled or regulated output vector
z	Regulated output vector
z_i	Subsystem controlled or regulated output of subsystem i

LIST OF FIGURES

LIST OF TABLES

CHAPTER 1

INTRODUCTION

1.1 Background

Advancement in high-strength materials, construction methodology, structural analysis capability as well as rapid urbanisation and development have considerably influenced urban structures, especially buildings and bridges. Hence, tall buildings and more flexible structures, with low damping and varying dynamic properties along different directions, are increasingly popular. Due to asymmetric and orthotropic properties, these structures are often stronger and stiffer in the longitudinal direction, but relatively weaker and softer in the lateral direction. However, these structures are often subjected to various lateral motions due to natural phenomena like earthquakes, wind and waves, as well as artificial phenomena like traffic loads, blast or impact forces. At or close to resonances, the resulting structural vibrations may pose serious problems of structural stability, integrity, safety and serviceability that result in discomfort to occupants, malfunctioning of sensitive equipments and even structural failure. The mitigation of these structural vibrations (forced or self-excited) is therefore of immediate importance.

1.2 Seismic studies and hazard analysis

Earthquakes are violent ground motions that are tectonic or volcanic in nature, as well as collapse or explosion-induced. Seismic ground motions consist of body waves (namely, longitudinal compressive P waves and transverse shear S waves) and surface waves (namely, Love waves and Rayleigh waves). The ground motions at

any location would be a probabilistic combination of all the motion waves (Loh and Chung, 2002).

The size of earthquake is normally measured on the intensity scale for the relative comparison of earthquake effects on a particular location, and the magnitude scale for the absolute earthquake energy released. The most commonly used intensity scale is the Modified Mercalli (MM) Scale (Wood and Neumann, 1931) and the most commonly used magnitude scale is the Richter Magnitude Scale (Richter C., 1935). Due to the large and variable velocities involved in strong motions, seismographs used to measure ground motions are normally accelerometers distributed across seismic regions. Actual earthquake records are derived from corrected seismograph measurements to account for environmental influences, measurement spillover and instrument variations.

Seismic hazard analysis is to estimate the largest earthquake that might occur in a region, especially during the service life of a particular structure. This involves assessing probabilistic earthquake occurrence and the return period as well as important earthquake characteristics like peak motions, frequency content, duration and attributes of strong pulses. During an earthquake, the resulting ground motions actually reaching a particular structure would depend on earthquake magnitude, distance to ruptured fault or excitation source, surrounding geology and local soil properties. Design earthquakes can be derived from scaled historical earthquake records, artificially generated strong motions from seismic hazard analysis, seismic building codes (Maguire and Wyatt, 1999) as well as critical seismic excitation methods (Takewaki, 2002). The variability of on-site conditions results in the wide variety of design earthquakes, which needs to be representative of the seismic region.

Under the design earthquakes, the actual responses of a structure would depend on its immediate ground motion, its dynamic properties and soil-structure interaction. The structural seismic vibration demand must be checked to be within safe specifications.

1.3 Seismic mitigation

When the seismic demand exceeds structural capacity, mitigation measures must be taken. Mitigation can be achieved by modifying geometric layout, masses, rigidities, energy-dissipating damping, and by providing passive or active counter forces. In general, seismic mitigation involves robust earthquake-resistant design, base isolation and structural control/retrofitting for new and current structures at both member and global levels.

1.3.1 Robust earthquake-resistant design

The conventional perspective is to re-design a structure for seismic-resistance. The criterion for robust design is to ensure that the seismic demand is satisfactorily met by the modified structure for the duration of its service life, including the various on-site uncertainties. Seismic analysis requires either peak seismic demands through the response spectra analysis (Chopra, 2000, 2002), or time history analysis (Hart and Wong, 2000) for both elastic and inelastic analyses, especially needed under severe earthquakes. An equivalent static load approach for the seismic demand is often taken to design for the maximum seismic force distribution, base shear and overturning moment as well as interstory drift, plastic hinge formation and rotation. Under robust design, the structural seismic demand can be met by modifying or changing the

structural configuration including modifying the surrounding soil properties, foundation design as well as superstructure design, through varying, adding or removing the use of different materials, layout, geometry, ties, supports and anchors. Service loadings and distributions can also be altered.

Modifications of superstructure (herein termed 'structure') to increase stiffness and damping include lateral load resisting systems of shear walls, core walls, non-sway frames, moment-resisting joints, braces, coupling elements and outriggers. The frame-core wall system is a highly effective form of lateral resisting system (Zhou, 1994). Appropriate mass distribution would ensure that induced seismic loads are minimised. However, the high variability of design earthquakes and the wider earthquake excitation spectrum than wind and wave loadings limit the effectiveness of robust design (Takewaki, 2001).

1.3.2 Base isolation

The concept of base isolation is to cut off or reduce the seismic motion transferred to the structure above the isolation system, thus effectively minimising the transmission of seismic excitation into the structure and reducing the seismic demand. Hence, effective base isolation requires highly flexible base connections for large deformation and/or large energy-dissipating hysteretic devices (Yang et al, 1995).

Base isolation measures include various forms of sliding systems, rollers, horizontal pads over the foundation, lead core rubber bearings, energy absorbers of solid, viscous hydraulic or pneumatic nature, and soft first story. Base isolation can also be used together with robust designs as enhanced passive structural mitigation measures considered to be a more mature technology (ATC-17, 1993). However,

modelling, constructional and maintenance difficulties as well as restrictions on the effective isolation bandwidth of passive mitigation limit the effectiveness of passive base isolation.

1.4 Structural control

The concept of seismic structural control or aseismic control involves the use of additional devices to modify the structural dynamic properties or energy dissipation capacity or both to ensure the assessed seismic demand is within the controlled structural capacity as well as to meet design specifications for desired structural responses. Structural control is generally considered when robust design and base isolation cannot reach the seismic mitigation specifications. Control solutions can also be extended to the upgrading, retrofitting and repair of existing structures. In general, structural control consists of passive and active controls (Nishitani and Inoue 2001, Soong and Spencer 2002), depending on the type of devices used, amount of external energy required and control algorithm or decision-making process using real-time measured data.

1.4.1 Passive control

A passive control system modifies the mass, stiffness and damping to resist seismic forces with no adaptation and no external power by using passive devices that impart forces developed in response to the seismic structural motion. Passive devices include braces and dynamic absorbers. Passive control is dominated by passive energy dissipation (PED) or damping, which are inherently stable, cost effective and does not interfere with the intrinsic dynamic properties such as mass, stiffness or

shape. Common passive damping devices include tuned mass or liquid dampers (TMD, TLD), fluid sloshing dampers, friction dampers and visco-elastic dampers. The drawbacks of passive damping are the effective bandwidth for aseismic control below which detrimental seismic amplification would result, and its inability to adjust to real-time dynamic conditions of widely variable spectrum, especially encountered in severe seismic excitations.

1.4.2 Active control

Active control (Soong, 1990) is the real-time input of corrective actuation forces, using external power sources, as determined by automatic decision-making process (controller) based on the measurements of structural responses and/or seismic motions. Hence, the active devices are adaptable to physical conditions through on-line computations, the control algorithm or controller must be stabilising so that no destabilising forces are imparted into the structure, and external power for injection of mechanical energy into the structure and/or operations of the control devices is necessary.

Kobori (1958, 1960) presented his seismic-response-control idea of incorporating automatic control into the seismic-resistant design of structures for the purpose of enhancing safety against severe earthquakes. Yao (1972) first demonstrated and inspired the idea and practical active civil engineering structural control schemes through the application of control theory to structural engineering. Overview of structural control concepts and applications (Soong 1990, Y.Fujino et al 1996, Housner et al 1997, Spencer and Sain 1997, Nishitani and Inoue 2001) provides full-scale applications and indicates the need for effective system integration, structure-controller interaction and control strategy optimization for reliable cost-

effective performance. Garg et al (2001) reported the current research activities in adaptive structures with emphasis on maximizing energy dissipation, adaptive damping systems and distributed control techniques are emphasized.

Five fundamental engineering principles (Nishitani and Inoue, 2001) have been proposed for the aseismic control of buildings:

1. To transfer the structural seismic energy to an auxiliary oscillator system (e.g. dynamic absorbers)
2. To reduce the flow of input seismic energy into the structure (e.g. base isolation)
3. To subject the structure to additional damping (e.g. passive damping)
4. To prevent structural resonance due to seismic influence (e.g. robust design)
5. To apply computer-controllable forces to the structure (e.g. active control)

Passive mitigation measures, discussed in the previous sections, cover the first four principles. Active control encompasses all five principles through the additions of sensors, control algorithm and actuators to the seismically-excited structure. Active control (Fig. 1.1.) is implemented as one of the following:

1. Open-loop or feedforward control: only measured excitations are used for computations of the actuations, applicable when the dynamic structural responses are exactly known
2. Closed-loop or feedback control: only measured structural responses are used for actuations, applicable when excitations are not modelled or measured
3. Closed-open-loop control: both measured structural responses and measured excitations are used for actuations

The ‘sensors’ herein means analogue devices to measure desired responses and/or excitations. Sensors used include conventional transducers and strain gauges, as well as piezoelectric, fibre optic, MEMS and other integrated sensory systems. The analogue measurements of the sensors have to be converted into equivalent digital signals using D/A converters for the processing by the digital controller.

The ‘controller’ herein means a control algorithm, where the basic task is to find a control strategy that uses the sensor measurements to calculate the control signal that is appropriate to send to the control devices (Fujino et al, 1996). Controllers can be designed as instantaneous, analogue or digital with associated sampling characteristics. In practice, digital controllers are preferred to analogue controllers, and instantaneous controllers are implemented digitally, sometimes with time delays (Ogata, 1994, 1996).

The ‘actuators’ herein means computer-operated analogue devices to execute the computed control actuation signals. Actuators can be force-inserting (when actuation strain is not a constraint), displacement-inserting (when actuation stress is not a constraint) and energy-inserting or energy-dissipating (Utku, 1998). Furthermore, actuators may be grouped into active, semi-active or hybrid. Active actuators continuously impart actuations, usually using large amounts of external power. Common active actuators include active mass drivers or dampers (Fujino et al 1996, Nishitani and Inoue 2001). Recently, desired fast response rate has prompted the application of stacked piezoelectric actuators (Kamada et al 1997, 1998), which overcome the actuation strain constraint by stacking piezoelectric actuators in layers.

1.4.3 Semi-active control

Semi-active control is active control through the use of semi-active actuators, in which only a limited amount of external power is needed and only at specific design occasions when the actuator characteristics or state is changed. Semi-active actuators are cost effective with good performance and inherently stable, i.e. no destabilising mechanical energy is injected into the controlled structure. Since external energy is only used to operate the semi-active actuators, they consume much less energy than active actuators and thus, more easily adopted for applications (Barroso et al 2002, Lynch and Law 2002). Semi-active controls include active variable stiffness (AVS) or damping (AVD), variable orifice or friction or viscous dampers, controllable fluid (ER, MR) dampers and even piezoelectric actuators with shunt damping (Fleming and Moheimani, 2003).

1.4.4 Hybrid control

Hybrid or composite control consists of a combination of active and passive control systems and/or hybrid actuators under directional actuations. The idea is to utilise the advantages of both active and passive control systems, while minimising their disadvantages, to increase overall reliability and mitigation performance. However, mechanical energy is injected into the structure, hence stability of the controlled structure must be checked. Hybrid controls include base isolation with active actuators (Yang et al, 1995) and hybrid mass dampers (HMD), some of which operate as TMD in longitudinal direction and HMD in lateral direction.

1.5 Literature review

The integration of the structural system with sensors and control devices poses great demands on the controller or control strategy (Garg et al, 2001). The control strategy is of prime importance, and needs to account for controlled stability, performance and optimality (Anderson and Moore, 1989). Controllers can be designed as linear or nonlinear. In linear controllers (Hart and Wong, 2000), the output actuations are a linear function of the structure model and sensor input measurements.

The performance of the controllers is often degraded in the presence of uncertainties and component failures (Frank et al, 1994) as well as incomplete and corrupted state information that can result in instability of the controlled structure. Moreover, active control also adds to the complexity due to inherent instability from the injection of destabilising mechanical energy due to deficient designs, especially in aseismic control of large-scale structures with numerous sensors and actuators.

1.5.1 Robust controller against system uncertainties

Conventionally, system model parameters are assumed unchanged, hence nominal throughout the service life of a structure. However, variable on-site conditions of the structural system as well as the seismic loading environment would cause uncertainties. The system uncertainties arising from sources such as unmodelled dynamics, non-linearities, disturbances and exogenous noises would violate the assumed nominal model that does not take these into consideration. Unmodelled dynamics can include variations in the masses, damping, stiffnesses, geometric nonlinearities resulting from P-delta effects, and material plasticity ignored in linearly elastic models. Under a controller based on nominal model, such system

uncertainties would lead to unmodelled controlled structural behaviour that can cause impaired performance and even instability.

Robust (insensitive) control against uncertainties is required for smooth operations. The aim is to design a robust controller that simultaneously stabilizes the closed-loop system (Choi et al 2001) and satisfying performance requirements (Xie et al 1992). Full state feedback control (Kalman 1960, Doyle et al 1989), which assumes perfect knowledge of the system states, has been studied extensively to minimise system states and actuation energy simultaneously. The most popular full state feedback controller is the linear quadratic regulator (LQR) (Anderson and Moore, 1989). However, the system states are rarely fully available for use in a control system. In addition, unmodelled noise fluctuations can occur in both the system and measurements. Specifically, loop transfer recovery (LTR) is needed to recover the original controlled structural properties of full state feedback control (Lu et al, 1998).

Lin et al (1994) claimed that for robust stabilization, the system uncertainties should take the form of a linear combination of the locations of the actuators (otherwise known as matched uncertainties). For other forms of system uncertainties (i.e. unmatched uncertainties), augmented controls are required (Krokavec et al 2000). Accounting for unstructured uncertainties (i.e. bounded in the squared Lesbegue space or L_2-sense, of which the squared Hardy space norm H_2 is only a subset) would lead to conservative controller design and inferior performance compared to that of accounting for structured uncertainties (i.e. bounded in the L_2-sense and with knowledge of its structure in the state-space governing equation) (Maciejowski 1989). Zames (1981) proposed an infinite Hardy space norm (H_∞)-control formulation using Riccati equation for the sensitivity robustness problem. This leads to a class of

solutions addressing the issue of stability, performance and optimality for linear systems with unmatched and matched, structured and unstructured uncertainties (e.g. Wang et al 2001), but no actuator failures and sensor uncertainty were considered.

1.5.2 Reliable controller against device malfunctions

Control devices, sensors and actuators, may suffer malfunctions or faults, especially during severe earthquakes, when sensing or control connections might be broken, interfaces with the structure dislocated and internal device failures occurred. Failures can be either insipient (soft) or partial failures, or total (hard) or complete failures of sensor(s) and/or actuator(s) (Frank et al, 1994). Sensor failures result in inaccurate or incomplete measurement inputs for the controller. Actuator failures result in inappropriate actuations and, in the case of active or hybrid actuators, possible detrimental or destabilising mechanical energy to be injected into the structure.

Robust control without consideration of possible failure of some actuators would result in unsatisfactory performance or instability if some failure does indeed occur. Hence, reliable (fault-tolerant) control against partial or complete breakdown of system components has been addressed (Veillette et al 1992, Yang et al 2001). However, solutions are feasible for only a class of reliable state feedback control with guaranteed stability and H_∞-norm performance where actuator failures are confined to a predefined subset of actuators (Seo et al 1996) with control optimality ignored.

1.5.3 Decentralised controller

Conventionally, a global, centralised controller is used, i.e. all computations of the actuations are performed by a single, global control algorithm using all sensor input measurements. However, centralised control is generally not suitable for large-scale control problems because computations increase faster than a linear rate with increases in system dimensionality (Lunze 1992) and it represents a single point of failure (Lynch and Law, 2001). Moreover, the performance of central control is degraded in the presence of uncertainties and device failures (Frank et al 1994) under severe earthquakes when power supplies failure and broken network connections would likely occur. Possible breakdown of the central control coordination is highly likely. Hence, there is practical interest and need to apply active control at the global structural level and further decentralize control for more effective distributed control of local subsystems (Cao et al 2000, Garg et al 2001, Lai et al 2002).

Decentralised controllers provide local subsystem controls using local feedback information only (Siljak, 1991). In large-scale complex systems, decentralised controllers with numerous, distributed sensing and control devices (Lunze 1992, Magana and Rodellar 1998, Luo et al 2002, Lynch and Law 2002) enable practical control distribution, reduced chance of catastrophic failure and less stringent requirement for stability. The attainable benefits of using decentralised control are high system performance under system uncertainties, greater stability robustness, improved control system performance in non-linear systems, and system installation modularity facilitating low-cost installations diagnostics and module replacements (Lukas, 1986). Cao et al (2000) proposed a decentralized control approach for two interconnected subsystems, where stability of the global structure can only be guaranteed when each subsystem has at least one working sensor and

actuator (Luo et al 2002). Magana and Rodellar (1998) have shown that a set of simpler decentralised controllers can have performance similar to a single global centralised controller under nominal conditions, and perform much better when system uncertainties and device failures occur.

1.6 Objective and Scope

The objective of this study is to develop a decentralised high performance robust reliable saturation controller that uses flexible tuning parameters and local information for independent control of subsystems for global stability, robustness, reliability and optimality for linear uncertain faulty systems under seismic excitations.

Under this objective, the scope of studies is as follows:

- Decentralised nominal saturation controller is designed for each subsystem, derived from decentralisation of the global linear nominal system, to ensure global closed-loop asymptotic stability with decentralised squared Hardy space norm (H_2)-optimality and seismic mitigation (or disturbance rejection) under noise-corrupted partial state measurement.
- Central robust reliable optimal controller is designed for global linear uncertain faulty system to ensure robustness against both structured and unstructured norm-bounded uncertainties as well as reliability against actuator failures confined to a predefined subset under noise-corrupted partial state measurement.
- Decentralised robust reliable saturation controller is designed for each subsystem, derived from decentralisation of the global linear uncertain faulty system, by combining both decentralised nominal saturation control and robust reliable control approaches.

1.7 Organisation of Thesis

Chapter 2 provides the formulation of the decentralised nominal saturation state feedback controller for nominal system without uncertainties under partial noise-corrupted sensor measurements. Chapter 3 provides the formulation of the central robust reliable controller for an uncertain system with admissible system uncertainties and a pre-defined set of possible actuator failures, under partial noise-corrupted sensor measurements. Chapter 4 develops the decentralised robust reliable saturation controller by combining the decentralisation methodology and the robust reliable control. Chapter 5 provides the conclusions and suggestions for further studies.

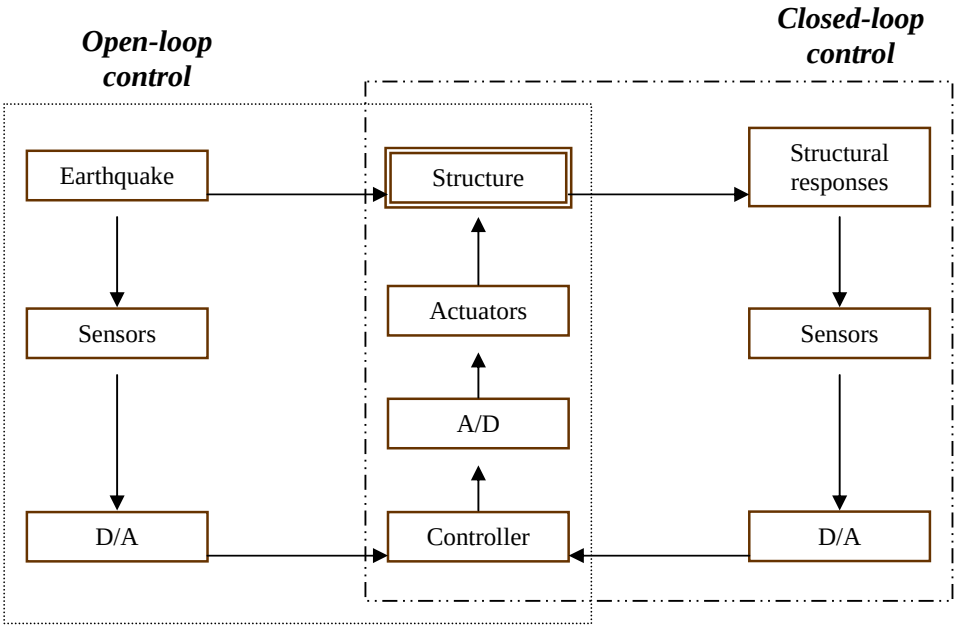

Figure 1.1: Schematic diagram of active control

CHAPTER 2

DECENTRALISED NOMINAL CONTROLLER

2.1 Introduction

In this chapter, the decentralised nominal saturation controller is designed for nominal linear systems without uncertainties under seismic excitation. The decentralised controllers use only local information for independent local control of subsystems. To cater for practical situations, the solution will be extended to account for partial noise-corrupted sensor measurements.

Based on the global state formulation, decentralisation into subsystems is performed where each subsystem contains at least one sensor and actuator pair. The decentralised control consists of a state-feedback control to regulate the local 'uncoupled' subsystem and a saturation control to account for the coupling terms (or inter-connections) and excitations. The former uses the closed-loop state-space Riccati equation optimal solution based LQR control approach to derive the full state-feedback gain for the undisturbed subsystem. The latter uses Lyapunov equation by Lyapunov's Direct Method to formulate the saturation control with the objective of attenuating the subsystem disturbances.

To account for noise-corrupted partial state feedback, observer-based control is implemented using the separation principle. A nominal 2DOF system is used to illustrate the effectiveness of decentralized control by comparing with results based on centralized nominal control. To illustrate that the method works for larger systems, a 20-DOF system is also presented where reduced order model is applied to simplify the problem.

2.2 Control Problem Formulation

2.2.1 Nominal Analytical Model

Consider an *n*-degree-of-freedom building structure subjected to one-dimensional horizontal earthquake ground acceleration $\ddot{x}_g(t)$. The global dynamic equation of motion can be derived using extended Hamilton's variational principle (Meirovitch, 2000) as:

$$M_s\ddot{\xi}(t)+C_s\dot{\xi}(t)+K_s\xi(t)+K_n[V(t)]=F_cU(t)-M_sl\ddot{x}_g(t) \tag{2.1}$$

where $\xi(t)\in\Re^n$ is the global displacement vector; $U(t)\in\Re^m$ is the nominal control voltage vectors to *m* groups of actuators; $M_s\in\Re^{nxn}$ is the global consistent mass matrix; $C_s\in\Re^{nxn}$ is the global nominal linear viscous damping matrices; $K_s\in\Re^{nxn}$ is the global nominal linear elastic stiffness matrices; $K_n[V(t)]\in\Re^n$ is the global nonlinear *n*-vector stiffness force that is assumed to be a function of *V(t)*, which is a function of the system responses with bounded coefficients; $F_c = p_c l_c$ is the global nominal control force distribution matrices, where $p_c\in\Re^{nxm}$ is the global actuation force distribution vector, $l_c\in\Re^{mxm}$ is the global nominal actuation force per unit voltage transformation matrices; and $l\in\Re^n$ is the global earthquake excitation influence vector.

For practical reasons, it is assumed that $n >> m$ (**assumption 1**); that is, there are fewer sensors and actuators pairs than the number of DOFs in the system. It is also assumed (**assumption 2**) in this paper that $\ddot{x}_g(t)$ is bounded.

2.2.2 Reduced-order State-Space Modelling

Under assumption 1, the global system described by (2.1), referred herein as full-order model (FOM), needs to be model-reduced to make the system manageable and for efficient design of *U(t)*. Model reduction using load-dependent Ritz vectors with Gram-Schmidt orthogonalisation (Chopra 2000, Krsyl et al 2001, Appendix: Robust Model Reduction) can be adopted to derive a detectable and stabilisable reduced-order model (ROM) with respect to known sensor and actuator locations. A system is detectable if all unstable modes are measured by sensors and regulated by the control algorithm. A system is stabilisable if all unstable modes are controlled by actuators.

Using the nominal matrices, the following Ritz vector transformation is derived:

$$\xi = \Psi q \tag{2.2}$$

where $\Psi \in \Re^{nxr}$ is the Ritz vector transformation matrix; $q \in \Re^{r}$ is the ROM global displacement vector corresponding to the desired master degrees of freedom for stabilisability and detectability.

Substituting (2.2) into (2.1), the ROM is given by:

$$M_r \ddot{q}(t) + C_r \dot{q}(t) + K_r q(t) + \Psi^T K_n [V(t)] = \Psi^T F_c U(t) - \Psi^T M_s l \ddot{x}_g(t) \tag{2.3}$$

where the reduced-order matrices are $M_r = \Psi^T M_s \Psi$, $C_r = \Psi^T C_s \Psi$, and $K_r = \Psi^T K_s \Psi$.

In the state space, (2.3) becomes a class of nominal systems with the following

form:

$$\begin{aligned} \dot{X}(t) &= AX(t) + BU(t) + X_n(t) + H\ddot{x}_g(t), \\ Y(t) &= CX(t) + \eta(t), \\ Z(t) &= CX(t) \end{aligned} \tag{2.4}$$

where the ROM global state vector is $X(t) = \begin{pmatrix} q \\ \dot{q} \end{pmatrix} \in \Re^{2r}$ of dimension (2rx1), input vector is $U(t) = [u_1,...,u_m]^T \in \Re^m$, measured output is $Y(t) \in \Re^m$ and controlled/regulated output is $Z(t) \in \Re^m$, $X_n(t) = \begin{pmatrix} 0 \\ -M_r^{-1}\Psi^T K_n[V(t)] \end{pmatrix}$ is the ROM global nonlinear stiffness component, $A = \begin{pmatrix} 0 & I \\ -M_r^{-1}K_r & -M_r^{-1}C_r \end{pmatrix} \in \Re^{2rx2r}$, $B = \begin{pmatrix} 0 \\ M_r^{-1}\Psi^T F_c \end{pmatrix} \in \Re^{mx2r}$, $C = \begin{pmatrix} -M_r^{-1}K_r & -M_r^{-1}C_r \end{pmatrix} \in \Re^{mx2r}$ and $H = \begin{pmatrix} 0 \\ -M_r^{-1}\Psi^T M_s l \end{pmatrix} \in \Re^{2r}$ are constant nominal system matrices. It is assumed that the system characterized by (A, B) is stabilisable.

2.2.3 Nominal Subsystem Model

Global state-decentralisation is carried out by decomposing the global state space model (2.4) completely into N_s ($N_s \le r \le m$) coupled subsystems:

$$\begin{aligned}
\dot{x}_i(t) &= \mathrm{A}_{\mathrm{ii}} x_i(t) + b_i u_{1i}(t) + h_i \ddot{x}_g(t) + \sum_{j=1,\, j\neq i}^{N_s} A_{ij} x_j(t) + x_{ni}(t), \\
y_i(t) &= C_{ii} x_i(t) + \sum_{j=1,\, j\neq i}^{N_s} C_{ij} x_j(t) + \eta_i(t), \\
z_i(t) &= C_{ii} x_i(t) + \sum_{j=1,\, j\neq i}^{N_s} C_{ij} x_j(t)
\end{aligned} \tag{2.5}$$

where $x_i(t)$ is the ith subsystem state, $u_{1i}(t)$ is nominal subsystem control voltage, $x_{ni}(t)$ is the subsystem nonlinear stiffness component, y_i the noise-corrupted subsystem measurement output, z_i the subsystem controlled or regulated output, A_{ii} and C_{ii} the system, and measurement and regulated output matrices of the nominal subsystem, A_{ij} and C_{ij} the nominal system, and measurement and regulated output inter-coupling matrices between subsystems i and j, $\forall i \neq j \quad (i, j = 1,..., N_s)$, b_i is the nominal subsystem control input matrices, and h_i is the subsystem excitation input matrix. The nonlinear stiffness and coupling components defined in the last two terms of (2.5a) are unknown but is assumed bounded (**assumption 3**) (Luo et al 2002).

The control task is to determine the decentralised nominal saturation feedback controller $u_{1i}(t)$ under noise-corrupted partial state measurement such that the closed-loop subsystem for (2.5) is asymptotically stable with decentralised H_2-optimality and disturbance rejection, i.e. optimal seismic mitigation w.r.t. minimisation of structural and control energies.

2.3 Decentralised Linear quadratic Regulator (LQR) Control for Nominal Subsystem Model

Using the decentralised control methodology (Magana and Rodellar 1998), let the decentralised nominal controller take the following form:

$$u_{1i}(t) = \hat{u}_{1i}(t) + \bar{u}_{1i}(t) \tag{2.6}$$

where $\hat{u}_{1i}(t) = -k_{1i}x_i(t)$ is the optimal regulation control for the undisturbed subsystem without seismic excitations, in which k_{1i} is the static full state feedback control gain of subsystem i in the nominal layer (in this study denoted as layer *1*) and $\bar{u}_{1i}$ is the augmented saturation (user-defined bounds or limits on the controls) control of the subsystem to account for interconnections between subsystems (inter-coupling) and disturbances.

To determine k_{1i}, define undisturbed and uncoupled subsystem from (2.5a):

$$\dot{x}_i(t) = \mathrm{A}_{\mathrm{ii}}x_i(t) + b_i\hat{u}_{1i}(t) \tag{2.7}$$

where (A_{ii}, b_i) is assumed stabilisable. The Linear Quadratic Regulator (LQR) can be used to design k_{1i} by minimising the following subsystem performance index:

$$J_{1i} = \int_0^\infty \left(x_i{}^T Q_{1i} x_i + \hat{u}_{1i}{}^T R_{1i}\hat{u}_{1i}\right)dt \tag{2.8}$$

where (A_{ii}, Q_{1i}) is assumed detectable, and Q_{1i} and R_{1i} are symmetric semi-positive-definite and symmetric positive-definite energy-weights respectively. The solution to (2.8) is considered as H_2-optimal. A solution is asymptotically stable when the system state x_i approaches zero equilibrium asymptotically. The sufficient condition for minimising (2.8) is the subsystem algebraic Riccati equation (ARE, Soong 1990):

$$A_{ii}{}^T P_{1i} + P_{1i}A_{ii} - P_{1i}b_i R_{1i}{}^{-1} b_i{}^T P_{1i} + Q_{1i} = 0 \tag{2.9}$$

where P_{1i} is the symmetric positive-definite (s.p.d.) solution to give the optimal nominal control gain as:

$$k_{1i} = R_{1i}^{-1} b_i P_{1i} \tag{2.10}$$

2.4 Nominal Augmented Saturation Subsystem Control

The second component $\bar{u}_{1i}$ is the augmented saturation subsystem control. Substituting (2.6) into (2.5a) yield the closed-loop linearly-controlled subsystem:

$$\dot{x}_i(t) = (\mathrm{A}_{\mathrm{ii}} - b_i k_{1i}) x_i(t) + b_i \bar{u}_{1i}(t) + e_{1i}(t) \tag{2.11}$$

where nominal subsystem disturbance vector is $e_{1i}(t) = \sum_{j=1, j\neq i}^{N_s} A_{ij} x_j(t) + h_i \ddot{x}_g(t) + x_{ni}(t)$.

When $e_{1i} = 0$, (2.11) is asymptotically stable and H_2-optimal. When $e_{1i} \neq 0$, under assumptions 2 and 3, $e_{1i}(t)$ is bounded and an augmented controller $\bar{u}_{1i}(t)$ can be specifically designed for desired subsystem disturbance rejection (Magana and Rodellar 1998). There exists a positive constant δ_{1i} which is known *a priori* such that $|e_{1i}(t)| \le \delta_{1i} = \left| \sum_{j=1, j\neq i}^{N_s} A_{ij} x_j(t) \right|_{\max} + |h_i \ddot{x}_g(t)|_{\max} + |x_{ni}(t)|_{\max}$ (**assumption 4**). For example, δ_{1i} can be derived from the uncontrolled responses under the target excitation (Magana and Rodellar 1998). The nominal decentralised augmented saturation controller of (2.6) can be expressed as:

$$\bar{u}_{1i}(t) = \begin{cases} \mathrm{sgn}(\mu_{1i}(t))\delta_{1i}, & |\mu_{1i}(t)| > \delta_{1i} \\ \mu_{1i}(t), & |\mu_{1i}(t)| \le \delta_{1i} \end{cases} \tag{2.12}$$

where $\bar{u}_{1i}(t)$ is a saturation controller that is limited by δ_{1i} in magnitude and $\mu_{1i}(t)$ in direction to maintain stability when $e_{1i} \neq 0$; $\mu_{1i}(t)$ is given as:

$$\mu_{1i}(t) = -\delta_{1i} b_i^T \tilde{P}_{1i} x_i \tag{2.13}$$

In (2.13), $\tilde{P}_{1i}$ is the s.p.d. solution of the following Lyapunov equation (Soong, 1990) of the closed-loop subsystem (2.11):

$$\left(\mathrm{A}_{\mathrm{ii}} - b_i k_{1i}\right)^T \tilde{P}_{1i} + \tilde{P}_{1i}\left(\mathrm{A}_{\mathrm{ii}} - b_i k_{1i}\right) = -\tilde{Q}_{1i} \tag{2.14}$$

where $\tilde{Q}_{1i}$ is the symmetric semi-positive-definite disturbance energy-weight matrix.

From (2.6), since $\hat{u}_{1i}(t)$ is asymptotically stable and $\bar{u}_{1i}(t)$ maintains stability of (2.11), $u_{1i}(t)$ is asymptotically stable with decentralised H_2-optimality and disturbance rejection with saturation control for a full-state feedback system. In practice, full-state feedback may not be realizable. If the actual nominal subsystem has partial state measurement with noise-corruption, then an observer-based control is more appropriate.

2.5 Loop Transfer Recovery (LTR) based Decentralised Nominal Saturation Controls

2.5.1 Need for LTR

Practical situations necessitate that only corrupted partial state feedback is available and (2.5) can be modified as follows:

$$\begin{aligned} \dot{x}_i(t) &= A_{ii}x_i(t) + b_i u_{1i}(t) + w_i(t), \\ y_i(t) &= C_{ii}x_i(t) + \overline{\eta}_i(t), \\ z_i(t) &= C_{ii}x_i(t) \end{aligned} \tag{2.15}$$

where $w_i(t) = \left[\sum_{j=1, j\neq i}^{N_s} A_{ij}x_j(t) + h_i \ddot{x}_g(t) + x_{ni}(t) \right] \in \Re^{2n}$ and

$\overline{\eta}_i(t) = \left[\sum_{j=1, j\neq i}^{N_s} C_{ij}x_j(t) + \eta_i(t) \right] \in \Re^{r}$ are assumed to be independent white noises, and $C_{ii} \neq I$ indicates partial state measurement. Conventionally, (2.15) can be modified in terms of the estimated state through an observer gain k_{f1i} based on the concept of Kalman filter as follows:

$$\dot{\hat{x}}_i(t) = A_{ii}\hat{x}_i(t) + b_i u_{1i}(t) + k_{f1i}[y_i(t) - C_{ii}\hat{x}_i(t)] \tag{2.16}$$

Using the separation principle (Chen, 2000), the decentralised nominal LQR control gain k_{1i} and the observer gain k_{f1i} can be designed separately. It is well known that the above observer-based feedback control of (2.16) would generally not guarantee all the properties of the full state feedback LQR (Chen 2000) because the open loop transfer function of both systems at the input point are different, resulting in an error, denoted as $E_{r1i}(s)$. To recover all the guaranteed LQR properties corresponding to the full-state feedback, loop transfer recovery (LTR) technique (Chen et al, 1991) is required to minimise the so-called subsystem LTR recovery error, $E_{r1i}(s)$.

The objective of this section is to design k_{f1i} such that the observer-based feedback control almost exactly matches the guaranteed properties of k_{1i}, which is equivalent to minimizing $E_{r1i}(s)$. It is assumed that the local subsystem (2.15) is

stabilisable, detectable, left invertible (inverse of transfer function matrix exists) and of minimum phase (stable zeros and poles) in order for LTR solution to exist (**assumption 5**).

2.5.2 CSS (Chen, Saberi, Sannuti) architecture-based control (Chen et al, 1991)

The control equation (2.15) can be re-cast into a simpler form where the influence of the control signals $b_i u_{1i}(t)$ on the state is not directly reflected but indirectly incorporated through the measured state $y_i(t)$. Hence, the CSS (Chen et al 1991) architecture based control law can be written as:

$$\begin{aligned} \dot{v}_i &= A_{ii} v_i + k_{f1i}(y_i - C_{ii} v_i) \\ u_{1i} &= -k_{1i} v_i \end{aligned} \tag{2.17}$$

where $k_{f1i} \in \Re^{2nxr}$ and $v_i \in \Re^{2n}$ is the CSS subsystem control state. The CSS subsystem controller complex frequency response function (FRF) or transfer function (TF) from $y_i(t)$ to $u_{1i}(t)$ is given by:

$$C_{fi}(s) = -k_{1i}\left(\Phi_i^{-1} + k_{f1i} C_{ii}\right)^{-1} k_{f1i} \tag{2.18}$$

where $\Phi_i^{-1} = sI - A_{ii}$ and s is the frequency variable

The actual control input with partial corrupted state feedback $y_i(t)$ in terms of the feedback estimated control input (2.15) is related by the transfer function L_{fi} (i.e. the achieved open-loop (without feedback considerations) transfer function of the nominal subsystem at the input point):

$$L_{fi}(s) = C_{fi}(s)C_{ii}\Phi_i b_i = -k_{1i}\left(\Phi_i^{-1} + k_{f1i}C_{ii}\right)^{-1} k_{f1i}C_{ii}\Phi_i b_i \tag{2.19}$$

However, if full state feedback is indeed available, the corresponding robust reliable LQR achieved open-loop transfer function L_{ci} from $x_i(=y_i)$ to u_{1i} would be

$$L_{ci}(s) = -k_{1i}\Phi_i b_i \tag{2.20}$$

The difference between (2.19) and (2.20) is defined as the recovery error

$$E_{r1i}(s) = L_{ci}(s) - L_{fi}(s) \tag{2.21}$$

and the objective of the full-order CSS architecture based control is to design k_{f1i} such that $E_{r1i}(s) \to 0$. It can be easily shown that (2.21) simplifies to:

$$E_{r1i}(s) = -k_{1i}\left(sI - A_{ii} + k_{f1i}C_{ii}\right)^{-1} b_i \tag{2.22}$$

To minimize E_{r1i}, consider an auxiliary subsystem given by

$$\sum_{aux}: \begin{cases} \dot{\tilde{x}}_i = A_{ii}^{\ T}\tilde{x}_i + C_{ii}^{\ T}\tilde{u}_i + k_{1i}^{\ T}\tilde{w}_i \\ \tilde{y}_i = \tilde{x}_i \\ \tilde{z}_i = b_i^{\ T}\tilde{x}_i \\ \tilde{u}_i = -k_{f1i}^{\ T}\tilde{x}_i \end{cases} \tag{2.23}$$

where $\tilde{x}_i$, $\tilde{u}_i$, $\tilde{w}_i$, $\tilde{y}_i$ and $\tilde{z}_i$ are the variables for state, control, excitation, sensor measurement and controlled output of the auxiliary subsystem respectively.

The closed-loop transfer function from $\tilde{w}_i$ to $\tilde{z}_i$ is given by:

$$T_{\tilde{z}\tilde{w}i} = b_i^T (sI - A_{ii}^T + C_{ii}^T k_{f1i}^T)^{-1} k_{1i}^T = -E_{r1i}^T(s) \tag{2.24}$$

Since $\|E_{r1i}(s)\|_{(.)} = \|E_{r1i}^T(s)\|_{(.)}$, any optimisation of the Hardy space norm (*H*-control) method (Chen 2000) can be used to design k_{fi} to minimize the desired *H*-norm of $T_{\tilde{z}\tilde{w}i}$ based on the system described by (2.23), thus minimizing E_{ri} and recovering the guaranteed decentralised nominal controller properties.

Therefore, the CSS-LTR concept is to replace x_i with a subsystem state v_i. Equation (2.6) can be re-written as:

$$u_{1i}(t) = -k_{1i} v_i(t) + \bar{u}_{1i}(t) \tag{2.25}$$

where k_{1i} is given in (2.10) and $\mu_{1i}(t)$ in (2.13) is replaced by:

$$\mu_{1i}(t) = -\delta_{1i} b_i^T \tilde{P}_{1i} v_i \tag{2.26}$$

2.5.3 Implementation

Flowchart for the design of the decentralised nominal control for each nominal subsystem is shown in Fig. 2.1. For pre-processing, Matlab is used to compute all structural data, state-space model and control gains. Simulink is used to numerically simulate the controlled system under earthquake excitation. For post-processing, Matlab is used to process and plot all output responses and controls.

2.6 Numerical illustration

2.6.1 2DOF nominal system

In this section, a numerical example of a 2-DOF system under El Centro

earthquake scaled to 0.1g (Fig. 2.2) is used to illustrate the effectiveness of the proposed layered decentralised control as opposed to central nominal LQR control. The 2-DOF system with two actuators in state-space form with $C_s / M_s = 1.2567$ and $K_s / M_s = 157.92$ (Hart and Wong, 2000) is given by:

$$\begin{pmatrix} \dot{x}_1 \\ \dot{x}_2 \\ \ddot{x}_1 \\ \ddot{x}_2 \end{pmatrix} = \begin{pmatrix} 0 & 0 & 1 & 0 \\ 0 & 0 & 0 & 1 \\ -315.84 & 157.92 & -2.5134 & 1.2567 \\ 157.92 & -157.92 & 1.2567 & -1.2567 \end{pmatrix} \begin{pmatrix} x_1 \\ x_2 \\ \dot{x}_1 \\ \dot{x}_2 \end{pmatrix} + \begin{pmatrix} 0 & 0 \\ 0 & 0 \\ 1 & 0 \\ 0 & 1 \end{pmatrix} \begin{pmatrix} u_1 \\ u_2 \end{pmatrix} + \begin{pmatrix} 0 \\ 0 \\ -1 \\ -1 \end{pmatrix} \ddot{x}_g + v(t)$$

$$\begin{pmatrix} y_1 \\ y_2 \end{pmatrix} = \begin{pmatrix} -315.84 & 157.92 & -2.5134 & 1.2567 \\ 157.92 & -157.92 & 1.2567 & -1.2567 \end{pmatrix} \begin{pmatrix} x_1 \\ x_2 \\ \dot{x}_1 \\ \dot{x}_2 \end{pmatrix} + w(t)$$

where *v(t)* and *w(t)* are the system and measurement noises.

For comparison purposes, a central LQR controller is designed for the global nominal system with $R = 0.01I$ and $Q = 100C^T C$ to give central control: $U = -KX$, where LQR gain $K = \begin{pmatrix} 31270 & -15635 & 346 & -140 \\ -15635 & 15635 & -140 & 206 \end{pmatrix}$ and LTR gain $K_f = \begin{pmatrix} -0.8 & -0.8 & 4999 & 0 \\ -0.8 & -1.6 & 0 & -4999 \end{pmatrix}^T$ using (2.23) for the global system.

After global state-decentralisation, the subsystem 1 is given below:

$$\begin{pmatrix} \dot{x}_1 \\ \ddot{x}_1 \end{pmatrix} = \left[\begin{pmatrix} 0 & 1 \\ -315.84 & -2.5134 \end{pmatrix} \begin{pmatrix} x_1 \\ \dot{x}_1 \end{pmatrix} + \begin{pmatrix} 0 & 0 \\ 157.92 & 1.2567 \end{pmatrix} \begin{pmatrix} x_2 \\ \dot{x}_2 \end{pmatrix} \right] + \begin{pmatrix} 0 \\ 1 \end{pmatrix} u_1 + \begin{pmatrix} 0 \\ -1 \end{pmatrix} \ddot{x}_g + v_1(t)$$

$$y_1 = \begin{pmatrix} -315.84 & -2.5134 \end{pmatrix} \begin{pmatrix} x_1 \\ \dot{x}_1 \end{pmatrix} + \begin{pmatrix} 157.92 & 1.2567 \end{pmatrix} \begin{pmatrix} x_2 \\ \dot{x}_2 \end{pmatrix} + w_1(t)$$

$$z_1 = \begin{pmatrix} -315.84 & -2.5134 \end{pmatrix} \begin{pmatrix} x_1 \\ \dot{x}_1 \end{pmatrix}$$

and the subsystem 2 is given below:

$$\begin{pmatrix} \dot{x}_2 \\ \ddot{x}_2 \end{pmatrix} = \left[\begin{pmatrix} 0 & 1 \\ -157.92 & -1.2567 \end{pmatrix} \begin{pmatrix} x_2 \\ \dot{x}_2 \end{pmatrix} + \begin{pmatrix} 0 & 0 \\ 157.92 & 1.2567 \end{pmatrix} \begin{pmatrix} x_1 \\ \dot{x}_1 \end{pmatrix} \right] + \begin{pmatrix} 0 \\ 1 \end{pmatrix} u_2 + \begin{pmatrix} 0 \\ -1 \end{pmatrix} \ddot{x}_g + v_2(t)$$

$$y_2 = \begin{pmatrix} 315.84 & 2.5134 \end{pmatrix} \begin{pmatrix} x_1 \\ \dot{x}_1 \end{pmatrix} + \begin{pmatrix} -157.92 & -1.2567 \end{pmatrix} \begin{pmatrix} x_2 \\ \dot{x}_2 \end{pmatrix} + w_2(t)$$

$$z_2 = \begin{pmatrix} -157.92 & -1.2567 \end{pmatrix} \begin{pmatrix} x_2 \\ \dot{x}_2 \end{pmatrix}$$

Notice that the local regulated output z_i is the undisturbed local acceleration. The nominal controller parameters are $R_{11} = R_{12} = 0.01$, $Q_{11} = 100 C_{11}{}^T C_{11}$, $Q_{22} = 100 C_{22}{}^T C_{22}$, $\varepsilon_{11} = \varepsilon_{12} = 8$, $\delta_{11} = \delta_{12} = 7.68$ and $\tilde{Q}_{11} = \tilde{Q}_{12} = diag(1,100)$ for damping control emphasis. From (2.9) and (2.10), the control gains are $k_{11} = \begin{pmatrix} 31270 & 352 \end{pmatrix}$ and $k_{12} = \begin{pmatrix} 15635 & 216 \end{pmatrix}$. From (2.23), the LTR gains are $k_{f11} = \begin{pmatrix} -0.379 & -499 \end{pmatrix}^T$ and $k_{f12} = \begin{pmatrix} -0.728 & -499 \end{pmatrix}^T$ respectively for subsystems 1 and 2. Since the controller gain coefficients are constant and bounded, and all disturbances are assumed bounded, then the controlled system responses are bounded.

Figures 2.3 and 2.4 show the drift, velocity drift and absolute acceleration for subsystem 1 and 2 respectively. Table 2.1 shows the maximum response quantities of the 2-DOF system under no control (Uncontrolled), central LQR control (LQR) and nominal decentralised control (Decen-n). Without any control, the magnitudes of the maximum inter-story drift, drift velocity and absolute acceleration are shown in columns (2) and (5) for subsystems 1 and 2 respectively. Under global central LQR control, the controlled responses are suitably mitigated, as shown in columns (3) and (6) for subsystems 1 and 2 respectively.

With decentralised nominal saturation controls, as shown in columns (4) and (7), the controlled responses and controls are comparable to that of the central LQR controls. The results show that for the nominal 2DOF system, a set of simpler decentralised nominal controllers can perform at least as good as a single global

centralised controller under similar peak control magnitude. This agrees with the findings of Magana and Rodellar (1998).

2.6.2 20DOF nominal system

Consider a nominal 20DOF shear-structural building model (Nishitani et al, 1998) with the following parameters: $m_1=m_2=\ldots=m_{19}=10^6 kg$, $m_{20}=7*10^5 kg$; $k_1=k_2=1.47GN/m$, $k_3=k_4=1.372GN/m$, $k_5=k_6=1.274GN/m$, $k_7=k_8=1.176GN/m$, $k_9=k_{10}=1.078GN/m$, $k_{11}=k_{12}=0.98GN/m$, $k_{13}=0.931GN/m$, $k_{14}=0.882GN/m$, $k_{15}=0.833GN/m$, $k_{16}=0.784GN/m$, $k_{17}=0.735GN/m$, $k_{18}=0.686GN/m$, $k_{19}=0.637GN/m$, $k_{20}=0.588GN/m$. The natural frequencies of the first two modes of the 20DOF FOM are: $\omega_1 = 2.68 rad/s$, $\omega_2 = 7.38 rad/s$. Sensors measure the absolute acceleration at 10th and 20th DOFs. Actuators are limited to provide maximum control forces of 1000kN (Ohtori et al, 1998) and two groups of 5 actuators are each placed at the base and 10th DOF respectively.

Reduced-order 2DOF model is derived using Ritz vectors with ROM natural frequencies: $\omega_{1r} = 2.68 rad/s$, $\omega_{2r} = 7.94 rad/s$. ω_{2r} is slightly larger than ω_2 to account for the influence of higher FOM modes. The 2DOF ROM is then used as the design model for both central LQR controller and decentralised nominal saturation controller following the procedure illustrated in section 2.6.1. The 2DOF ROM system with two groups of actuators in state-space form is given by:

$$\begin{pmatrix}\dot{x}_1\\ \dot{x}_2\\ \ddot{x}_1\\ \ddot{x}_2\end{pmatrix}=\begin{pmatrix}0 & 0 & 1 & 0\\ 0 & 0 & 0 & 1\\ -7.2980 & 2.7761 & -0.0730 & 0.0278\\ 2.7761 & -62.8417 & 0.0278 & -0.6284\end{pmatrix}\begin{pmatrix}x_1\\ x_2\\ \dot{x}_1\\ \dot{x}_2\end{pmatrix}+\begin{pmatrix}0 & 0\\ 0 & 0\\ -12.1596 & -8.9808\\ 53.0676 & -27.8441\end{pmatrix}\begin{pmatrix}u_1\\ u_2\end{pmatrix}$$
$$+\begin{pmatrix}0\\ 0\\ 4022\\ -1530\end{pmatrix}\ddot{x}_g+v(t)$$

$$\begin{pmatrix}y_1\\ y_2\end{pmatrix}=\begin{pmatrix}-7.2980 & 2.7761 & -0.0730 & 0.0278\\ 2.7761 & -62.8417 & 0.0278 & -0.6284\end{pmatrix}\begin{pmatrix}x_1\\ x_2\\ \dot{x}_1\\ \dot{x}_2\end{pmatrix}+w(t)$$

where *v(t)* and *w(t)* are the system and measurement noises.

For comparison purposes, a central LQR controller is designed for the global nominal system with $R=0.01I$ and $Q=100C^TC$ to give central control: $U=-KX$, where LQR gain $K=\begin{pmatrix}-608 & 5565 & -8.6 & 57\\ -490 & -2930 & -9.6 & -31\end{pmatrix}$ and LTR gain $K_f=\begin{pmatrix}-14 & -0.6 & -69439 & 13620\\ -0.6 & -1.6 & 29848 & -299330\end{pmatrix}^T$ using (2.23) for the global system.

After global state-decentralisation, the subsystem 1 is given below:

$$\begin{pmatrix}\dot{x}_1\\ \ddot{x}_1\end{pmatrix}=\left[\begin{pmatrix}0 & 1\\ -7.2980 & -0.0730\end{pmatrix}\begin{pmatrix}x_1\\ \dot{x}_1\end{pmatrix}+\begin{pmatrix}0 & 0\\ 2.7761 & 0.0278\end{pmatrix}\begin{pmatrix}x_2\\ \dot{x}_2\end{pmatrix}\right]+\begin{pmatrix}0\\ -12.1596\end{pmatrix}u_1$$
$$+\begin{pmatrix}0\\ 4022\end{pmatrix}\ddot{x}_g+v_1(t),$$

$$y_1=\begin{pmatrix}-7.2980 & -0.0730\end{pmatrix}\begin{pmatrix}x_1\\ \dot{x}_1\end{pmatrix}+\begin{pmatrix}2.7761 & 0.0278\end{pmatrix}\begin{pmatrix}x_2\\ \dot{x}_2\end{pmatrix}+w_1(t),$$

$$z_1 = \begin{pmatrix} -7.2980 & -0.0730 \end{pmatrix} \begin{pmatrix} x_1 \\ \dot{x}_1 \end{pmatrix}$$

and the subsystem 2 is given below:

$$\begin{pmatrix} \dot{x}_2 \\ \ddot{x}_2 \end{pmatrix} = \left[\begin{pmatrix} 0 & 1 \\ -62.8417 & -0.6284 \end{pmatrix} \begin{pmatrix} x_2 \\ \dot{x}_2 \end{pmatrix} + \begin{pmatrix} 0 & 0 \\ 2.7761 & 0.0278 \end{pmatrix} \begin{pmatrix} x_1 \\ \dot{x}_1 \end{pmatrix} \right] + \begin{pmatrix} 0 \\ -27.8441 \end{pmatrix} u_2 ,$$
$$+ \begin{pmatrix} 0 \\ -1530 \end{pmatrix} \ddot{x}_g + v_2(t)$$

$$y_2 = \begin{pmatrix} 2.7761 & 0.0278 \end{pmatrix} \begin{pmatrix} x_1 \\ \dot{x}_1 \end{pmatrix} + \begin{pmatrix} -62.8417 & -0.6284 \end{pmatrix} \begin{pmatrix} x_2 \\ \dot{x}_2 \end{pmatrix} + w_2(t),$$

$$z_2 = \begin{pmatrix} -62.8417 & -0.6284 \end{pmatrix} \begin{pmatrix} x_2 \\ \dot{x}_2 \end{pmatrix}$$

Notice that the local regulated output z_i is the undisturbed local acceleration. The nominal controller parameters are $R_{11} = R_{12} = 0.01$, $Q_{11} = 100 C_{11}{}^T C_{11}$, $Q_{22} = 100 C_{22}{}^T C_{22}$, $\varepsilon_{11} = \varepsilon_{12} = 8$, $\delta_{11} = \delta_{12} = 7.68$ and $\tilde{Q}_{11} = \tilde{Q}_{12} = diag(1,100)$ for damping control emphasis. From (2.9) and (2.10), the control gains are $k_{11} = \begin{pmatrix} -729 & -13 \end{pmatrix}$ and $k_{12} = \begin{pmatrix} -6282 & -66 \end{pmatrix}$. From (2.23), the LTR gains are $k_{f11} = \begin{pmatrix} -12 & --6079 \end{pmatrix}^T$ and $k_{f12} = \begin{pmatrix} -2 & -13921 \end{pmatrix}^T$ respectively for subsystems 1 and 2. Since the controller gain coefficients are constant and bounded, and all disturbances are assumed bounded, then the controlled system responses are bounded.

Figures 2.5 and 2.6 show the inter-storey drift, drift velocity and absolute acceleration for the 10th DOF and 20th DOF respectively. Table 2.2 shows the maximum response quantities of the 10th and 20th DOFs of the 20DOF system under no control (Uncontrolled), central LQR control (LQR) and nominal decentralised control (Decen-n).

The results show that without any control, the magnitudes of the maximum inter-story drift, drift velocity and absolute acceleration are shown in columns (2) and

(5). Under global central LQR control, the controlled responses are suitably mitigated, as shown in columns (3) and (6). With decentralised nominal saturation controls, as shown in columns (4) and (7), the controlled responses are comparable to the central LQR controlled responses. Hence, this reinforces the findings from the 2DOF system and also shows that decentralized nominal saturation controls work as well using Ritz-ROM.

Table 2.1: Maximum Responses of Nominal 2DOF system

Cases (1)	Subsystem 1			Subsystem 2		
	No control (2)	LQR (3)	Decen-n (4)	No control (5)	LQR (6)	Decen-n (7)
Drift (cm)	1.94	0.01	0.01	1.18	0.005	0.005
Drift vel. (cm/s)	14.4	0.34	0.34	9.18	0.2	0.15
Abs. acc. (cm/s^2)	120.9	85.71	85.71	186.3	85.83	86.37

Table 2.2: Maximum Responses of Nominal 20DOF system

Cases (1)	10^{th} DOF			20^{th} DOF		
	No control (2)	LQR (3)	Decen-n (4)	No control (5)	LQR (6)	Decen-n (7)
Drift (cm)	0.65	0.01	0.007	0.17	0.008	0.009
Drift vel. (cm/s)	2.73	0.52	0.27	1.35	0.33	0.41
Abs. acc. (cm/s^2)	101	85.58	85.82	141	86.62	85.68

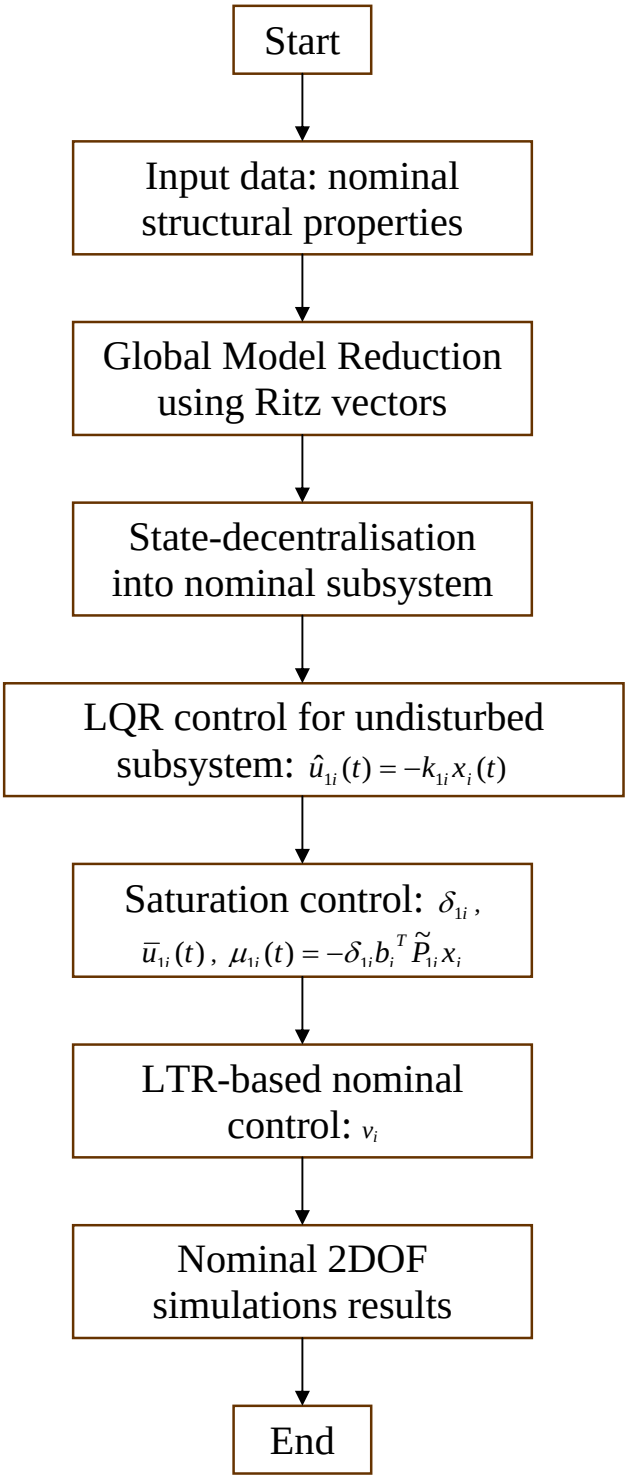

Figure 2.1: Flowchart for Design of Decentralised Nominal Saturation Control

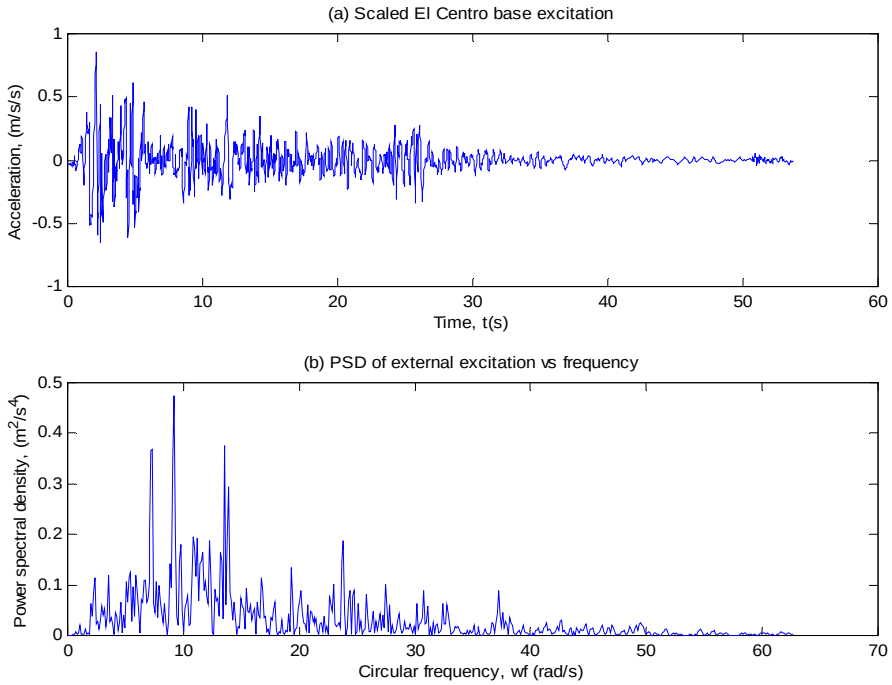

Figure 2.2: El Centro earthquake scaled to 0.1g and PSD

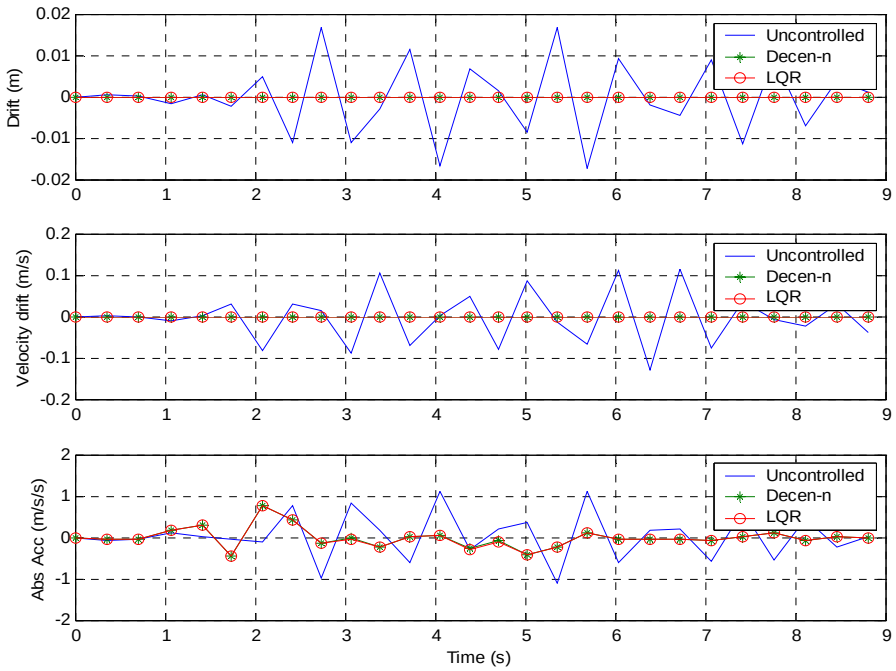

Figure 2.3: Subsystem 1 responses and controls for nominal 2DOF system

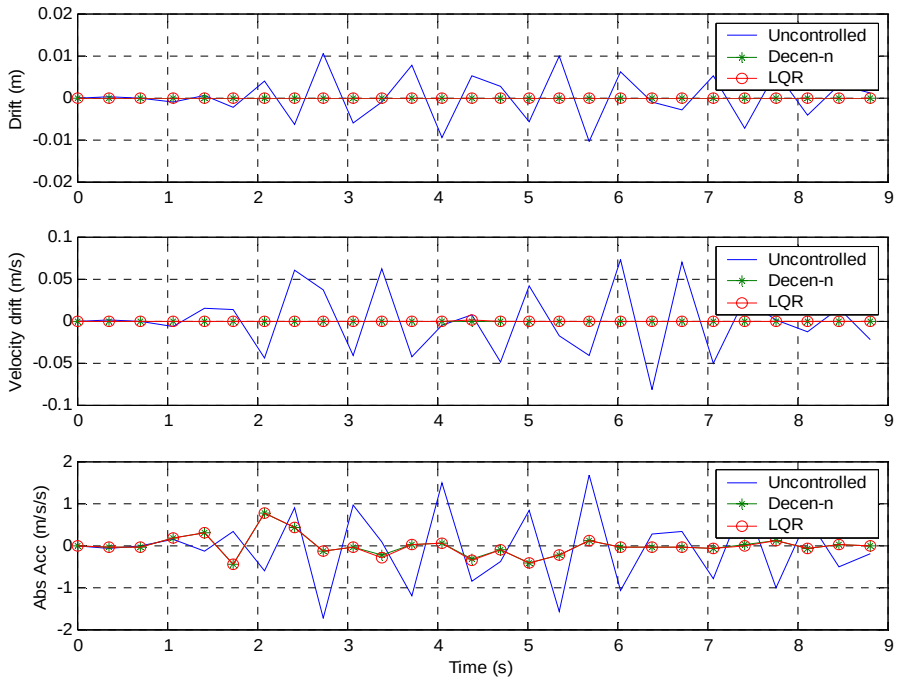

Figure 2.4: Subsystem 2 responses and controls for nominal 2DOF system

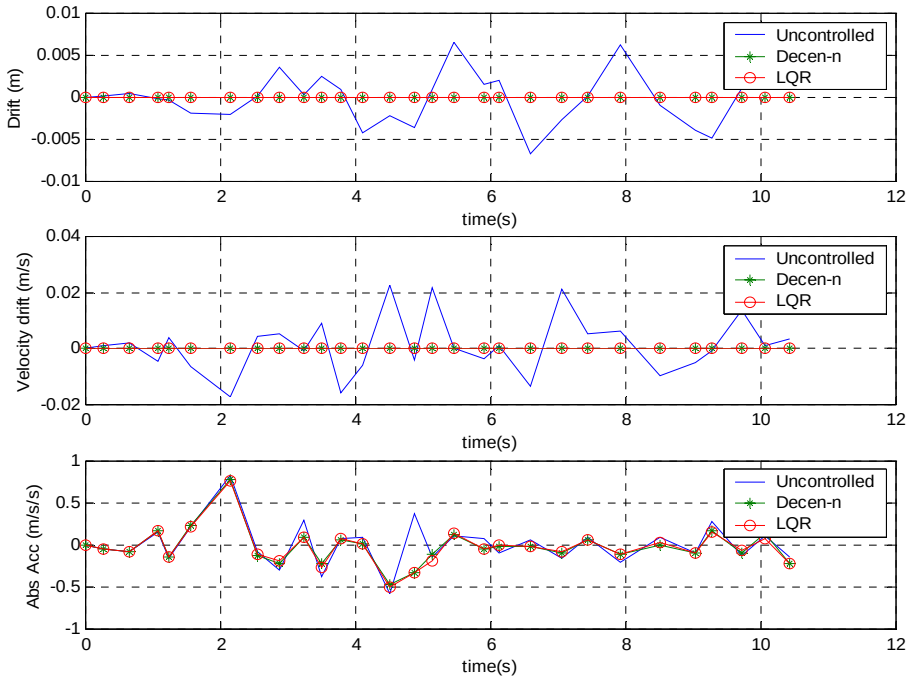

Figure 2.5: Responses and controls for 10th DOF of nominal 20DOF system

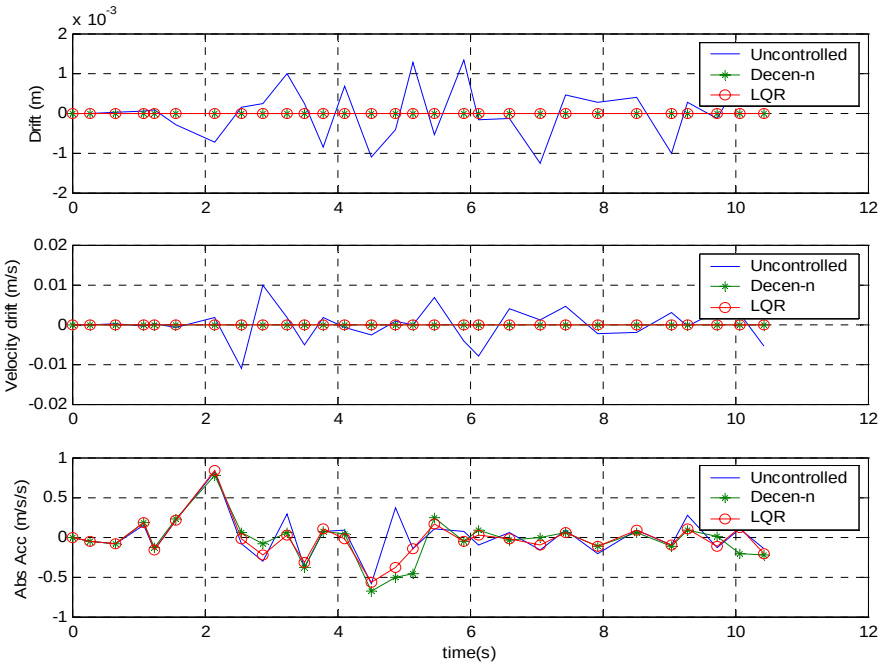

Figure 2.6: Responses and controls for 20th DOF of nominal 20DOF system

CHAPTER 3

CENTRAL ROBUST RELIABLE CONTROLLER

3.1 Introduction

The previous chapter presents the solution for the decentralised nominal control using LTR technique with LQR and saturation controllers for noise-corrupted partial state feedback systems. In many practical situations, additional complexities arise when uncertainties are present and some control sensors and actuators may fail during service. This is addressed in this chapter where the robust reliable optimal controller is proposed for linear uncertain systems under seismic excitation.

As in the previous chapter, full state feedback is considered. Firstly, the system uncertainties are decomposed. Using closed-loop state-space Riccati-based control approach, the full state-feedback gain is derived from the solution of the formulated Algebraic Riccati Equation (ARE). The full state feedback gain is formulated to be robust against both structured and unstructured norm-bounded uncertainties as well as reliable against actuator failures confined to a predefined subset. Secondly, to account for noise-corrupted partial state feedback, LTR-based robust reliable control is implemented using the separation principle to account for noise-corrupted partial state feedback under practical considerations. For illustration, both the nominal and uncertain 2DOF systems under robust reliable optimal control, central LQR control and decentralised nominal saturation control are presented.

3.2 Control Problem Formulation

3.2.1 Analytical Model with Uncertainties

Consider an *n*-degree-of-freedom building subjected to one-dimensional horizontal earthquake ground acceleration $\ddot{x}_g(t)$. By modifying (2.1), the global uncertain dynamic equation of motion inclusive of all uncertainties, perturbations and disturbances can be derived using extended Hamilton's variational principle (Meirovitch, 2000) as:

$$M_s\ddot{\xi}(t)+(C_s+\Delta C_s)\dot{\xi}(t)+(K_s+\Delta K_s)\xi(t)=(F_c+\Delta F_c)U(t)-M_s(l+\Delta l)\ddot{x}_g(t) \quad (3.1)$$

where $\xi(t)\in\Re^n$ is the global displacement vector; $U(t)\in\Re^m$ is the nominal control voltage vectors to *m* groups of actuators; $M_s\in\Re^{nxn}$ is the global consistent mass matrix; $C_s\in\Re^{nxn}$ and $\Delta C_s\in\Re^{nxn}$ are the global nominal and uncertain linear viscous damping matrices; $K_s\in\Re^{nxn}$ and $\Delta K_s\in\Re^{nxn}$ are the global nominal and uncertain linear elastic stiffness matrices; $F_c = p_c l_c$ and $\Delta F_c = p_c \Delta l_c$ are the global nominal and uncertain control force distribution matrices, where $p_c\in\Re^{nxm}$ is the global actuation force distribution vector, $l_c\in\Re^{mxm}$ and $\Delta l_c\in\Re^{mxm}$ are the global nominal and uncertain actuation force per unit voltage transformation matrices; and $l\in\Re^n$ and $\Delta l\in\Re^n$ are the global nominal and uncertain earthquake excitation influence vectors.

In the state space, (3.1) becomes a class of uncertain systems with the following form:

$$\begin{aligned} \dot{x}(t) &= (A + \Delta A)x(t) + Bu(t) + (H + \Delta H)w(t), \\ y(t) &= x(t), \\ z(t) &= (C + \Delta C)x(t) \end{aligned} \tag{3.2}$$

where $A \in \Re^{2nx2n}$, $C = \begin{pmatrix} -M_s^{-1}K_s & -M_s^{-1}C_s \end{pmatrix} \in \Re^{rx2n}$ and $H = \begin{pmatrix} 0 \\ -l \end{pmatrix} \in \Re^{2nxd}$ are the constant nominal system, regulated output influence and disturbance influence matrices, respectively. Note that $d=n$ for earthquake excitations. $x(t) = \begin{pmatrix} \xi \\ \dot{\xi} \end{pmatrix} \in \Re^{2n}$ is the full state vector, $u(t) = [u_1,...,u_m]^T \in \Re^m$ is the control input vector, $y(t) \in \Re^{2n}$ is the vector of sensor measurements chosen here for full state measurements, $z(t) \in \Re^r$ the regulated output vector and $w(t) \in \Re^d$ the disturbance vector. Structured uncertainties for the system are denoted as $\Delta A \in \Re^{2nx2n}$ and the controller influence matrix as $B = \begin{pmatrix} 0 \\ M_s^{-1}F_c + M_s^{-1}\Delta F_c \end{pmatrix} \in \Re^{2nxm}$. Unstructured uncertainties for the norm-bounded sensors and the disturbance input are $\Delta C = \begin{pmatrix} -M_s^{-1}\Delta K_s & -M_s^{-1}\Delta C_s \end{pmatrix} \in \Re^{rx2n}$ and $\Delta H = \begin{pmatrix} 0 \\ -\Delta l \end{pmatrix} \in \Re^{2nxd}$ respectively, where $0 \le \|\Delta C\|_2 \le \delta_c$ and $0 \le \|\Delta H\|_2 \le \delta_h$.

Formulating (3.2) in state space form of (3.1), the system and system uncertainty matrices are:

$$A = \begin{pmatrix} 0 & I \\ -M_s^{-1}K_s & -M_s^{-1}C_s \end{pmatrix}, \ \Delta A = \begin{pmatrix} 0 & 0 \\ -M_s^{-1}\Delta K_s & -M_s^{-1}\Delta C_s \end{pmatrix} \tag{3.3}$$

Without loss of generality, the components in ΔA can be decomposed (Khargoneka et al 1990) as

$$M_s^{-1}\Delta C_s = D_c F_c(t) E_c,\ M_s^{-1}\Delta K_s = D_k F_k(t) E_k \tag{3.4}$$

where $D_c,\ D_k,\ E_c,\ E_k \in \Re^{nxn}$ are known real constant matrices, and $F_c(t),\ F_k(t) \in \Re^{nxn}$ are bounded uncertain matrix with Lebesgue measurable elements such that $F_c(t)^T F_c(t) \le I$ and $F_k(t)^T F_k(t) \le I$. Hence,

$$\Delta A = DF(t)E \tag{3.5}$$

where

$$D = \begin{pmatrix} 0 & 0 \\ D_k & D_c \end{pmatrix},\ F(t) = \begin{pmatrix} -F_k(t) & 0 \\ 0 & -F_c(t) \end{pmatrix},\ E = \begin{pmatrix} E_k & 0 \\ 0 & E_c \end{pmatrix} \tag{3.6}$$

3.2.2 Assumptions

In addition to the assumption of full state feedback and no measurement noise implied in (1b), the following assumptions are made in formulating the control problem:

(a) The uncertainties have known bounds; that is, $(C_s + \Delta C_s) \in [C_s^-, C_s^+]$, $(K_s + \Delta K_s) \in [K_s^-, K_s^+]$, $(F_c + \Delta F_c) \in [F_c^-, F_c^+]$ and $U \in [U^-, U^+]$ where C_s^-, C_s^+, K_s^-, K_s^+, F_c^-, F_c^+, U^- and U^+ are known quantities.

(b) The actuators can be divided into two mutually exclusive sets, where one set of predefined actuators susceptible to failures is denoted by $\Omega \subseteq \{1,...,m\}$ and the other set of actuators that never fail is denoted by $\overline{\Omega} = \{1,...,m\} - \Omega$. The control input

influence matrix can be decomposed as (Seo et al 1996):

$$B = B_{\Omega} + B_{\overline{\Omega}} \tag{3.7}$$

where $B_{\Omega} \in \Re^{2nxm}$ and $B_{\overline{\Omega}} \in \Re^{2nxm}$ are formed from B by zeroing out columns corresponding to Ω and $\overline{\Omega}$ respectively. Note that actuator failures can be either partial failures if the actuator(s) or group(s) of actuators are operating at less than full working capacity; or total failures if the actuator(s) or group(s) of actuators are not working at all.

(c) $(A, B_{\overline{\Omega}})$ is stabilisable. That is, the unstable modes can be controlled by the actuators.

(d) The vector of time-varying outputs of failed actuators $u_F(t)$ is bounded, i.e. $u_F(t) \in [0, u_{sat}]$, where u_{sat} is the pre-defined actuator saturation function.

3.2.3 Closed-loop System

Amongst the pre-defined set of possible actuators that may fail, let the actual set of actuators that failed at time t be denoted as ω, where $\omega \subseteq \Omega$. By decomposing B as $B_{\omega} + B_{\overline{\omega}}$, where $B_{\overline{\Omega}} \le B_{\overline{\omega}} \le B$ and $0 \le B_{\omega} \le B_{\Omega}$, and assuming a control law with static feedback gain $K_c \in \Re^{mx2n}$:

$$u(t) = -K_c x(t) \tag{3.8}$$

then the closed-loop system for (3.2) can be written as:

$$\begin{aligned} \dot{x}(t) &= A_c x(t) + B_c w_F(t), \\ y(t) &= x(t), \\ z(t) &= C_c x(t) \end{aligned} \tag{3.9}$$

where $A_c = A + \Delta A - B_{\bar{\omega}} K_c$, $B_c = \begin{pmatrix} H + \Delta H & B_\omega \end{pmatrix}$, $C_c = C + \Delta C$, $w_F = \begin{pmatrix} w^T & u_F^T \end{pmatrix}^T$, in which $w_F(t) \in \Re^{d+m}$ is augmented disturbance vector and $u_F(t) \in \Re^m$ is the control input vector with elements corresponding to working actuators being zero.

3.2.4 Control Tasks

The objective is to design a linear state feedback control law (3.8) for the closed-loop system (3.9) with admissible uncertainties and allowable actuator failures under assumptions stated in Section 3.2.2 such that despite the actuator faults, the controller provides (a) robust α-degree relative asymptotic stability (i.e. the real part of the eigenvalue of A_c is less than negative of a pre-defined positive value, α):

$$\mathrm{Re}\{\lambda(A_c)\} < -\alpha < 0 \tag{3.10}$$

(b) robust augmented disturbance transmission that is H_∞–norm bounded within a prescribed level δ:

$$\left\| T_{zw_F} \right\|_\infty = \left\| C_c \left(sI - A_c \right)^{-1} B_c \right\|_\infty \le \delta \tag{3.11}$$

and (c) H_2 optimal by minimizing the performance index:

$$J = \int_0^\infty \left[x^T \tilde{Q} x + u^T \tilde{R} u \right] dt \tag{3.12}$$

where $\tilde{Q}:\tilde{Q}\geq 0,\tilde{Q}\in\Re^{2nx2n}$ is symmetric and semi-positive definite and $\tilde{R}:\tilde{R}>0,\tilde{R}\in\Re^{mxm}$ is symmetric and positive definite. Note that (3.11) implies that the control output is quadratically stable (Seo and Kim, 1996) despite actuator failures, i.e.

$$\|z\|_2 \leq \delta \|w_F\|_2 \tag{3.13}$$

3.3 Robust Reliable Optimal Full State-Feedback Control

3.3.1 Robust reliable control under system uncertainties

Objectives (3.11-3.12) can be achieved for scalars $\alpha \geq 0$, $\delta > 0$ and $\varepsilon > 0$ if there exists a matrix $P > 0$ such that (Wang et al 2001)

$$(A_c + \alpha I)^T P + P(A_c + \alpha I) + \frac{\varepsilon}{\delta} P B_c B_c{}^T P + \frac{1}{\varepsilon\delta} C_c{}^T C_c < 0 \tag{3.14}$$

Assuming that K_c can be expressed as

$$K_c = \frac{1}{2\beta} B_{\bar{\omega}}{}^T P \tag{3.15}$$

where $\beta > 0$ is a pre-defined scalar used to scale K_c. Substituting (3.9) and (3.15) into the LHS of (3.14) gives

$$
\begin{aligned}
&(A_c+\alpha I)^T P + P(A_c+\alpha I) + \frac{\varepsilon}{\delta} PB_c B_c{}^T P + \frac{1}{\varepsilon\delta} C_c{}^T C_c \\
&= \left(A+\Delta A - \frac{1}{2\beta} B_{\bar{\omega}} B_{\bar{\omega}}{}^T P + \alpha I \right)^T P + P\left(A+\Delta A - \frac{1}{2\beta} B_{\bar{\omega}} B_{\bar{\omega}}{}^T P + \alpha I \right) \\
&+ \frac{\varepsilon}{\delta} P\begin{pmatrix} H+\Delta H & B_\omega \end{pmatrix} \begin{pmatrix} H^T+\Delta H^T \\ B_\omega{}^T \end{pmatrix} P + \frac{1}{\varepsilon\delta}(C+\Delta C)^T (C+\Delta C) \\
&= (A+\alpha I)^T P + \Delta A^T P + P(A+\alpha I) + P\Delta A - \frac{1}{\beta} PB_{\bar{\omega}} B_{\bar{\omega}}{}^T P \\
&+ \frac{\varepsilon}{\delta} P\left[HH^T + \Delta H\Delta H^T + H\Delta H^T + \Delta HH^T + B_\omega B_\omega{}^T \right] P \\
&+ \frac{1}{\varepsilon\delta}\left[C^T C + \Delta C^T \Delta C + C^T \Delta C + \Delta C^T C \right]
\end{aligned}
\tag{3.16}
$$

Using the inequality that for any rectangular matrices X and Y with scalar $\xi > 0$ (Wang et al, 2001),

$$
\xi XX^T + \frac{1}{\xi} YY^T \pm \left(XY^T + YX^T \right) \geq 0 \tag{3.17}
$$

the following inequalities can be derived:

$$
\begin{aligned}
&C^T C + \Delta C^T C + \Delta C^T \Delta C + C^T \Delta C \\
&\leq (1+\varepsilon_2) C^T C + (1+\frac{1}{\varepsilon_2}) \Delta C^T \Delta C \\
&\leq (1+\varepsilon_2) C^T C + (1+\frac{1}{\varepsilon_2}) \delta_c{}^2 I
\end{aligned}
\tag{3.18}
$$

for $\varepsilon_2 > 0$.

$$\begin{aligned} & B_\omega B_\omega{}^T + HH^T + \Delta H\Delta H^T + (H\Delta H^T + \Delta HH^T) \\ & \le B_\omega B_\omega{}^T + HH^T + \Delta H\Delta H^T + \left(\varepsilon_3 HH^T + \frac{1}{\varepsilon_3}\Delta H\Delta H^T\right) \\ & = B_\omega B_\omega{}^T + (1+\varepsilon_3)HH^T + (1+\frac{1}{\varepsilon_3})\Delta H\Delta H^T \\ & \le B_\omega B_\omega{}^T + (1+\varepsilon_3)HH^T + (1+\frac{1}{\varepsilon_3})\delta_h{}^2 I \end{aligned} \tag{3.19}$$

for $\varepsilon_3 > 0$.

$$-\frac{1}{\beta}PB_{\bar{\omega}}B_{\bar{\omega}}{}^T P \le -PB_{\bar{\omega}}B_{\bar{\omega}}{}^T P \tag{3.20}$$

for $0 < \beta \le 1$.

$$\Delta A^T P + P\Delta A \le \varepsilon_1 \Delta A\Delta A^T + \frac{1}{\varepsilon_1}PP^T \tag{3.21}$$

for $\varepsilon_1 > 0$. Let $X = \sqrt{\varepsilon_4}D^T P - \frac{1}{\sqrt{\varepsilon_4}}F(t)E$ where scalar $\varepsilon_4 > 0$. Then inequality $X^T X \ge 0$ gives:

$$\dot{\left[\sqrt{\varepsilon_4}PD - \frac{1}{\sqrt{\varepsilon_4}}E^T F^T(t)\right]}\left[\sqrt{\varepsilon_4}D^T P - \frac{1}{\sqrt{\varepsilon_4}}F(t)E\right] \ge 0 \tag{3.22}$$

Substitute (3.5) and (3.22) into (3.21) gives

$$\Delta A^T P + P\Delta A \le \varepsilon_1 PT_A P + \frac{1}{\varepsilon_1}U_A \tag{3.23}$$

where

$$T_A = DD^T = \begin{pmatrix} 0 & 0 \\ 0 & D_k D_k{}^T + D_c D_c{}^T \end{pmatrix},\ U_A = E^T E = \begin{pmatrix} E_k{}^T E_k & 0 \\ 0 & E_c{}^T E_c \end{pmatrix} \qquad (3.24)$$

Hence, substituting (3.18-3.20, 3.23) and the following expansion

$$\begin{aligned} B_\Omega B_\Omega{}^T &= B_\omega B_\omega{}^T + B_{\Omega-\omega} B_{\Omega-\omega}{}^T \\ B_{\bar{\Omega}} B_{\bar{\Omega}}{}^T &= B_{\bar{\omega}} B_{\bar{\omega}}{}^T - B_{\Omega-\omega} B_{\Omega-\omega}{}^T \end{aligned} \quad \Rightarrow \quad \begin{aligned} B_\omega B_\omega{}^T &= B_\Omega B_\Omega{}^T - B_{\Omega-\omega} B_{\Omega-\omega}{}^T \\ B_{\bar{\omega}} B_{\bar{\omega}}{}^T &= B_{\bar{\Omega}} B_{\bar{\Omega}}{}^T + B_{\Omega-\omega} B_{\Omega-\omega}{}^T \end{aligned} \qquad (3.25)$$

into (3.16) gives

$$
\begin{aligned}
&(A+\alpha I)^T P + \Delta A^T P + P(A+\alpha I) + P\Delta A - \frac{1}{\beta} P B_{\bar{\varpi}} B_{\bar{\varpi}}{}^T P \\
&+ \frac{\varepsilon}{\delta} P\left[HH^T + \Delta H \Delta H^T + H\Delta H^T + \Delta H H^T + B_{\omega} B_{\omega}{}^T\right] P \\
&+ \frac{1}{\varepsilon\delta}\left[C^T C + \Delta C^T \Delta C + C^T \Delta C + \Delta C^T C\right] \\
&\le (A+\alpha I)^T P + P(A+\alpha I) + \varepsilon_1 P B T_{mA} B^T P + \frac{1}{\varepsilon_1} U_{mA} \\
&- P\left(B_{\bar{\Omega}} B_{\bar{\Omega}}{}^T + B_{\Omega-\omega} B_{\Omega-\omega}{}^T\right) P + \frac{\varepsilon}{\delta} P\left(B_{\Omega} B_{\Omega}{}^T - B_{\Omega-\omega} B_{\Omega-\omega}{}^T\right) P \\
&+ \frac{\varepsilon}{\delta} P\left[(1+\varepsilon_3) HH^T + (1+\frac{1}{\varepsilon_3})\delta_h{}^2 I\right] P \\
&+ \frac{1}{\varepsilon\delta}\left[(1+\varepsilon_2) C^T C + (1+\frac{1}{\varepsilon_2})\delta_c{}^2 I\right] + Q - Q \\
&= (A+\alpha I)^T P + P(A+\alpha I) + \varepsilon_1 P T_A P + \frac{1}{\varepsilon_1} U_A \\
&- P\left(B_{\bar{\Omega}} B_{\bar{\Omega}}{}^T\right) P + \frac{\varepsilon}{\delta} P\left(B_{\Omega} B_{\Omega}{}^T\right) P \\
&+ \frac{\varepsilon}{\delta} P\left[(1+\varepsilon_3) HH^T + (1+\frac{1}{\varepsilon_3})\delta_h{}^2 I\right] P \\
&+ \frac{1}{\varepsilon\delta}\left[(1+\varepsilon_2) C^T C + (1+\frac{1}{\varepsilon_2})\delta_c{}^2 I\right] + Q \\
&- \left(1+\frac{\varepsilon}{\delta}\right) P\left(B_{\Omega-\omega} B_{\Omega-\omega}{}^T\right) P - Q
\end{aligned}
\tag{3.26}
$$

for $Q > 0$. From (3.26), for (3.14) to hold,

$$
\begin{aligned}
&(A+\alpha I)^T P + P(A+\alpha I) + \varepsilon_1 P T_A P + \frac{1}{\varepsilon_1} U_A \\
&- P\left(B_{\bar{\Omega}} B_{\bar{\Omega}}{}^T\right) P + \frac{\varepsilon}{\delta} P\left(B_{\Omega} B_{\Omega}{}^T\right) P + \frac{\varepsilon}{\delta} P\left[(1+\varepsilon_3) HH^T + (1+\frac{1}{\varepsilon_3})\delta_h{}^2 I\right] P \\
&+ \frac{1}{\varepsilon\delta}\left[(1+\varepsilon_2) C^T C + (1+\frac{1}{\varepsilon_2})\delta_c{}^2 I\right] + Q = 0
\end{aligned}
\tag{3.27}
$$

which can be cast in the algebraic Riccati equation (ARE) form as

$$(A+\alpha I)^T P + P(A+\alpha I) - PRP + \overline{Q} = 0 \tag{3.28}$$

where

$$R = B_{\overline{\Omega}} B_{\overline{\Omega}}{}^T - \varepsilon_1 T_A - \frac{\varepsilon}{\delta}\left[B_\Omega B_\Omega{}^T + (1+\varepsilon_3) HH^T + (1+\frac{1}{\varepsilon_3})\delta_h{}^2 I \right] \tag{3.29}$$

$$\overline{Q} = \frac{1}{\varepsilon_1} U_A + \frac{1}{\varepsilon\delta}\left[(1+\varepsilon_2) C^T C + (1+\frac{1}{\varepsilon_2})\delta_c{}^2 I \right] + Q \tag{3.30}$$

To solve the ARE (3.28) implies $\overline{Q} \geq 0$ and *R>0,* hence the following condition need to be satisfied:

$$\underline{\sigma}\left(\frac{1}{\beta} B_{\overline{\Omega}} B_{\overline{\Omega}}{}^T \right) > \overline{\sigma}\left\{ (\varepsilon_1 T_A) + \frac{\varepsilon}{\delta}\left[B_\Omega B_\Omega{}^T + (1+\varepsilon_3) HH^T + (1+\frac{1}{\varepsilon_3})\delta_h{}^2 I \right] \right\} > 0 \tag{3.31}$$

α and δ are selected based on user robustness specifications. Tuning scalars ε, ε_1, ε_2 and ε_3 should be chosen to ensure that both *R* (3.29) and $\overline{Q}$ (3.30) are positive-definite as well as selecting β to achieve H_2-optimality given in (3.12). For $R > 0$, increase δ and decrease ε and β. For $\overline{Q} > 0$, increase ε_2 and *Q*; and decrease ε_1 and δ.

3.3.2 Robust reliable control under matched system uncertainties

For system where *B* takes the form $\begin{pmatrix} 0 \\ \overline{B} \end{pmatrix}$, $\overline{B} \neq 0$, and the uncertainties are

matched (or can be decomposed) in the manner

$$\Delta K_s = \overline{B}\Delta \mathrm{K_m}, \qquad \Delta C_s = \overline{B}\Delta C_{\mathrm{m}} \tag{3.32}$$

the system uncertainties can be re-written as

$$\Delta A = BA_m,\ A_m = \begin{pmatrix} -\Delta K_m & -\Delta C_m \end{pmatrix} \tag{3.33}$$

in which $A_m \in \Re^{mx2n}$, $\Delta C_m \in \Re^{mxn}$ and $\Delta K_m \in \Re^{mxn}$. Following the same argument in Section 3.3.1, it can be shown that

$$\Delta A^T P + P\Delta A \le \varepsilon_1 PBT_{mA}B^T P + \frac{1}{\varepsilon_1}U_{mA} \tag{3.34}$$

where

$$T_{mA} = D_{mk}{D_{mk}}^T + D_{mc}{D_{mc}}^T,\ U_{mA} = \begin{pmatrix} {E_{mk}}^T E_{mk} & 0 \\ 0 & {E_{mc}}^T E_{mc} \end{pmatrix} \tag{3.35}$$

in which

$$\Delta \mathrm{C_m} = D_{mc}F_{mc}(t)E_{mc},\ \Delta K_{\mathrm{m}} = D_{mk}F_{mk}(t)E_{mk} \tag{3.36}$$

The ARE in (3.28) holds with

$$R = B_{\bar{\Omega}} B_{\bar{\Omega}}{}^{T} - \varepsilon_1 B T_{mA} B^{T} - \frac{\varepsilon}{\delta}\left[B_{\Omega} B_{\Omega}{}^{T} + (1+\varepsilon_3) H H^{T} + (1+\frac{1}{\varepsilon_3})\delta_h{}^{2} I \right] \tag{3.37}$$

$$\bar{Q} = \frac{1}{\varepsilon_1} U_{mA} + \frac{1}{\varepsilon\delta}\left[(1+\varepsilon_2) C^{T} C + (1+\frac{1}{\varepsilon_2})\delta_c{}^{2} I \right] + Q \tag{3.38}$$

3.3.3 Robust reliable H_2-optimal control

From (3.8), (3.12) can be written as

$$J = \int_0^{\infty} \left[x^{T} \left(\tilde{Q} + K^{T} \tilde{R} K \right) x \right] dt = \int_0^{\infty} \left[x^{T} \hat{Q} x \right] dt \tag{3.39}$$

where $\hat{Q} = \tilde{Q} + K^{T} \tilde{R} K$. From (3.9) and (3.15), $A_c = A + \Delta A - \frac{1}{2\beta} B_{\bar{\omega}} B_{\bar{\omega}}{}^{T} P$.

If (3.28) holds and since the closed-loop system is asymptotically stable as guaranteed under (3.10) and A_c is stable, for (3.39) to be minimized, the following Lyapunov equation must hold

$$A_c{}^{T} P + P A_c = -\hat{Q} \tag{3.40}$$

under the condition that $\hat{Q} \in \Re^{2nx2n}$ is positive semi-definite matrix. Taking $\tilde{R} = 2\beta I > 0$ and re-writing (3.15) as $K_c = R^{-1} B_{\bar{\omega}}{}^{T} P$, it can be shown through (3.40) that

$$\tilde{Q} = -(A_c^{T} P + P A_c + P B_{\bar{\omega}} \tilde{R}^{-1} B_{\bar{\omega}}{}^{T} P) \tag{3.41}$$

Objective (3.10) implies A_c is negative definite and (3.14) implies P is s.p.d. to ensure admissible solution of (3.28), then $\tilde{Q} \geq 0$. Adding the ARE in (3.28) with (3.40) gives:

$$\begin{aligned} &2\alpha P - \frac{1}{\beta} P\left(B_{\bar{\Omega}} B_{\bar{\Omega}}{}^T\right) P + \frac{\varepsilon}{\delta} P\left(B_{\Omega} B_{\Omega}{}^T\right) P + \frac{1}{2\beta} P B_{\bar{\varpi}} B_{\bar{\varpi}}{}^T P \\ &+ \frac{\varepsilon}{\delta} P\left[(1+\varepsilon_3) H H^T + (1+\frac{1}{\varepsilon_3})\delta_h{}^2 I\right] P + \frac{1}{\varepsilon\delta}\left[(1+\varepsilon_2) C^T C + (1+\frac{1}{\varepsilon_2})\delta_c{}^2 I\right] + Q \geq 0 \end{aligned} \tag{3.42}$$

The detectability of $(A, \tilde{Q}^{1/2})$ is assumed for unstable modes to be reflected in (3.12). This can be used to check whether H_2-optimality has been achieved for the robust reliable controller. Satisfying (3.42) therefore implies that under closed-loop linear system conditions, (3.12) is satisfied such that the controller provides infinite gain margin and at least 60° phase margin for all admissible uncertainties and allowable actuator failures.

In addition to being fault-tolerant, if the allowable actuator failures can be actively monitored, then fault compensation using state feedback (Tao et al 2001) can be used to completely attenuate the effects of all failures.

3.4 Partial Noise-corrupted State Feedback Control

In this section, conditions for system (3.2) would be relaxed to include corrupted partial state feedback, CSS LTR (Chen et al 1991) can be used to recover the properties of the robust reliable LQR controller of the previous section.

3.4.1 LTR Problem

In the previous section where for the system described by (3.2), the robust

reliable LQR control gain K_c in (3.8) can be computed using (3.15). Practical situations necessitate that only corrupted partial state feedback is available and (3.2) can be modified as follows:

$$\begin{aligned} \dot{x}(t) &= (A + \Delta A)x(t) + Bu(t) + w(t), \\ y(t) &= (C + \Delta C)x(t) + \eta(t), \\ z(t) &= (C + \Delta C)x(t) \end{aligned} \tag{3.43}$$

where $w(t) \in \Re^{2n}$ and $\eta(t) \in \Re^{r}$ are independent white noises, and $C \neq I$ indicates partial state measurement. Conventionally, (3.43) can be modified in terms of the estimated state through an observer gain K_f based on the concept of Kalman filter, noting that only nominal matrices are used since uncertainties ΔA and ΔC are not measurable:

$$\dot{\hat{x}}(t) = A\hat{x}(t) + Bu(t) + K_f[y(t) - C\hat{x}(t)] \tag{3.44}$$

It is well known that an observer-based feedback control would generally not guarantee all the properties of the full state feedback LQR. This can be overcome by using loop transfer recovery (LTR) technique where the objective is to design K_f such that the observer-based feedback control almost or exactly matches the guaranteed properties of K_c under the following assumptions:

(a) (A, C) is detectable. That is, all the unstable modes are captured by the sensors.

(b) $E[w(t)] = 0$ with $E[w(t)w^T(\tau)] = Q_f\delta(t-\tau)$, $Q_f = Q_f^T \geq 0$.

(c) $E[\eta(t)] = 0$ with $E[\eta(t)\eta^T(\tau)] = R_f\delta(t-\tau)$, $R_f = R_f^T \geq 0$.

(d) (A, Q_f) is stabilisable.

(e) System (3.43) is left invertible and of minimum phase, i.e. no unstable closed right

half plane poles (roots of the FRF denominator) and zeros (roots of the FRF numerator) on the root locus plot. This is required for LTR to be realizable.

3.4.2 Full-order CSS architecture-based control

The control equation (3.43) can be re-cast in a simpler form where the influence of the control signals *Bu(t)* on the state is not directly reflected but indirectly incorporated through the measured state *y(t)*. Hence, the full-order CSS (Chen et al 1991) architecture based control law can be written as:

$$\begin{aligned} \dot{v}(t) &= Av(t) + K_f[y(t) - Cv], \\ u(t) &= -K_c v(t) \end{aligned} \tag{3.45}$$

where $K_f \in \Re^{2nxr}$ and $v \in \Re^{2n}$ is the CSS control state. The CSS controller transfer function from *y(t)* to $-u(t)$ is given by

$$C_f(s) = K_c\left(\Phi^{-1} + K_f C\right)^{-1} K_f \tag{3.46}$$

where $\Phi^{-1} = sI - A$ and *s* is the frequency variable.

The actual control input with partial corrupted state feedback *y(t)* in terms of the feedback estimated control input (3.45) is related by the transfer function L_f (i.e. the achieved open-loop transfer function L_f of the nominal plant at the input point)

$$L_f(s) = C_f(s)C\Phi B = K_c\left(\Phi^{-1} + K_f C\right)^{-1} K_f C\Phi B \tag{3.47}$$

However, if full state feedback is indeed available, the corresponding robust

reliable LQR achieved open-loop transfer function L_c would be

$$L_c(s) = K_c \Phi B \tag{3.48}$$

The difference between (3.47) and (3.48) is defined as the recovery error

$$E_r(s) = L_c(s) - L_f(s) \tag{3.49}$$

and the objective of the full-order CSS architecture based control is to design K_f such that $E_r(s) \to 0$. Chen et al (1991) has shown that (3.49) can be simplified to

$$E_r(s) = K_c\left(\Phi^{-1} + K_f C\right)^{-1} B \tag{3.50}$$

Based on (3.50), an auxiliary system can be created, described by

$$\sum_{aux}: \begin{cases} \dot{\tilde{x}} = A^T \tilde{x} + C^T \tilde{u} + {k_c}^T \tilde{w} \\ \tilde{y} = \tilde{x} \\ \tilde{z} = B^T \tilde{x} \\ \tilde{u} = -{K_f}^T \tilde{x} \end{cases} \tag{3.51}$$

which has the closed-loop transfer function from $\tilde{w}$ to $\tilde{z}$

$$T_{\tilde{z}\tilde{w}} = B^T (\Phi^{-T} + C^T {K_f}^T)^{-1} {K_c}^T = {E_r}^T(s) \tag{3.52}$$

Since $\|E_r(s)\|_{(.)} = \left\|{E_r}^T(s)\right\|_{(.)}$, any *H*-control method (Chen, 2000) can be employed to design K_f such that the desired *H*-norm of $T_{\tilde{z}\tilde{w}}$, and hence E_r is

minimized.

3.5 Computational implementation

Calculation of the robust reliable control gain and implementation follow the flowchart shown in Fig. 3.1. For pre-processing, MATLAB™ is used to compute all structural data, state-space model and control gains. SIMULINK™ is used to numerically simulate the controlled system under earthquake excitation. For post-processing, MATLAB is used to process and plot all output responses and controls.

3.6 Numerical illustration

3.6.1 2DOF uncertain system

A numerical example of a 2-DOF system under scaled El Centro earthquake to 0.1g (Fig. 2.2) is used to illustrate the effectiveness of the robust reliable optimal control as opposed to central nominal full state-feedback LQR control and decentralised nominal saturation control of Chapter 2. Consider the same 2-DOF system with two actuators, but with allowable uncertainties below in state-space:

$$\begin{pmatrix} \dot{x}_1 \\ \dot{x}_2 \\ \ddot{x}_1 \\ \ddot{x}_2 \end{pmatrix} = \begin{pmatrix} 1 & 0 & 0 & 0 \\ 0 & 1 & 0 & 0 \\ 0 & 0 & 1+\alpha_A & 0 \\ 0 & 0 & 0 & 1+\alpha_A \end{pmatrix} \begin{pmatrix} 0 & 0 & 1 & 0 \\ 0 & 0 & 0 & 1 \\ -315.84 & 157.92 & -2.5134 & 1.2567 \\ 157.92 & -157.92 & 1.2567 & -1.2567 \end{pmatrix} \begin{pmatrix} x_1 \\ x_2 \\ \dot{x}_1 \\ \dot{x}_2 \end{pmatrix}$$

$$+ \alpha_B \begin{pmatrix} 0 & 0 \\ 0 & 0 \\ 1 & 0 \\ 0 & 1 \end{pmatrix} \begin{pmatrix} u_1 \\ u_2 \end{pmatrix} + \begin{pmatrix} 0 \\ 0 \\ -1 \\ -1 \end{pmatrix} \ddot{x}_g + v(t)$$

$$\begin{pmatrix} y_1 \\ y_2 \end{pmatrix} = \alpha_c \begin{pmatrix} -315.84 & 157.92 & -2.5134 & 1.2567 \\ 157.92 & -157.92 & 1.2567 & -1.2567 \end{pmatrix} \begin{pmatrix} x_1 \\ x_2 \\ \dot{x}_1 \\ \dot{x}_2 \end{pmatrix} + w(t)$$

where parameters $\alpha_A \in [-0.1, 0.1]$, $\alpha_B \in [-1, 1]$ and $\alpha_C \in [-1, 1]$ are used to specify

uncertainties. System is nominal when $\alpha_A = 0$, $\alpha_B = 1$ and $\alpha_C = 1$. Assume that $u_F{}^T = (0 \quad 0)$. The nominal central LQR and decentralised nominal saturation controllers parameters are provided in section 2.6.1.

For $\alpha_A = -0.1$, $\alpha_B = 0.5$ and $\alpha_C = 0.9$, the central robust reliable optimal controller parameters are $\alpha = 0.5$, $\beta = 1$, $\delta = 0.01$, $\delta_c = \delta_h = 0$, $\varepsilon_1 = \varepsilon_2 = \varepsilon_3 = 10^{-2}$, $\varepsilon = 10^{-5}$, $Q = 0.01I$ and $B_\Omega = B_\omega = 0.5B$. From (3.15) and (3.27), the robust reliable control gains are $K_c = \begin{pmatrix} 416020 & -205630 & 3430 & -1640 \\ -212090 & 220080 & -1690 & 1880 \end{pmatrix}$; and using section 3.4, LTR gains are $K_f = \begin{pmatrix} -1 & -1 & -99999 & 0 \\ -1 & -2 & 0 & -99999 \end{pmatrix}^T$.

The controlled responses using central LQR, decentralised nominal controls (Decen-n) and robust reliable optimal controls (rrLQR) are shown in Figs. 3.2-3.3 for the nominal 2DOF global system as well as in Figs. 3.4-3.5 for the uncertain 2DOF global system, inclusive of uncontrolled responses. Tables 3.1 and 3.2 show the maximum absolute peak responses of the nominal and uncertain 2DOF systems respectively under central full state-feedback (LQR) controls, decentralised nominal controls and robust reliable optimal controls. Under global central LQR control, the controlled responses and controls are suitably mitigated, as shown in columns (2) and (5) for subsystems 1 and 2 respectively. The LQR controls for uncertain system is double that of the nominal system due to half actuator failure for linear state feedback.

With nominal decentralised saturation controls, as shown in columns (3) and (6), the controlled responses are consistently better than that of the central LQR controls for both nominal and uncertain systems. With robust reliable optimal controls, as shown in columns (4) and (7), the controlled responses are consistently better than both central LQR control and decentralized nominal saturation controls for

both nominal and uncertain systems. Better control performance is achieved for nominal system with lesser uncertainties and actuator failures. The controlled absolute accelerations are comparable for all controls due to the emphasis on acceleration control of the regulated outputs.

3.6.2 20DOF uncertain system

Consider the same 2DOF ROM for the 20DOF shear-structural building model in section 2.6.2, but with allowable uncertainties below in state-space:

$$\begin{pmatrix}\dot{x}_1\\ \dot{x}_2\\ \ddot{x}_1\\ \ddot{x}_2\end{pmatrix}=\begin{pmatrix}1 & 0 & 0 & 0\\ 0 & 1 & 0 & 0\\ 0 & 0 & 1+\alpha_A & 0\\ 0 & 0 & 0 & 1+\alpha_A\end{pmatrix}\begin{pmatrix}0 & 0 & 1 & 0\\ 0 & 0 & 0 & 1\\ -7.2980 & 2.7761 & -0.0730 & 0.0278\\ 2.7761 & -62.8417 & 0.0278 & -0.6284\end{pmatrix}\begin{pmatrix}x_1\\ x_2\\ \dot{x}_1\\ \dot{x}_2\end{pmatrix}$$
$$+\alpha_B\begin{pmatrix}0 & 0\\ 0 & 0\\ -12.1596 & -8.9808\\ 53.0676 & -27.8441\end{pmatrix}\begin{pmatrix}u_1\\ u_2\end{pmatrix}+\begin{pmatrix}0\\ 0\\ 4022\\ -1530\end{pmatrix}\ddot{x}_g+v(t)$$

$$\begin{pmatrix}y_1\\ y_2\end{pmatrix}=\alpha_c\begin{pmatrix}-7.2980 & 2.7761 & -0.0730 & 0.0278\\ 2.7761 & -62.8417 & 0.0278 & -0.6284\end{pmatrix}\begin{pmatrix}x_1\\ x_2\\ \dot{x}_1\\ \dot{x}_2\end{pmatrix}+w(t)$$

Using the same uncertainty settings and controller parameters as section 3.6.1, and from (3.15) and (3.27), the robust reliable control gains are $K_c=\begin{pmatrix}-493000 & 22682000 & -5000 & 227000\\ -3815000 & -11930000 & -38000 & -119000\end{pmatrix}$; and using section 3.4, LTR gains are $K_f=\begin{pmatrix}-15 & -1 & -694410 & 136370\\ -1 & -2 & 298450 & -2993300\end{pmatrix}^T$.

The controlled responses using central LQR, decentralised nominal controls (Decen-n) and robust reliable optimal controls (rrLQR) are shown in Figs. 3.6-3.7 for the nominal 20DOF global system as well as in Figs. 3.8-3.9 for the uncertain 20DOF

global system, inclusive of uncontrolled responses. Tables 3.3 and 3.4 show the maximum absolute peak responses for the 10^{th} and 20^{th} DOFs of the nominal and uncertain 20DOF systems respectively under central full state-feedback (LQR) controls, decentralised nominal controls and robust reliable optimal controls. The uncontrolled responses of the 20DOF system is shown in Table 2.2. Under global central LQR control, the controlled responses and controls are suitably mitigated, as shown in columns (2) and (5) for 10^{th} and 20^{th} DOF respectively.

With nominal decentralised saturation controls, as shown in columns (3) and (6), the controlled responses are consistently better that of the central LQR controls. With robust reliable optimal controls, as shown in columns (4) and (7), the controlled responses are consistently better than both central LQR control and decentralized nominal saturation controls for both nominal and uncertain systems. Better control performance is achieved for nominal system with lesser uncertainties and actuator failures.

The results show that for both nominal and uncertain systems with and without Ritz model reduction, robust reliable optimal controls perform much better than both central nominal LQR as well as nominal decentralised controls. In addition, robust reliable optimal control performs better under the nominal system than under the uncertain system, when system uncertainties and/or device failures do occur. Robust reliable control system always outperforms nominal central and decentralised control systems, hence illustrating that superior control performance is achieved at the expense of greater controller design & implementation complexity. This agrees with the findings of Wang et al (2001) that robust control performs better than nominal controls when uncertainties do occur.

Table 3.1: Peak Responses and Controls for Nominal 2DOF System

Cases (1)	Subsystem 1			Subsystem 2		
	LQR (2)	Decen-n (3)	rrLQR (4)	LQR (5)	Decen-n (6)	rrLQR (7)
Drift (cm)	0.01	0.01	0.0007	0.005	0.005	0.0003
Drift vel. (cm/s)	0.34	0.34	0.03	0.2	0.15	0.015
Abs. acc. (cm/s^2)	85.71	85.71	85.50	85.83	86.37	85.49
Control (V)	0.8489	0.8489	0.8541	0.8500	0.8556	0.8544

Table 3.2: Peak Responses and Controls for Uncertain 2DOF System

Cases (1)	Subsystem 1			Subsystem 2		
	LQR (2)	Decen-n (3)	rrLQR (4)	LQR (5)	Decen-n (6)	rrLQR (7)
Drift (cm)	0.02	0.02	0.001	0.01	0.01	0.0007
Drift vel. (cm/s)	0.75	0.73	0.07	0.40	0.35	0.04
Abs. acc. (cm/s^2)	86.02	86.13	85.46	86.51	86.93	85.62
Control (V)	1.6903	1.6896	1.7069	1.7055	1.7064	1.7104

Table 3.3: Peak Responses for Nominal 20DOF System

Cases (1)	10^{th} DOF			20^{th} DOF		
	LQR (2)	Decen-n (3)	rrLQR (4)	LQR (5)	Decen-n (6)	rrLQR (7)
Drift (cm)	0.007	0.003	0.000001	0.004	0.004	0.0000005
Drift vel. (cm/s)	0.27	0.12	0.00006	0.17	0.18	0.00002
Abs. acc. (cm/s^2)	85.49	85.48	85.38	86.08	85.67	85.38

Table 3.4: Peak Responses for Uncertain 20DOF System

Cases (1)	10^{th} DOF			20^{th} DOF		
	LQR (2)	Decen-n (3)	rrLQR (4)	LQR (5)	Decen-n (6)	rrLQR (7)
Drift (cm)	0.01	0.007	0.000003	0.008	0.009	0.000001
Drift vel. (cm/s)	0.52	0.27	0.0001	0.33	0.41	0.00005
Abs. acc. (cm/s^2)	85.58	85.82	85.46	86.62	85.68	85.48

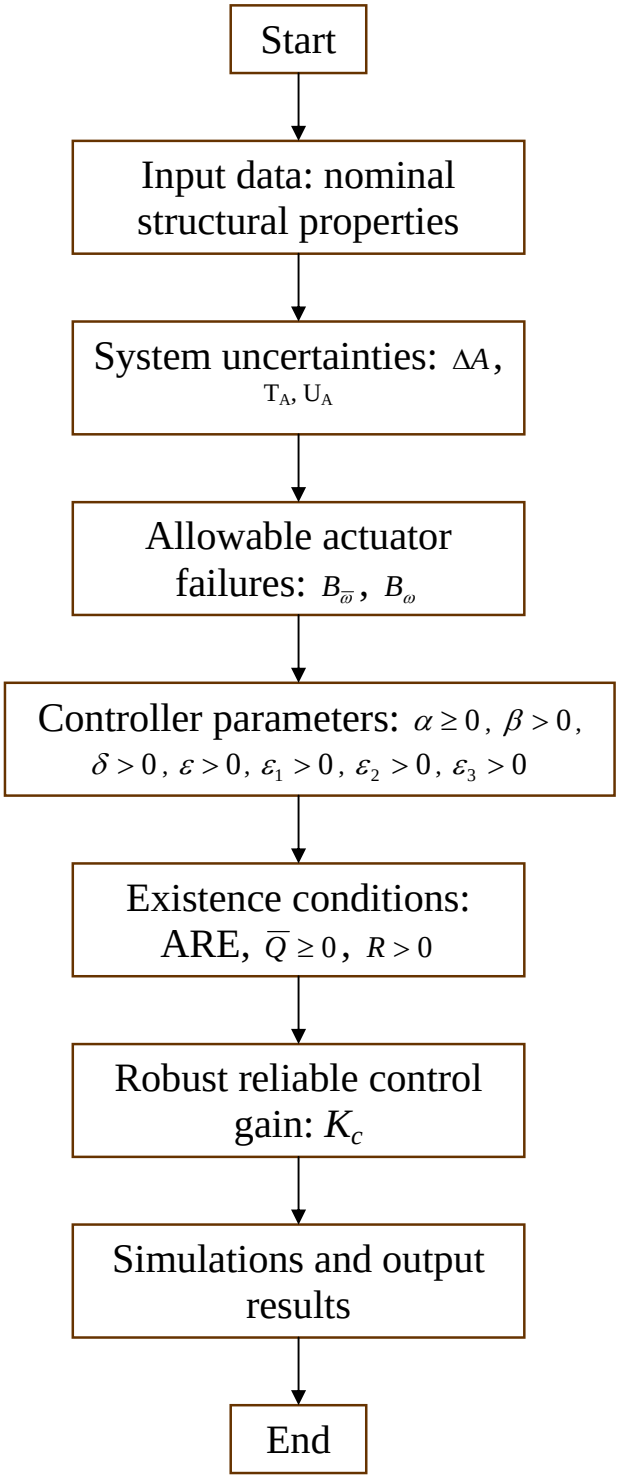

Figure 3.1: Flowchart for Robust Reliable Control Gain Calculation

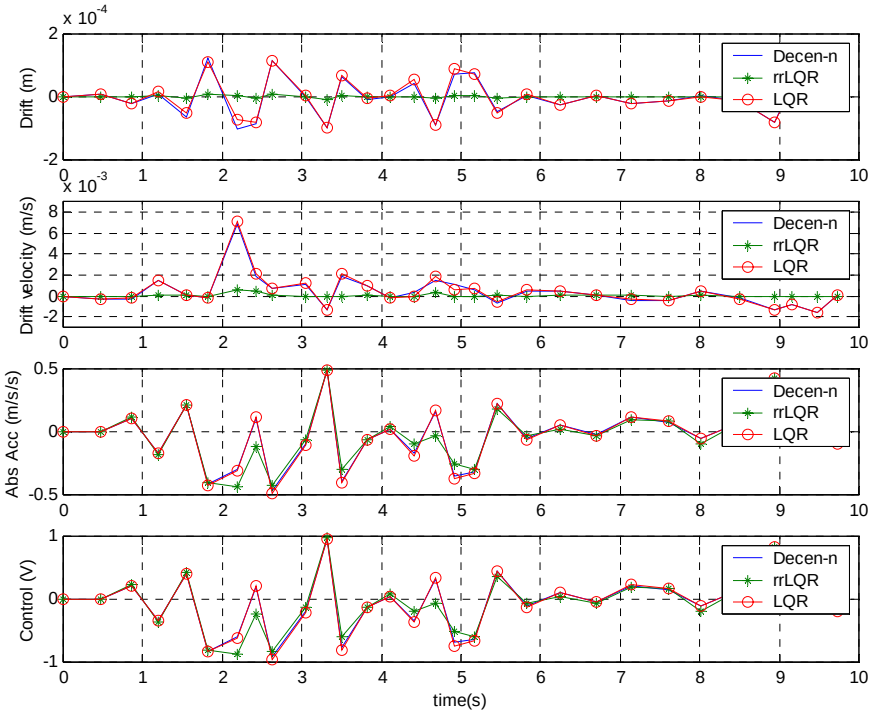

Figure 3.2: Subsystem 1 responses and controls for nominal 2DOF system

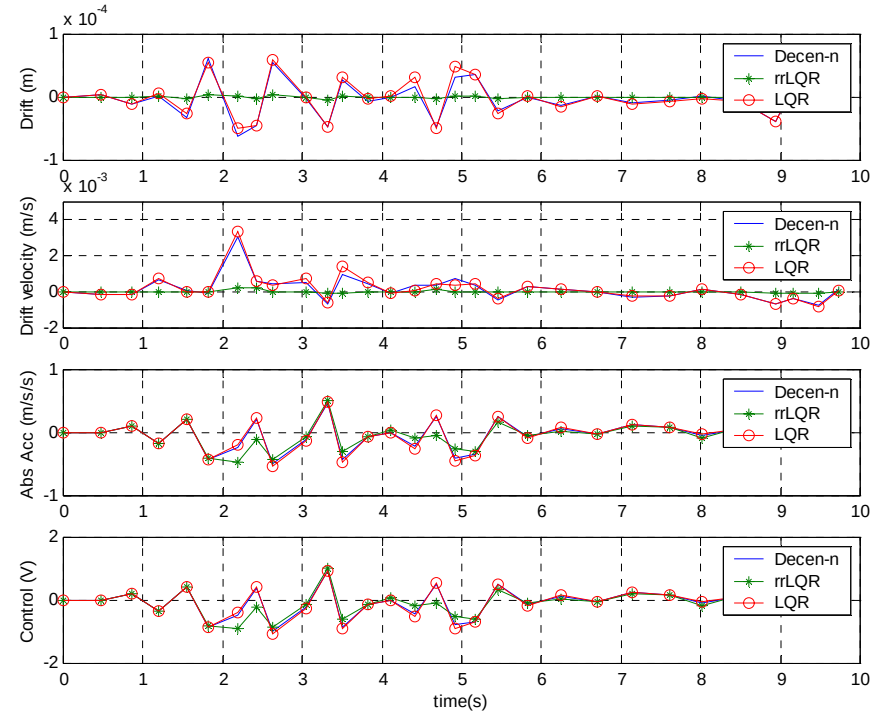

Figure 3.3: Subsystem 2 responses and controls for nominal 2DOF system

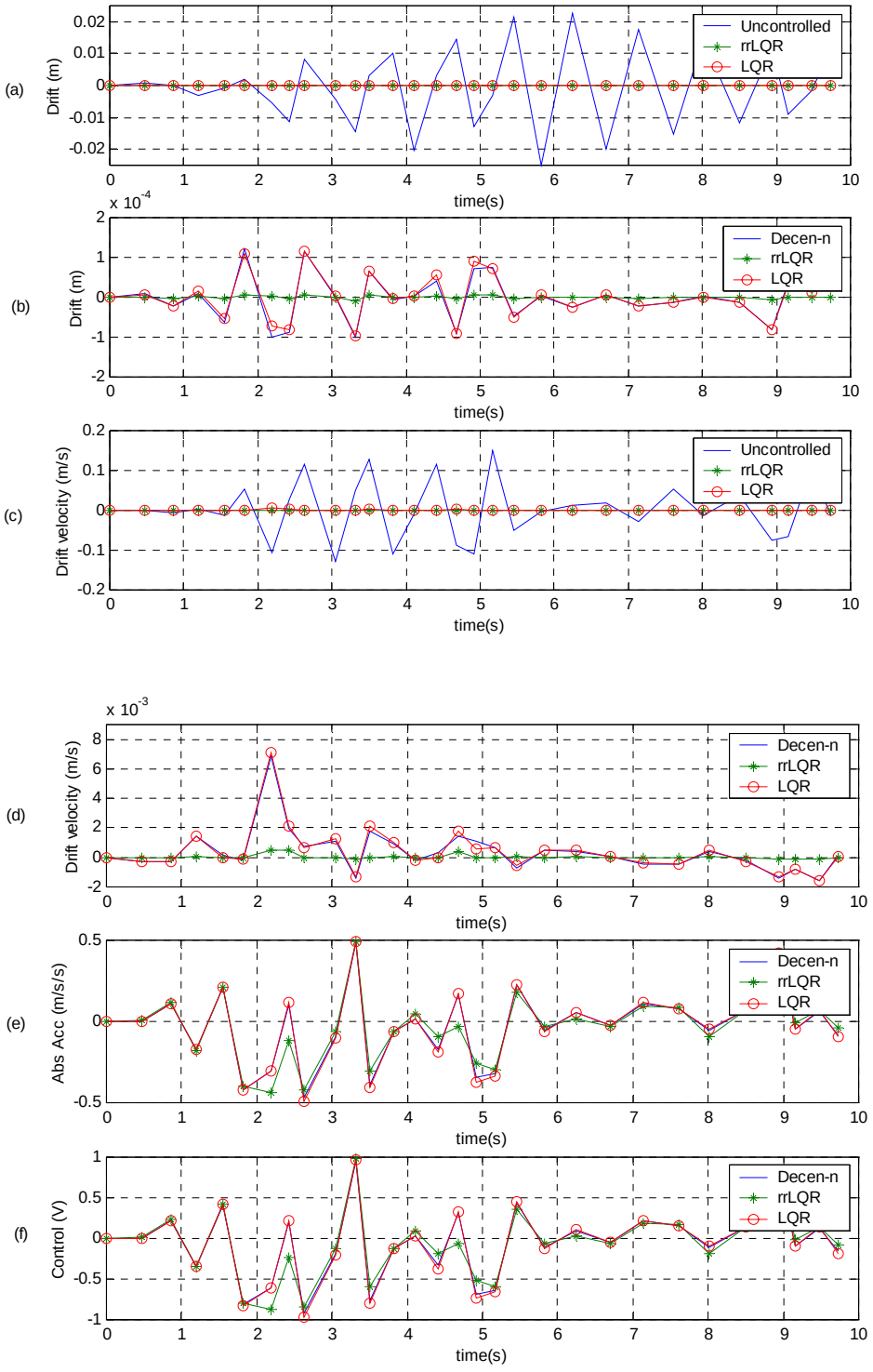

Figure 3.4: Comparisons of subsystem 1 responses under central LQR and decentralised nominal controls and robust reliable optimal controls for uncertain 2DOF system – (a) drifts including uncontrolled drifts; (b) controlled drifts; (c) velocity drifts including uncontrolled; (d) controlled velocity drifts; (e) absolute acceleration; (f) controls

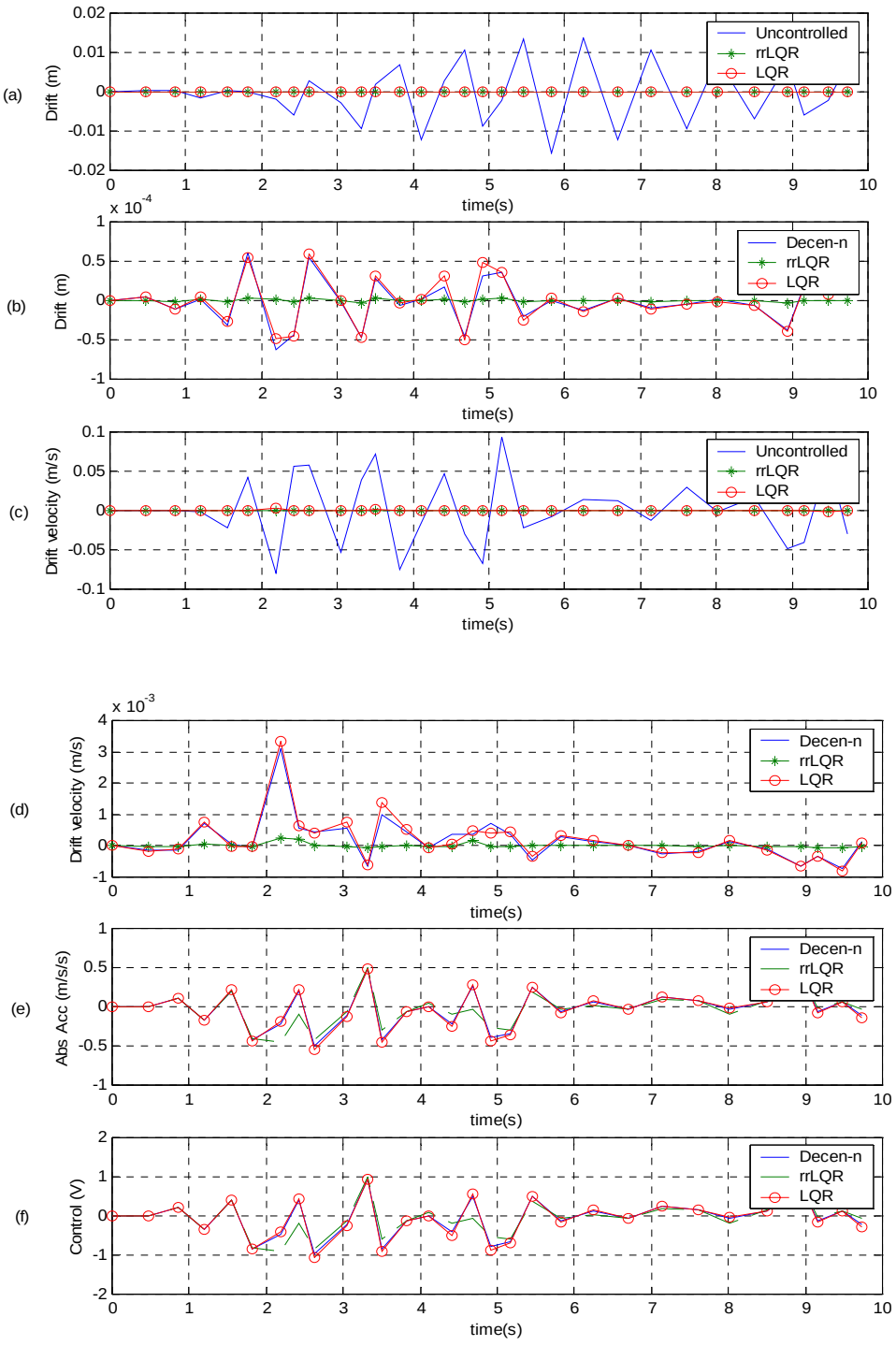

Figure 3.5: Comparisons of subsystem 2 responses under central LQR and decentralised nominal controls and robust reliable optimal controls for uncertain 2DOF system – (a) drifts including uncontrolled drifts; (b) controlled drifts; (c) velocity drifts including uncontrolled; (d) controlled velocity drifts; (e) absolute acceleration; (f) controls

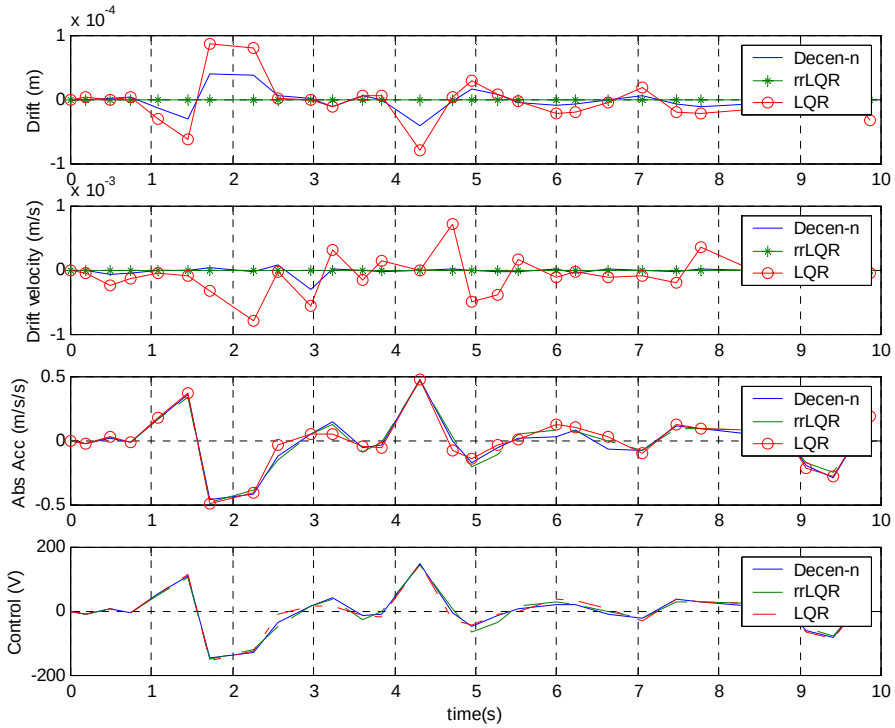

Figure 3.6: Responses and controls for 10th DOF of nominal 20DOF system

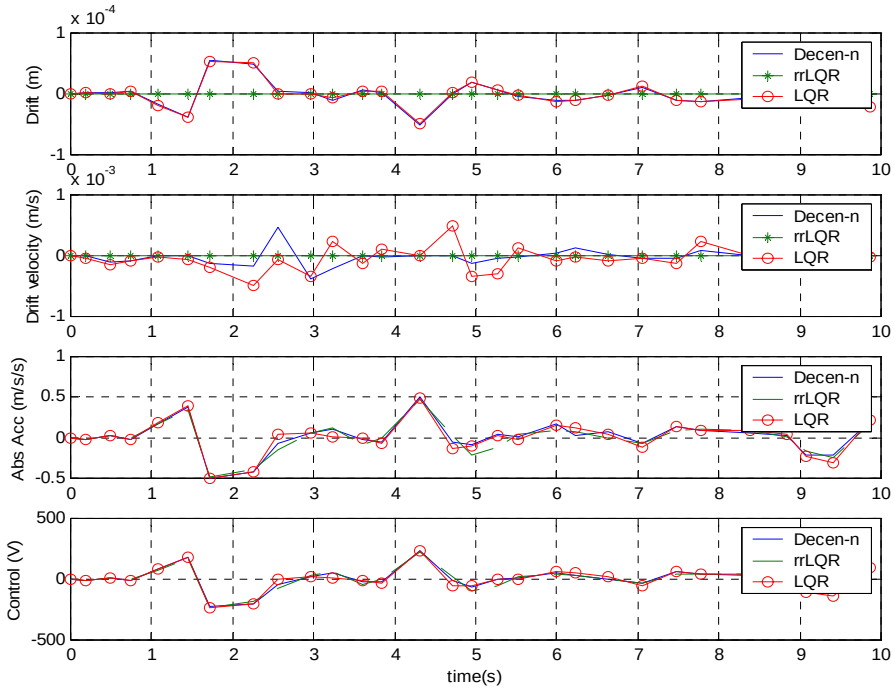

Figure 3.7: Responses and controls for 20th DOF of nominal 20DOF system

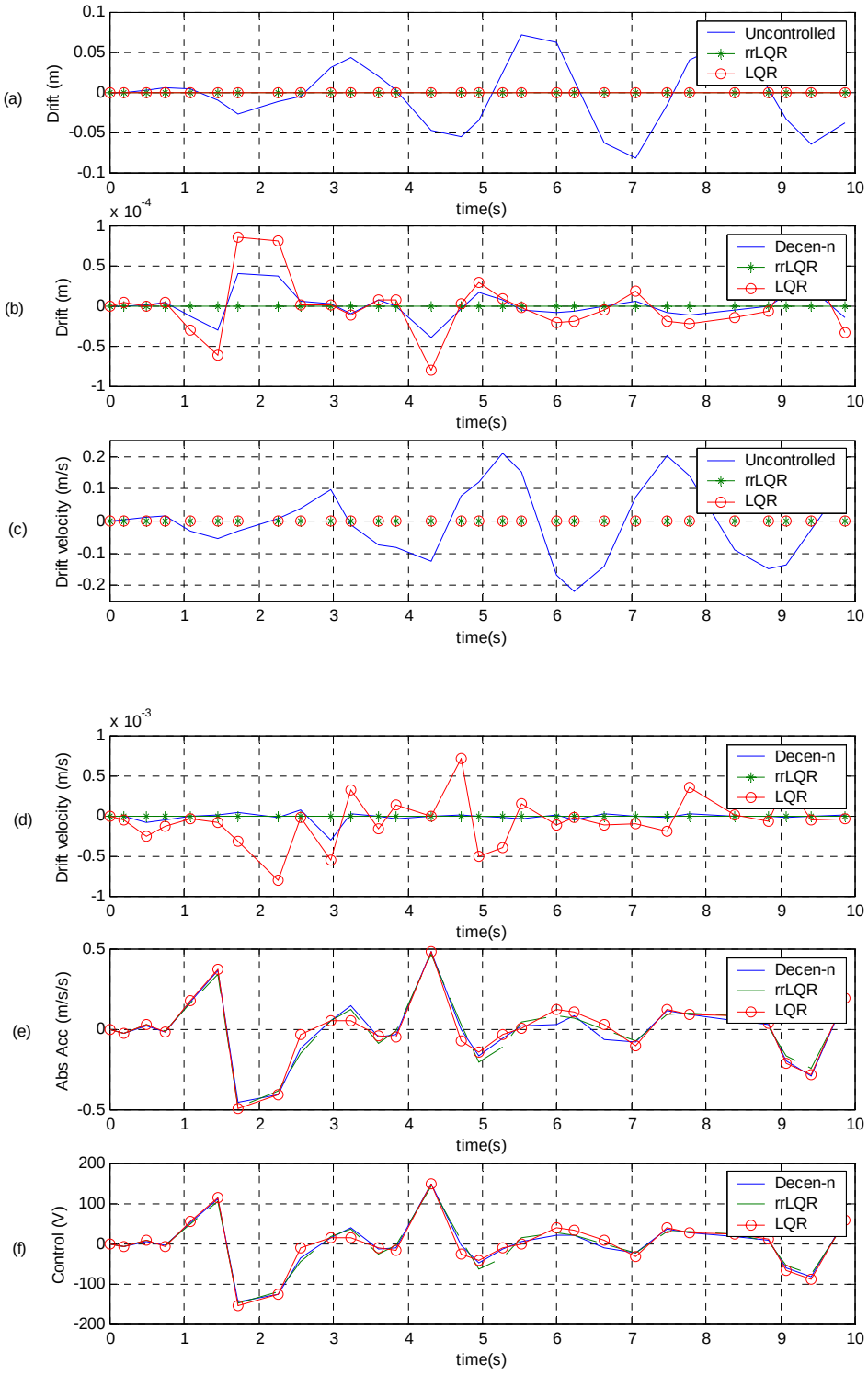

Figure 3.8: Comparisons of responses for 10th DOF of uncertain 20DOF system under central LQR and decentralised nominal controls and robust reliable optimal controls – (a) drifts including uncontrolled drifts; (b) controlled drifts; (c) velocity drifts including uncontrolled; (d) controlled velocity drifts; (e) absolute acceleration; (f) controls

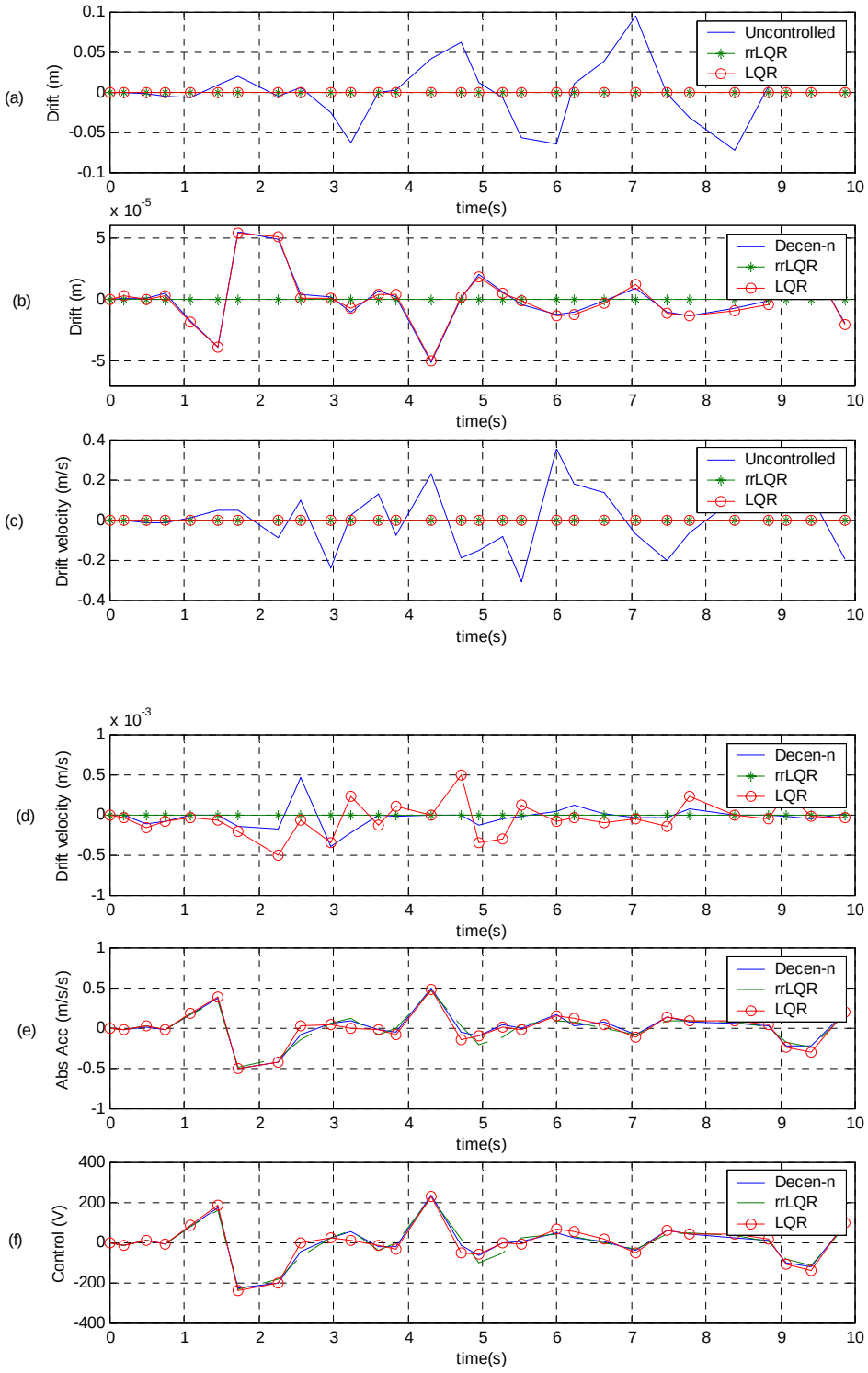

Figure 3.9: Comparisons of responses for 20th DOF of uncertain 20DOF system under central LQR and decentralised nominal controls and robust reliable optimal controls – (a) drifts including uncontrolled drifts; (b) controlled drifts; (c) velocity drifts including uncontrolled; (d) controlled velocity drifts; (e) absolute acceleration; (f) controls

CHAPTER 4

DECENTRALISED ROBUST RELIABLE CONTROL

4.1 Introduction

The previous chapters present the solutions for the decentralised nominal saturation control and the central robust reliable optimal control for corrupted partial feedback systems. In this chapter, the decentralised robust reliable saturation controller is proposed for linear uncertain systems under seismic excitation. By combining the decentralisation methodology with the robust reliable optimal control, the decentralised controllers use only local information for independent local robust reliable control of uncertain subsystems.

As in the previous chapters, full state feedback is considered. Firstly, the system uncertainties are decomposed. Using closed-loop state-space Riccati-based control approach, the full state-feedback gain is derived from the solution of the formulated ARE. The decentralised full state feedback gain is formulated to be robust against both structured and unstructured norm-bounded uncertainties as well as reliable against actuator failures confined to a predefined subset. Secondly, the effects of subsystem inter-coupling and nonlinear stiffness are attenuated by employing saturation control formulated using Lyapunov equation. Finally, to account for noise-corrupted partial state feedback, observer-based robust reliable control is implemented using the separation principle. For illustration, the decentralised controls of both nominal and uncertain 2-DOF systems are presented.

4.2 Control Problem Formulation

4.2.1 Analytical Model with Uncertainties

Consider an *n*-degree-of-freedom building subjected to one-dimensional horizontal earthquake ground acceleration $\ddot{x}_g(t)$. By modifying (2.1), the global uncertain dynamic equation of motion inclusive of all uncertainties, perturbations and disturbances can be derived using extended Hamilton's variational principle (Meirovitch, 2000) as:

$$M_s\ddot{\xi}(t)+(C_s+\Delta C_s)\dot{\xi}(t)+(K_s+\Delta K_s)\xi(t)+K_n[V(t)]=(F_c+\Delta F_c)U(t)-M_s l\ddot{x}_g(t) \quad (4.1)$$

where $\xi(t)\in\Re^n$ is the global displacement vector; $U(t)\in\Re^m$ is the nominal control voltage vectors to *m* groups of actuators; $M_s\in\Re^{nxn}$ is the global consistent mass matrix; $C_s\in\Re^{nxn}$ and $\Delta C_s\in\Re^{nxn}$ are the global nominal and uncertain linear viscous damping matrices; $K_s\in\Re^{nxn}$ and $\Delta K_s\in\Re^{nxn}$ are the global nominal and uncertain linear elastic stiffness matrices; $K_n[V(t)]\in\Re^n$ is the global nonlinear *n*-vector stiffness force that is assumed to be a function of *V(t)*, which is a function of the system responses with bounded coefficients; $F_c = p_c l_c$ and $\Delta F_c = p_c \Delta l_c$ are the global nominal and uncertain control force distribution matrices, where $p_c\in\Re^{nxm}$ is the global actuation force distribution vector, $l_c\in\Re^{mxm}$ and $\Delta l_c\in\Re^{mxm}$ are the global nominal and uncertain actuation force per unit voltage transformation matrices; and $l\in\Re^n$ is the global earthquake excitation influence vector.

It is assumed (**assumption 6**) that the uncertainties have known bounds; that is, $(C_s+\Delta C_s)\in[C_s^-, C_s^+]$, $(K_s+\Delta K_s)\in[K_s^-, K_s^+]$, $(F_c+\Delta F_c)\in[F_c^-, F_c^+]$ and

$U \in \left[U^-, U^+\right]$ where C_s^-, C_s^+, K_s^-, K_s^+, F_c^-, F_c^+, U^- and U^+ are known quantities.

4.2.2 Reduced-order State-Space Modelling

Under assumption 1, the global uncertain FOM can be model-reduced to make the problem tractable and for efficient design of *U(t)*. Model reduction using load-dependent Ritz vectors with Gram-Schmidt orthogonalisation (Chopra 2000, Krsyl et al 2001, Appendix: Robust Model Reduction) is performed to derive a detectable and stabilisable reduced-order model (ROM) with respect to known sensor and actuator locations.

Using both uncertain and nominal matrices of (4.1), the following Ritz vector transformation (Sestieri, 2000) is derived:

$$\xi = \Psi_u q \tag{4.2}$$

where $\Psi_u \in \Re^{nxr}$ is the Ritz vector transformation matrix of the uncertain FOM; $q \in \Re^r$ is the ROM global displacement vector corresponding to the desired master degrees of freedom for stabilisability and detectability.

Substituting (4.2) into (4.1), ROM is given by:

$$\begin{aligned} &M_r \ddot{q}(t) + \left(C_r + \Delta C_r\right)\dot{q}(t) + \left(K_r + \Delta K_r\right)q(t) + \Psi^T K_n\left[V(t)\right] \\ &= \Psi^T \left(F_c + \Delta F_c\right)U(t) - \Psi^T M_s l \ddot{x}_g(t) \end{aligned} \tag{4.3}$$

where the reduced-order matrices are $M_r = \Psi_u{}^T M_s \Psi_u$, $C_r = \Psi_u{}^T C_s \Psi_u$, $\Delta C_r = \Psi_u{}^T \Delta C_s \Psi_u$, $K_r = \Psi_u{}^T K_s \Psi_u$ and $\Delta K_r = \Psi_u{}^T \Delta K_s \Psi_u$.

In the state space, (4.3) becomes a class of uncertain systems with the following form:

$$\begin{aligned} \dot{X}(t) &= (A+\Delta A)X(t) + (B+\Delta B)U(t) + X_n(t) + H\ddot{x}_g(t), \\ Y(t) &= (C+\Delta C)X(t) + \eta(t), \\ Z(t) &= (C+\Delta C)X(t) \end{aligned} \tag{4.4}$$

where ROM global state vector is $X(t) = \begin{pmatrix} q \\ \dot{q} \end{pmatrix} \in \Re^{2r}$, input vector is $U(t) = [u_1,...,u_m]^T \in \Re^m$, measured output is $Y(t) \in \Re^m$ and controlled/regulated output is $Z(t) \in \Re^m$; $X_n(t) = \begin{pmatrix} 0 \\ -M_r^{-1}\Psi_u^T K_n[V(t)] \end{pmatrix}$ is the ROM global nonlinear stiffness component; $A = \begin{pmatrix} 0 & I \\ -M_r^{-1}K_r & -M_r^{-1}C_r \end{pmatrix} \in \Re^{2rx2r}$, $B = \begin{pmatrix} 0 \\ M_r^{-1}\Psi_u^T F_c \end{pmatrix} \in \Re^{2rxm}$, $C = \begin{pmatrix} -M_r^{-1}K_r & -M_r^{-1}C_r \end{pmatrix} \in \Re^{mx2r}$ and $H = \begin{pmatrix} 0 \\ -M_r^{-1}\Psi_u^T M_s l \end{pmatrix} \in \Re^{2r}$ are constant nominal system matrices; $\Delta A = \begin{pmatrix} 0 & 0 \\ -M_r^{-1}\Delta K_r & -M_r^{-1}\Delta C_r \end{pmatrix} \in \Re^{2rx2r}$, $\Delta B = \begin{pmatrix} 0 \\ M_r^{-1}\Psi_u^T \Delta F_c \end{pmatrix} \in \Re^{2rxm}$ and $\Delta C = \begin{pmatrix} -M_r^{-1}\Delta K_r & -M_r^{-1}\Delta C_r \end{pmatrix} \in \Re^{mx2r}$ are uncertain system matrices; $\eta(t) \in \Re^m$ are independent white noises. Structured uncertainties for the system and the input are ΔA and ΔB respectively. Norm-bounded unstructured uncertainty for the sensor measurement is ΔC, where $0 \le \|\Delta C\|_2 \le \delta_c$.

Fix two mutually exclusive groups of actuators, where one set of predefined actuators susceptible to failures is denoted by $\Omega \subseteq \{1,...,m\}$ and the other set of

actuators that never fail is denoted by $\overline{\Omega} = \{1,...,m\} - \Omega$. Then the following decomposition (Seo and Kim 1996) can be performed (**assumption 7**):

$$B + \Delta B = B_{\Omega} + B_{\overline{\Omega}} \tag{4.5}$$

where $B_{\Omega} \in \Re^{2nxm}$ and $B_{\overline{\Omega}} \in \Re^{2nxm}$ are formed from B by zeroing out columns corresponding to Ω and $\overline{\Omega}$ respectively. Then using (4.5), define $B_{\overline{\omega}} : B_{\overline{\Omega}} \le B_{\overline{\omega}} \le B$ and $B_{\omega} : 0 \le B_{\omega} \le B_{\Omega}$ such that $B_{\omega} + B_{\overline{\omega}} = B + \Delta B$, where $\overline{\omega}$ is the set of actuators that are still working and satisfies $\overline{\Omega} \subseteq \overline{\omega} \subseteq \{1,...,m\}$; ω is the set of actuators that actually fails and satisfies $\omega \subseteq \Omega$. Note that actuator failures can be either partial failures if the actuator(s) or group(s) of actuators are operating at less than full working capacity; or total failures if the actuator(s) or group(s) of actuators are not working at all.

It is also assumed that $(A, B_{\overline{\Omega}})$ is stabilisable (**assumption 8**).

4.2.3 Uncertain Subsystem Model

Decompose the global state space model (4.4) completely into N_s ($N_s \le r \le m$) coupled subsystems:

$$\begin{aligned}
\dot{x}_i(t) &= (A_{ii} + \Delta A_{ii})x_i(t) + (b_i + \Delta b_i)u_{2i}(t) + h_i \ddot{x}_g(t) + \sum_{j=1, j\neq i}^{N_s} (A_{ij} + \Delta A_{ij})x_j(t) + x_{ni}(t), \\
y_i(t) &= (C_{ii} + \Delta C_{ii})x_i(t) + \sum_{j=1, j\neq i}^{N_s} (C_{ij} + \Delta C_{ij})x_j(t) + \eta_i(t), \\
z_i(t) &= (C_{ii} + \Delta C_{ii})x_i(t) + \sum_{j=1, j\neq i}^{N_s} (C_{ij} + \Delta C_{ij})x_j(t)
\end{aligned} \tag{4.6}$$

where $x_i(t)$ is the ith subsystem state, $u_{2i}(t)$ is subsystem control voltage, $x_{ni}(t)$ is the subsystem nonlinear stiffness component; y_i is noise-corrupted subsystem measurement output; z_i is subsystem controlled or regulated output; A_{ij} and C_{ij} are the nominal system, measurement and regulated output inter-coupling between subsystems i and j, $\forall i \neq j$ $(i, j = 1,..., N_s)$; b_i is the nominal subsystem control input matrices; h_i is the subsystem excitation input matrix; the subsystem uncertainties ΔA_{ii}, ΔA_{ij}, Δb_i, ΔC_{ii}, ΔC_{ij} are bounded as described in assumption 6.

The control task is to determine the uncertain (denoted in this thesis as layer 2) subsystem feedback control $u_{2i}(t)$ such that the closed-loop subsystem for (4.6) with admissible uncertainties and allowable actuator failures (4.5) provides relative asymptotic stability with robust reliable decentralised H_∞-norm disturbance rejection and H_2-optimality with saturation control.

4.3 Decentralised Robust Reliable Control for Uncertain Subsystem Model

Using the decentralised control methodology (Magana and Rodellar 1998), let the decentralised nominal controller take the following form:

$$u_{2i}(t) = \hat{u}_{2i}(t) + \bar{u}_{2i}(t) \tag{4.7}$$

where $\hat{u}_{2i}(t) = -k_{2i} x_i(t)$ is the optimal regulation control for the undisturbed subsystem, k_{2i} is the static robust reliable state feedback control gain of subsystem i in uncertain layer *2* and $\bar{u}_{2i}$ is the augmented saturation subsystem control.

4.3.1 Decentralised Robust Reliable Control Problem

From (4.6), define the following subsystem *i* that is ground-excited, but without inter-coupling and nonlinear stiffness as follows:

$$\begin{aligned} \dot{x}_i(t) &= (A_{ii} + \Delta A_{ii})x_i(t) + (b_i + \Delta b_i)\hat{u}_{2i}(t) + h_i \ddot{x}_g(t), \\ y_i(t) &= x_i(t), \\ z_i(t) &= (C_{ii} + \Delta C_{ii})x_i(t) \end{aligned} \tag{4.8}$$

where admissible subsystem actuator failure(s) can be derived with (4.5) to give relevant subsystem control location matrices: $b_{\Omega i}$, $b_{\overline{\Omega} i}$, $b_{\omega i}$ and $b_{\overline{\omega} i}$; $(A_{ii}, b_{\overline{\omega} i})$ is stabilisable, as implied under assumption 8. Following Khargoneka et al (1990), the admissible bounded uncertainties ΔA_{ii} can be decomposed as follows:

$$\Delta A_{ii} = D_i F_i(t) E_i \tag{4.9}$$

where D_i, E_i are known real constant matrices with $F_i(t)$ is a bounded uncertain matrix with Lebesgue measurable elements such that $F_i(t)^T F_i(t) \le I$.

Assume the following linear full state-feedback control law for (4.8):

$$\hat{u}_{2i}(t) = -k_{2i} x_i(t) \tag{4.10}$$

then the closed-loop system for (4.8) can be written as:

$$\begin{aligned} \dot{x}_i(t) &= A_{ci} x_i(t) + B_{ci} w_{Fi}(t), \\ y_i(t) &= x_i(t), \\ z_i(t) &= C_{ci} x_i(t) \end{aligned} \tag{4.11}$$

where $A_{ci} = A_{ii} + \Delta A_{ii} - b_{\bar{\omega}i} k_{2i}$, $B_{ci} = \begin{pmatrix} h_i & b_{\omega i} \end{pmatrix}$, $C_{ci} = C_{ii} + \Delta C_{ii}$, $w_{Fi} = \begin{pmatrix} \ddot{x}_g{}^T & u_{Fi}^T \end{pmatrix}^T$, in which $w_{Fi}(t) \in \Re^{d+m}$ is the augmented subsystem excitation vector and $u_{Fi}(t) \in \Re^m$ is the subsystem input vector with elements corresponding to working actuators being zero.

The objective is to design a linear state feedback control law (4.10) for the closed-loop system (4.11), such that despite the presence of admissible uncertainties and allowable actuator failures, the controller provides (a) robust α_i-degree subsystem relative asymptotic stability, that is,

$$\mathrm{Re}\{\lambda(A_{ci})\} < -\alpha_i < 0 \tag{4.12}$$

(b) robust subsystem augmented disturbance transmission that is H_∞–norm bounded within a prescribed level δ:

$$\left\| T_{z_i w_{Fi}} \right\|_\infty = \left\| C_{ci} \left(sI - A_{ci} \right)^{-1} B_{ci} \right\|_\infty \le \delta \tag{4.13}$$

and (c) H_2-optimal by minimizing the subsystem performance index:

$$J_{2i} = \int_0^\infty \left[x_i{}^T \tilde{Q}_{2i} x_i + \hat{u}_{2i}{}^T \tilde{R}_{2i} \hat{u}_{2i} \right] dt \tag{4.14}$$

where $\tilde{Q}_{2i} : \tilde{Q}_{2i} \ge 0$ is symmetric and semi-positive definite and $\tilde{R}_{2i} : \tilde{R}_{2i} > 0$ is s.p.d. Note that (4.13) implies that the control output is quadratically stable (Seo and Kim, 1996) despite actuator failures, i.e.

$$\|z_i\|_2 \le \delta \|w_{Fi}\|_2 \tag{4.15}$$

4.3.2 Decentralised Robust Reliable Full State-Feedback Control

Objectives (4.12-4.13) can be achieved for scalars $\alpha_i \ge 0$, $\delta > 0$ and $\varepsilon_i > 0$ if there exists a matrix $P_{2i} > 0$ such that (Wang et al 2001):

$$(A_{ci} + \alpha_i I)^T P_{2i} + P_{2i}(A_{ci} + \alpha_i I) + \frac{\varepsilon_i}{\delta} P_{2i} B_{ci} B_{ci}^T P_{2i} + \frac{1}{\varepsilon_i \delta} C_{ci}^T C_{ci} < 0 \tag{4.16}$$

Assuming that k_{2i} can be expressed as:

$$k_{2i} = \frac{1}{2\beta_i} b_{\bar{\omega}i}^T P_{2i} \tag{4.17}$$

where $\beta_i > 0$ is a pre-defined subsystem scalar used to scale k_{2i}. Substituting (4.11) and (4.17) into the LHS of (4.16) gives:

$$\begin{aligned}
&(A_{ci} + \alpha_i I)^T P_{2i} + P_{2i}(A_{ci} + \alpha_i I) + \frac{\varepsilon_i}{\delta} P_{2i} B_{ci} B_{ci}^T P_{2i} + \frac{1}{\varepsilon_i \delta} C_{ci}^T C_{ci} \\
&= \left(A_{ii} + \Delta A_{ii} - \frac{1}{2\beta_i} b_{\bar{\omega}i} b_{\bar{\omega}i}^T P_{2i} + \alpha_i I \right)^T P_{2i} + P_{2i} \left(A_{ii} + \Delta A_{ii} - \frac{1}{2\beta_i} b_{\bar{\omega}i} b_{\bar{\omega}i}^T P_{2i} + \alpha_i I \right) \\
&+ \frac{\varepsilon_i}{\delta} P_{2i} \begin{pmatrix} h_i & b_{\omega i} \end{pmatrix} \begin{pmatrix} h_i^T \\ b_{\omega i}^T \end{pmatrix} P_{2i} + \frac{1}{\varepsilon_i \delta} (C_{ii} + \Delta C_{ii})^T (C_{ii} + \Delta C_{ii}) \\
&= (A_{ii} + \alpha_i I)^T P_{2i} + \Delta A_{ii}^T P_{2i} + P_{2i}(A_{ii} + \alpha_i I) + P_{2i} \Delta A_{ii} - \frac{1}{\beta_i} P_{2i} b_{\bar{\omega}i} b_{\bar{\omega}i}^T P_{2i} \\
&+ \frac{\varepsilon_i}{\delta} P_{2i} \left[h_i h_i^T + b_{\omega i} b_{\omega i}^T \right] P_{2i} + \frac{1}{\varepsilon_i \delta} \left[C_{ii}^T C_{ii} + \Delta C_{ii}^T \Delta C_{ii} + C_{ii}^T \Delta C_{ii} + \Delta C_{ii}^T C_{ii} \right]
\end{aligned} \tag{4.18}$$

Using the inequality that for any rectangular matrices X and Y with scalar $\upsilon > 0$ (Wang et al, 2001),

$$\upsilon XX^T + \frac{1}{\upsilon} YY^T \pm \left(XY^T + YX^T \right) \geq 0 \tag{4.19}$$

the following inequalities can be derived:

$$\Delta A_{ii}^T P_{2i} + P_{2i} \Delta A_{ii} \leq \varepsilon_{1i} \Delta A_{ii} \Delta A_{ii}^T + \frac{1}{\varepsilon_{1i}} P_{2i} P_{2i}^T \tag{4.20}$$

for $\varepsilon_{1i} > 0$. Let $X_i = \sqrt{\varepsilon_{4i}} D_i^T P_{2i} - \frac{1}{\sqrt{\varepsilon_{4i}}} F_i(t) E_i$ where scalar $\varepsilon_{4i} > 0$. Then inequality $X_i^T X_i \geq 0$ gives:

$$\left[\sqrt{\varepsilon_{4i}} P_{2i} D_i - \frac{1}{\sqrt{\varepsilon_{4i}}} E_i^T F_i^T(t) \right] \left[\sqrt{\varepsilon_{4i}} D_i^T P_{2i} - \frac{1}{\sqrt{\varepsilon_{4i}}} F_i(t) E_i \right] \geq 0 \tag{4.21}$$

Substitute (4.9) and (4.21) into (4.20) gives:

$$\Delta A_{ii}^T P_{2i} + P_{2i} \Delta A_{ii} \leq \varepsilon_{1i} P_{2i} T_{Ai} P_{2i} + \frac{1}{\varepsilon_{1i}} U_{Ai} \tag{4.22}$$

where

$$T_{Ai} = D_i D_i^T, \; U_{Ai} = E_i^T E_i \tag{4.23}$$

and,

$$
\begin{aligned}
&C_{ii}{}^{T}C_{ii} + \Delta C_{ii}{}^{T}C_{ii} + \Delta C_{ii}{}^{T}\Delta C_{ii} + C_{ii}{}^{T}\Delta C_{ii} \\
&\le (1+\varepsilon_{2i})C_{ii}{}^{T}C_{ii} + (1+\frac{1}{\varepsilon_{2i}})\Delta C_{ii}{}^{T}\Delta C_{ii} \\
&\le (1+\varepsilon_{2i})C_{ii}{}^{T}C_{ii} + (1+\frac{1}{\varepsilon_{2i}})\delta_{c}{}^{2}I
\end{aligned}
\tag{4.24}
$$

for $\varepsilon_{2i} > 0$.

$$
-\frac{1}{\beta_i}P_{2i}b_{\bar{\omega}i}b_{\bar{\omega}i}{}^{T}P_{2i} \le -P_{2i}b_{\bar{\omega}i}b_{\bar{\omega}i}{}^{T}P_{2i} \tag{4.25}
$$

for $0 < \beta_i \le 1$.

Hence, substituting (4.20, 4.24, 4.25) and the following expansion:

$$
\begin{aligned}
b_{\Omega i}b_{\Omega i}{}^{T} &= b_{\omega i}b_{\omega i}{}^{T} + b_{\Omega i-\omega i}b_{\Omega i-\omega i}{}^{T} \\
b_{\bar{\Omega}i}b_{\bar{\Omega}i}{}^{T} &= b_{\bar{\omega}i}b_{\bar{\omega}i}{}^{T} + b_{\bar{\Omega}i-\bar{\omega}i}b_{\bar{\Omega}i-\bar{\omega}i}{}^{T}
\end{aligned}
\quad\Rightarrow\quad
\begin{aligned}
b_{\omega i}b_{\omega i}{}^{T} &= b_{\Omega i}b_{\Omega i}{}^{T} - b_{\Omega i-\omega i}b_{\Omega i-\omega i}{}^{T} \\
b_{\bar{\omega}i}b_{\bar{\omega}i}{}^{T} &= b_{\bar{\Omega}i}b_{\bar{\Omega}i}{}^{T} - b_{\bar{\Omega}i-\bar{\omega}i}b_{\bar{\Omega}i-\bar{\omega}i}{}^{T}
\end{aligned}
\tag{4.26}
$$

into (4.18) gives:

$$
\begin{aligned}
&\left(A_{ii}+\alpha_i I\right)^{T}P_{2i} + \Delta A_{ii}{}^{T}P_{2i} + P_{2i}\left(A_{ii}+\alpha_i I\right) + P_{2i}\Delta A_{ii} - \frac{1}{\beta_i}P_{2i}b_{\bar{\omega}i}b_{\bar{\omega}i}{}^{T}P_{2i} \\
&+\frac{\varepsilon_i}{\delta}P_{2i}\left[h_i h_i{}^{T} + b_{\omega i}b_{\omega i}{}^{T}\right]P_{2i} + \frac{1}{\varepsilon_i\delta}\left[C_{ii}{}^{T}C_{ii} + \Delta C_{ii}{}^{T}\Delta C_{ii} + C_{ii}{}^{T}\Delta C_{ii} + \Delta C_{ii}{}^{T}C_{ii}\right] \\
&\le \left(A_{ii}+\alpha_i I\right)^{T}P_{2i} + P_{2i}\left(A_{ii}+\alpha_i I\right) + \varepsilon_{1i}P_{2i}T_{Ai}P_{2i} + \frac{1}{\varepsilon_{1i}}U_{Ai} - P_{2i}\left(b_{\bar{\Omega}i}b_{\bar{\Omega}i}{}^{T}\right)P_{2i} \\
&+\frac{\varepsilon_i}{\delta}P_{2i}\left(b_{\Omega i}b_{\Omega i}{}^{T}\right)P_{2i} + \frac{\varepsilon_i}{\delta}P_{2i}\left[h_i h_i{}^{T}\right]P_{2i} + \frac{1}{\varepsilon_i\delta}\left[(1+\varepsilon_{2i})C_{ii}{}^{T}C_{ii} + (1+\frac{1}{\varepsilon_{2i}})\delta_{c}{}^{2}I\right] + Q_{2i} \\
&-\left(1+\frac{\varepsilon_i}{\delta}\right)P_{2i}\left(b_{\Omega i-\omega i}b_{\Omega i-\omega i}{}^{T}\right)P_{2i} - Q_{2i}
\end{aligned}
\tag{4.27}
$$

for $Q_{2i} > 0$. From (4.27), for (4.16) to hold,

$$\begin{aligned}&(A_{ii}+\alpha_i I)^T P_{2i}+P_{2i}(A_{ii}+\alpha_i I)+\varepsilon_{1i}P_{2i}T_{Ai}P_{2i}+\frac{1}{\varepsilon_{1i}}U_{Ai}-P_{2i}\left(b_{\overline{\Omega}i}b_{\overline{\Omega}i}{}^T\right)P_{2i}\\&+\frac{\varepsilon_i}{\delta}P_{2i}\left(b_{\Omega i}b_{\Omega i}{}^T\right)P_{2i}+\frac{\varepsilon_i}{\delta}P_{2i}\left[h_i h_i{}^T\right]P_{2i}+\frac{1}{\varepsilon_i\delta}\left[(1+\varepsilon_{2i})C_{ii}{}^T C_{ii}+(1+\frac{1}{\varepsilon_{2i}})\delta_c{}^2 I\right]+Q_{2i}\\&=0\end{aligned} \quad (4.28)$$

which can be cast in the algebraic Riccati form as:

$$(A_{ii}+\alpha_i I)^T P_{2i}+P_{2i}(A_{ii}+\alpha_i I)-P_{2i}R_{2i}P_{2i}+\overline{Q}_{2i}=0 \quad (4.29)$$

where

$$R_{2i}=\frac{1}{\beta_i}b_{\overline{\Omega}i}b_{\overline{\Omega}i}{}^T-\varepsilon_{1i}b_{\overline{\omega}i}T_{Ai}b_{\overline{\omega}i}{}^T-\frac{\varepsilon_i}{\delta_i}\left[b_{\Omega i}b_{\Omega i}{}^T+h_i h_i{}^T\right] \quad (4.30)$$

$$\overline{Q}_{2i}=\frac{1}{\varepsilon_{1i}}U_{Ai}+\frac{1}{\varepsilon_i\delta_i}\left[(1+\varepsilon_{2i})C_{ii}{}^T C_{ii}+(1+\frac{1}{\varepsilon_{2i}})\delta_{ci}{}^2 I\right]+Q_{2i} \quad (4.31)$$

where R_{2i} and $\overline{Q}_{2i}$ are positive-definite design uncertainty weighting matrices; T_{Ai} and U_{Ai} are as defined in (4.23) and $\|\Delta C_{ii}\|_2 \le \delta_c$ with control law of (4.10) in which k_{2i} is given in (4.17).

Existence of admissible solution to the ARE implies $\overline{Q}_{2i} \ge 0$ and $R_{2i}>0$, hence the following condition must be satisfied:

$$\underline{\sigma}\left(\frac{1}{\beta_i}b_{\overline{\Omega}i}b_{\overline{\Omega}i}{}^T\right)>\overline{\sigma}\left\{\left(\varepsilon_{i1}T_{Ai}\right)+\frac{\varepsilon_i}{\delta}\left[b_{\Omega i}b_{\Omega i}{}^T+h_i h_i{}^T\right]\right\}>0 \quad (4.32)$$

α_i and β_i are selected based on user robustness specifications. Tuning scalars ε_i, ε_{1i} and ε_{2i} should be chosen to ensure that both R_{2i} and $\overline{Q}_{2i}$ are positive-definite as well as selecting β_i to achieve decentralised H_2-optimality given in (4.14).

4.3.3 Decentralised Robust Reliable H_2-Optimal Control

From (4.10), (4.14) can be written as:

$$J_{2i} = \int_0^\infty \left[x_i{}^T \left(\tilde{Q}_{2i} + k_{2i}{}^T \tilde{R}_{2i} k_{2i} \right) x_i \right] dt = \int_0^\infty \left[x_i{}^T \hat{Q}_{2i} x_i \right] dt \tag{4.33}$$

where $\hat{Q}_{2i} = \tilde{Q}_{2i} + k_{2i}{}^T \tilde{R}_{2i} k_{2i}$. If (4.29) holds and since the closed-loop system (4.11) is asymptotically stable as guaranteed under (4.12) and A_c is stable, then for (4.33) to be minimized, the following Lyapunov equation must hold:

$$A_{ci}{}^T P_{2i} + P_{2i} A_{ci} = -\hat{Q}_{2i} \tag{4.34}$$

under the condition that $\hat{Q}_{2i} \in \Re^{2nx2n}$ is positive semi-definite matrix. Taking $\tilde{R}_{2i} = 2\beta_i I > 0$ and re-writing (4.17) as $k_{2i} = \tilde{R}_{2i}{}^{-1} b_{\bar{\omega}i}{}^T P_{2i}$, it can be shown through (4.34) that:

$$\tilde{Q}_{2i} = -(A_{ci}^T P_{2i} + P_{2i} A_{ci} + P_{2i} b_{\bar{\omega}i} \tilde{R}_{2i}{}^{-1} b_{\bar{\omega}i}{}^T P_{2i}) \tag{4.35}$$

Objective (4.12) implies A_{ci} is negative definite and (4.16) implies P_{2i} is s.p.d. to ensure admissible solution of (4.29), then $\tilde{Q}_{2i} \geq 0$. Adding the ARE in (4.29) with (4.34) gives:

$$\begin{aligned} &2\alpha_i P_{2i} - \frac{1}{\beta_i} P_{2i}\left(b_{\bar{\Omega}i} b_{\bar{\Omega}i}{}^T\right) P_{2i} + \frac{\varepsilon_i}{\delta_i} P_{2i}\left(b_{\Omega i} b_{\Omega i}{}^T\right) P_{2i} + \frac{1}{2\beta_i} P_{2i} b_{\bar{\omega}i} b_{\bar{\omega}i}{}^T P_{2i} \\ &+ \frac{\varepsilon_i}{\delta_i} P_{2i}\left[(1+\varepsilon_{3i}) h_i h_i{}^T\right] P_{2i} + \frac{1}{\varepsilon_i \delta_i}\left[(1+\varepsilon_{2i}) C_{ii}{}^T C_{ii} + (1+\frac{1}{\varepsilon_{2i}})\delta_{ci}{}^2 I\right] + Q_{2i} \geq 0 \end{aligned} \tag{4.36}$$

The detectability of $(A_{ii}, \tilde{Q}_{2i}{}^{1/2})$ is assumed for unstable modes to be reflected in (4.14). This can be used to check whether H_2-optimality has been achieved for the robust reliable controller. Satisfying (4.36) therefore implies that under closed-loop linear system conditions, (4.14) is satisfied such that the controller provides infinite gain margin and at least 60° phase margin for all admissible uncertainties and allowable actuator failures.

By satisfying (4.29-4.31, 4.36), the uncertain layer linear feedback controller with control gain (4.17) guarantees relative α_i-degree asymptotic stability with robust reliable decentralised H_∞-norm excitation rejection and H_2-optimality for subsystem (4.8). In addition to being fault-tolerant, if the allowable actuator failures can be actively monitored, then fault compensation using state feedback (Tao et al 2001) can be used to completely attenuate the effects of all failures.

4.4 Augmented Saturation Subsystem Control

Based on the above, the closed-loop linearly-controlled subsystem of (4.6) under robust reliable controls in view of (4.7) can be re-written as:

$$\begin{aligned} \dot{x}_i(t) &= \left(A_{ii} + \Delta A_{ii} - b_{\overline{\omega}i} k_{2i}\right) x_i(t) + b_{\omega i} \overline{u}_{2i}(t) + e_{2i}(t), \\ y_i(t) &= x_i(t), \\ z_i(t) &= \left(C_{ii} + \Delta C_{ii}\right) x_i(t) \end{aligned} \tag{4.37}$$

where the uncertain subsystem disturbance vector is $e_{2i}(t) = \sum_{j=1, j\neq i}^{N_s} A_{ij} x_j(t) + x_{ni}(t) + \left(b_{\omega i} \quad h_i\right)\begin{pmatrix} u_{Fi}(t) \\ \ddot{x}_g(t) \end{pmatrix}$. When $e_{2i} = 0$, which corresponds to (4.11), (4.37) is α_i-degree asymptotically stable. When $e_{2i} \neq 0$, under assumptions 7-8 and bounded arbitrary excitation $\ddot{x}_g$ and actuator failure signals u_{Fi}, $e_{2i}(t)$ is a bounded function such that the robust reliable augmented controller $\overline{u}_{2i}(t)$ in (4.7) can be specifically designed for desired subsystem disturbance rejection (Magana and Rodellar 1998).

It is assumed that positive subsystem constant δ_{2i} exists and given or known *a priori* such that $\left|e_{2i}(t)\right| \leq \delta_{2i} = \left|\sum_{j=1, j\neq i}^{N_s} A_{ij} x_j(t)\right|_{\max} + \left|x_{ni}(t)\right|_{\max} + \left|\left(b_{\omega i} \quad h_i\right)\begin{pmatrix} u_{Fi}(t) \\ \ddot{x}_g(t) \end{pmatrix}\right|_{\max}$ (**Assumption 9**). For example, δ_{2i} can be derived from the uncontrolled responses under the target excitation (Magana and Rodellar 1998).

Under Assumption 9, the robust reliable decentralised augmented saturation controller is given as:

$$\overline{u}_{2i}(t) = \begin{cases} \operatorname{sgn}\left(\mu_{2i}(t)\right)\delta_{2i}, & \left|\mu_{2i}(t)\right| > \delta_{2i} \\ \mu_{2i}(t), & \left|\mu_{2i}(t)\right| \leq \delta_{2i} \end{cases} \tag{4.38}$$

where $\overline{u}_{2i}(t)$ is a saturation controller that is limited by δ_{2i} in magnitude and $\mu_{2i}(t)$ in direction; $\mu_{2i}(t)$ is given as:

$$\mu_{2i}(t) = -\delta_{2i} b_i^T \tilde{P}_{2i} x_i \tag{4.39}$$

where $\tilde{P}_{2i}$ is the s.p.d. solution of the following Lyapunov equation of the closed-loop subsystem (4.37):

$$\left(A_{ii} + \Delta A_{ii} - b_{\bar{\omega}i} k_{2i}\right)^T \tilde{P}_{2i} + \tilde{P}_{2i}\left(A_{ii} + \Delta A_{ii} - b_{\bar{\omega}i} k_{2i}\right) = -\breve{Q}_{2i} \tag{4.40}$$

where $\breve{Q}_{2i}$ is the symmetric semi-positive-definite disturbance energy-weighting matrix.

4.5 LTR-based Decentralised Robust Reliable Saturation Controls

Following the LTR procedure in section 2.5, (4.6) can be modified as follows:

$$\begin{aligned} \dot{x}_i(t) &= A_{ii} x_i(t) + b_{\bar{\omega}i} u_{2i}(t) + w_{2i}(t), \\ y_i(t) &= C_{ii} x_i(t) + \bar{\eta}_{2i}(t), \\ z_i(t) &= C_{ii} x_i(t) + \sum_{j=1, j\neq i}^{N_s} C_{ij} x_j(t) \end{aligned} \tag{4.41}$$

where $w_{2i}(t) = \left[\Delta A_{ii} x_i(t) + b_{\omega i} u_{2i}(t) + h_i \ddot{x}_g(t) + \sum_{j=1, j\neq i}^{N_s}\left(A_{ij} + \Delta A_{ij}\right) x_j(t) + x_{ni}(t)\right] \in \Re^{2n}$

and $\bar{\eta}_{2i}(t) = \left[\Delta C_{ii} x_i(t) + \sum_{j=1, j\neq i}^{N_s}\left(C_{ij} + \Delta C_{ij}\right) x_j(t) + \eta_i(t)\right] \in \Re^{r}$ are assumed to be independent white noises, and $C_{ii} \neq I$ indicates partial state measurement. Under assumption 5, the full-order LTR-based control law for layer *2* can be written as:

$$\begin{aligned} \dot{v}_i &= A_{ii} v_i + k_{f2i}(y_i - C_{ii} v_i) \\ u_{2i} &= -k_{2i} v_i \end{aligned} \tag{4.42}$$

where the CSS subsystem control state is $v_i \in \Re^{2n}$ and the LTR gain for layer *2* is $k_{f2i} \in \Re^{2nxr}$, which is derived following the procedure in section 2.5 by replacing k_{f1i}, k_{1i}, b_i and $E_{r1i}(s)$ with k_{f2i}, k_{2i}, $b_{\bar{\omega}i}$ and $E_{r2i}(s)$ respectively.

Replace (4.7) with the CSS-LTR subsystem state as follows:

$$u_{2i}(t) = -k_{2i} v_i(t) + \bar{u}_{2i}(t) \tag{4.43}$$

where k_{2i} is given in (4.17) and $\mu_{2i}(t)$ in (4.39) is replaced by:

$$\mu_{2i}(t) = -\delta_{2i} b_{\bar{\omega}i}{}^T \tilde{P}_{2i} v_i \tag{4.44}$$

4.6 Computational implementation

Computation and implementation of the layered decentralized controls follow the flowchart shown in Fig. 4.1. For pre-processing, MATLAB™ is used to compute all structural data, state-space model and control gains. SIMULINK™ is used to numerically simulate the controlled system under earthquake excitation. For post-processing, MATLAB is used to process and plot all output responses and controls.

4.7 Numerical illustration

4.7.1 2DOF uncertain system

A numerical example of a 2-DOF system under scaled El Centro earthquake to

0.1g (Fig. 2.2) is used to illustrate the effectiveness of the decentralised robust reliable saturation control as opposed to central nominal full state-feedback LQR control and decentralised nominal saturation control of Chapter 2. Consider the same 2-DOF system with two actuators, but with allowable uncertainties below in state-space:

$$\begin{pmatrix}\dot{x}_1\\ \dot{x}_2\\ \ddot{x}_1\\ \ddot{x}_2\end{pmatrix}=\begin{pmatrix}1 & 0 & 0 & 0\\ 0 & 1 & 0 & 0\\ 0 & 0 & 1+\alpha_A & 0\\ 0 & 0 & 0 & 1+\alpha_A\end{pmatrix}\begin{pmatrix}0 & 0 & 1 & 0\\ 0 & 0 & 0 & 1\\ -315.84 & 157.92 & -2.5134 & 1.2567\\ 157.92 & -157.92 & 1.2567 & -1.2567\end{pmatrix}\begin{pmatrix}x_1\\ x_2\\ \dot{x}_1\\ \dot{x}_2\end{pmatrix},$$
$$+\alpha_B\begin{pmatrix}0 & 0\\ 0 & 0\\ 1 & 0\\ 0 & 1\end{pmatrix}\begin{pmatrix}u_1\\ u_2\end{pmatrix}+\begin{pmatrix}0\\ 0\\ -1\\ -1\end{pmatrix}\ddot{x}_g+v(t)$$

$$\begin{pmatrix}y_1\\ y_2\end{pmatrix}=\alpha_c\begin{pmatrix}-315.84 & 157.92 & -2.5134 & 1.2567\\ 157.92 & -157.92 & 1.2567 & -1.2567\end{pmatrix}\begin{pmatrix}x_1\\ x_2\\ \dot{x}_1\\ \dot{x}_2\end{pmatrix}+w(t)$$

where parameters $\alpha_A\in[-0.1,0.1]$, $\alpha_B\in[-1,1]$ and $\alpha_C\in[-1,1]$ are used to specify uncertainties. System is nominal when $\alpha_A=0$, $\alpha_B=1$ and $\alpha_C=1$. Assume that $u_F{}^T=(0\quad 0)$. To illustrate the performance effectiveness, the nominal natural frequencies encompass the PSD peaks of the El Centro excitation used.

After state decentralisation, the subsystem 1 is given below:

$$\begin{pmatrix}\dot{x}_1\\ \ddot{x}_1\end{pmatrix}=\begin{pmatrix}1 & 0\\ 0 & 1+\alpha_A\end{pmatrix}\left[\begin{pmatrix}0 & 1\\ -315.84 & -2.5134\end{pmatrix}\begin{pmatrix}x_1\\ \dot{x}_1\end{pmatrix}+\begin{pmatrix}0 & 0\\ 157.92 & 1.2567\end{pmatrix}\begin{pmatrix}x_2\\ \dot{x}_2\end{pmatrix}\right]+\alpha_B\begin{pmatrix}0\\ 1\end{pmatrix}u_1,$$
$$+\begin{pmatrix}0\\ -1\end{pmatrix}\ddot{x}_g+v_1(t)$$

$$y_1=\alpha_c\begin{pmatrix}-315.84 & -2.5134\end{pmatrix}\begin{pmatrix}x_1\\ \dot{x}_1\end{pmatrix}+\alpha_c\begin{pmatrix}157.92 & 1.2567\end{pmatrix}\begin{pmatrix}x_2\\ \dot{x}_2\end{pmatrix}+w_1(t),$$

$$z_1=\begin{pmatrix}-315.84 & -2.5134\end{pmatrix}\begin{pmatrix}x_1\\ \dot{x}_1\end{pmatrix}$$

and the subsystem 2 is given below:

$$\begin{pmatrix}\dot{x}_2\\ \ddot{x}_2\end{pmatrix}=\begin{pmatrix}1 & 0\\ 0 & 1+\alpha_A\end{pmatrix}\left[\begin{pmatrix}0 & 1\\ -157.92 & -1.2567\end{pmatrix}\begin{pmatrix}x_2\\ \dot{x}_2\end{pmatrix}+\begin{pmatrix}0 & 0\\ 157.92 & 1.2567\end{pmatrix}\begin{pmatrix}x_1\\ \dot{x}_1\end{pmatrix}\right]+\alpha_B\begin{pmatrix}0\\ 1\end{pmatrix}u_2 ,$$
$$+\begin{pmatrix}0\\ -1\end{pmatrix}\ddot{x}_g+v_2(t)$$

$$y_2=\alpha_c\begin{pmatrix}315.84 & 2.5134\end{pmatrix}\begin{pmatrix}x_1\\ \dot{x}_1\end{pmatrix}+\alpha_c\begin{pmatrix}-157.92 & -1.2567\end{pmatrix}\begin{pmatrix}x_2\\ \dot{x}_2\end{pmatrix}+w_2(t),$$

$$z_2=\begin{pmatrix}-157.92 & -1.2567\end{pmatrix}\begin{pmatrix}x_2\\ \dot{x}_2\end{pmatrix}$$

Notice that the local regulated output z_i is the undisturbed local acceleration.

The nominal controller parameters are provided in section 2.6.1.

For $\alpha_A=-0.1$, $\alpha_B=0.5$ and $\alpha_C=0.9$, the robust reliable controller parameters are $\alpha_1=\alpha_2=0.5$, $\beta_1=\beta_2=0.01$, $\delta_1=\delta_2=0.01$, $\delta_c=\delta_h=0$, $\varepsilon_1=\varepsilon_2=10^{-5}$, $\varepsilon_{11}=\varepsilon_{12}=0.01$, $\varepsilon_{21}=\varepsilon_{22}=0.01$, $\varepsilon_{31}=\varepsilon_{32}=0.01$, $R_{11}=R_{12}=0.01$, $Q_{21}=Q_{22}=0.01I$, $T_{A1}=T_{A2}=diag(0,2)$, $U_{A1}=diag(997.5,0.0632)$, $U_{A2}=diag(249.4,0.0158)$, $b_{\Omega 1}=b_{\omega 1}=b_{\Omega 2}=b_{\omega 2}=\begin{pmatrix}0 & 0.5\end{pmatrix}^T$, $\varepsilon_{11}=\varepsilon_{12}=8$, $\delta_{11}=\delta_{12}=7.68$ and $\tilde{Q}_{21}=\tilde{Q}_{22}=diag(1,100)$. From (4.17) and (4.29), the robust reliable control gains are $k_{21}=\begin{pmatrix}5.02 & 0.04\end{pmatrix}*10^6$, $k_{22}=\begin{pmatrix}2.51 & 0.02\end{pmatrix}*10^6$; and using section 4.6, LTR gains are $k_{f21}=\begin{pmatrix}-0.363 & -249\end{pmatrix}^T$ and $k_{f22}=\begin{pmatrix}-0.677 & -249\end{pmatrix}^T$.

The controlled responses using central robust reliable controls (rrLQR), decentralised nominal controls (Decen-n) and decentralised robust reliable controls (Decen-rr) are shown in Figs. 4.2-4.3 for the nominal 2DOF global system as well as in Figs. 4.4-4.5 for the uncertain 2DOF global system, inclusive of uncontrolled responses. Tables 4.1 and 4.2 show the absolute peak responses and controls of the

nominal and uncertain 2DOF systems respectively under central full state-feedback robust reliable (rrLQR) controls, decentralised nominal controls and decentralised robust reliable controls. Under central robust reliable LQR controls, the controlled responses and controls are suitably mitigated, as shown in columns (2) and (5) for subsystems 1 and 2 respectively. Under nominal decentralised saturation controls, as shown in columns (3) and (6), the controlled responses are consistently poorer than that of the central robust reliable LQR controls for both nominal and uncertain systems.

With decentralised robust reliable saturation controls, as shown in columns (4) and (7), the controlled responses are comparable to central robust reliable control, and consistently better than decentralized nominal saturation controls for both nominal and uncertain systems. Better control performance is achieved for nominal system with lesser uncertainties and actuator failures. The controlled absolute accelerations are comparable for all controls due to the emphasis on acceleration control of the regulated outputs. These results follow the findings from the previous two chapters.

4.7.2 20DOF uncertain system

Consider the same uncertain 2DOF ROM for the 20DOF shear-structural building model in section 3.6.2. After global state-decentralisation, the subsystem 1 is given below:

$$\begin{pmatrix}\dot{x}_1\\ \ddot{x}_1\end{pmatrix}=\begin{pmatrix}1 & 0\\ 0 & 1+\alpha_A\end{pmatrix}\left[\begin{pmatrix}0 & 1\\ -7.2980 & -0.0730\end{pmatrix}\begin{pmatrix}x_1\\ \dot{x}_1\end{pmatrix}+\begin{pmatrix}0 & 0\\ 2.7761 & 0.0278\end{pmatrix}\begin{pmatrix}x_2\\ \dot{x}_2\end{pmatrix}\right],$$
$$+\alpha_B\begin{pmatrix}0\\ -12.1596\end{pmatrix}u_1+\begin{pmatrix}0\\ 4022\end{pmatrix}\ddot{x}_g+v_1(t)$$

$$y_1=\alpha_c\begin{pmatrix}-7.2980 & -0.0730\end{pmatrix}\begin{pmatrix}x_1\\ \dot{x}_1\end{pmatrix}+\alpha_c\begin{pmatrix}2.7761 & 0.0278\end{pmatrix}\begin{pmatrix}x_2\\ \dot{x}_2\end{pmatrix}+w_1(t),$$

$$z_1 = \begin{pmatrix} -7.2980 & -0.0730 \end{pmatrix} \begin{pmatrix} x_1 \\ \dot{x}_1 \end{pmatrix}$$

and the subsystem 2 is given below:

$$\begin{pmatrix} \dot{x}_2 \\ \ddot{x}_2 \end{pmatrix} = \begin{pmatrix} 1 & 0 \\ 0 & 1+\alpha_A \end{pmatrix} \left[\begin{pmatrix} 0 & 1 \\ -62.8417 & -0.6284 \end{pmatrix} \begin{pmatrix} x_2 \\ \dot{x}_2 \end{pmatrix} + \begin{pmatrix} 0 & 0 \\ 2.7761 & 0.0278 \end{pmatrix} \begin{pmatrix} x_1 \\ \dot{x}_1 \end{pmatrix} \right],$$
$$+ \alpha_B \begin{pmatrix} 0 \\ -27.8441 \end{pmatrix} u_2 + \begin{pmatrix} 0 \\ -1530 \end{pmatrix} \ddot{x}_g + v_2(t)$$

$$y_2 = \alpha_c \begin{pmatrix} 2.7761 & 0.0278 \end{pmatrix} \begin{pmatrix} x_1 \\ \dot{x}_1 \end{pmatrix} + \alpha_c \begin{pmatrix} -62.8417 & -0.6284 \end{pmatrix} \begin{pmatrix} x_2 \\ \dot{x}_2 \end{pmatrix} + w_2(t),$$

$$z_2 = \begin{pmatrix} -62.8417 & -0.6284 \end{pmatrix} \begin{pmatrix} x_2 \\ \dot{x}_2 \end{pmatrix}$$

The nominal controller and central robust reliable controller parameters are provided in sections 2.6.2 and 3.6.2 respectively. The uncertainty settings and robust reliable controller parameters follow section 4.7.1. From (4.17) and (4.29), the decentralised robust reliable control gains are $k_{21} = \begin{pmatrix} -729 & -13 \end{pmatrix}$, $k_{22} = \begin{pmatrix} -6282 & -66 \end{pmatrix}$; and using section 4.6, LTR gains are $k_{f21} = \begin{pmatrix} -12 & -6079 \end{pmatrix}^T$ and $k_{f22} = \begin{pmatrix} -2 & -13921 \end{pmatrix}^T$.

The controlled responses using central robust reliable controls (rrLQR), decentralised nominal controls (Decen-n) and decentralised robust reliable controls (Decen-rr) are shown in Figs. 4.2-4.3 for the nominal 2DOF global system as well as in Figs. 4.4-4.5 for the uncertain 2DOF global system, inclusive of uncontrolled responses. Tables 4.1 and 4.2 show the absolute peak responses and controls of the nominal and uncertain 2DOF systems respectively under central full state-feedback robust reliable (rrLQR) controls, decentralised nominal controls and decentralised robust reliable controls. Under central robust reliable LQR controls, the controlled responses and controls are suitably mitigated, as shown in columns (2) and (5) for

subsystems 1 and 2 respectively. Under nominal decentralised saturation controls, as shown in columns (3) and (6), the controlled responses are consistently poorer than that of the central robust reliable LQR controls for both nominal and uncertain systems.

With decentralised robust reliable saturation controls, as shown in columns (4) and (7), the controlled responses are comparable to central robust reliable control, and consistently better than decentralized nominal saturation controls for both nominal and uncertain systems. Better control performance is achieved for nominal system with lesser uncertainties and actuator failures. The controlled absolute accelerations are comparable for all controls due to the emphasis on acceleration control of the regulated outputs.

The results show that for both linear nominal and uncertain systems, a set of simpler decentralised controllers can have performance at least as good as a single global centralised controller under similar peak control magnitude. Robust reliable controls perform consistently better than nominal controls for both nominal and uncertain systems under both central and decentralised control systems. By combining decentralisation and robust reliable control approaches, the decentralised robust reliable controls perform consistently better than decentralised nominal controls, with comparable performance to central robust reliable controls, when system uncertainties and/or device failures do occur. Hence, this agrees with the findings of Lukas (1996) that the attainable benefits of decentralised control are high system performance under system uncertainties, greater stability robustness and improved control system performance.

Table 4.1: Peak Responses and Controls for Nominal 2DOF System

Cases (1)	Subsystem 1			Subsystem 2		
	rrLQR (2)	Decen-n (3)	Decen-rr (4)	rrLQR (5)	Decen-n (6)	Decen-rr (7)
Drift (cm)	0.0007	0.01	0.006	0.0003	0.005	0.0003
Drift vel. (cm/s)	0.03	0.34	0.03	0.015	0.15	0.015
Abs. acc. (cm/s^2)	85.50	85.72	85.50	85.49	86.37	85.79
Control (V)	0.8541	0.8489	0.8545	0.8544	0.8556	0.8574

Table 4.2: Peak Responses and Controls for Uncertain 2DOF System

Cases (1)	Subsystem 1			Subsystem 2		
	rrLQR (2)	Decen-n (3)	Decen-rr (4)	rrLQR (5)	Decen-n (6)	Decen-rr (7)
Drift (cm)	0.001	0.02	0.006	0.0007	0.01	0.0006
Drift vel. (cm/s)	0.07	0.73	0.06	0.04	0.35	0.03
Abs. acc. (cm/s^2)	85.46	86.13	85.6	85.62	86.93	85.93
Control (V)	1.7069	1.6896	1.7101	1.7104	1.7064	1.7168

Table 4.3: Peak Responses for Nominal 20DOF System

Cases (1)	10^{th} DOF			20^{th} DOF		
	rrLQR (2)	Decen-n (3)	Decen-rr (4)	rrLQR (5)	Decen-n (6)	Decen-rr (7)
Drift (cm)	0.000001	0.003	0.0000007	0.000005	0.004	0.0000009
Drift vel. (cm/s)	0.00006	0.12	0.00003	0.00002	0.18	0.00004
Abs. acc. (cm/s^2)	85.38	85.48	85.48	85.38	85.67	85.50

Table 4.4: Peak Responses for Uncertain 20DOF System

Cases (1)	10^{th} DOF			20^{th} DOF		
	rrLQR (2)	Decen-n (3)	Decen-rr (4)	rrLQR (5)	Decen-n (6)	Decen-rr (7)
Drift (cm)	0.000003	0.007	0.000001	0.000001	0.009	0.000002
Drift vel. (cm/s)	0.0001	0.27	0.00006	0.00005	0.41	0.00008
Abs. acc. (cm/s^2)	85.46	85.82	85.48	85.48	85.68	85.51

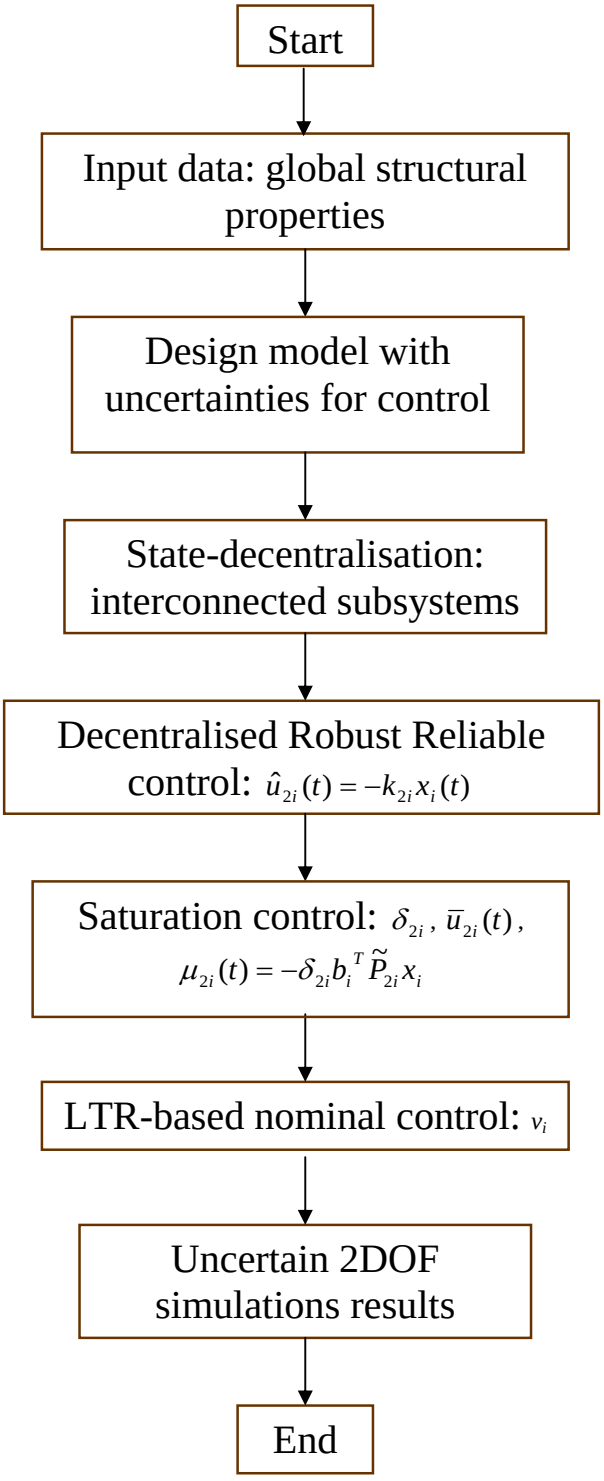

Figure 4.1: Flowchart for Decentralised Robust Reliable Saturation Control

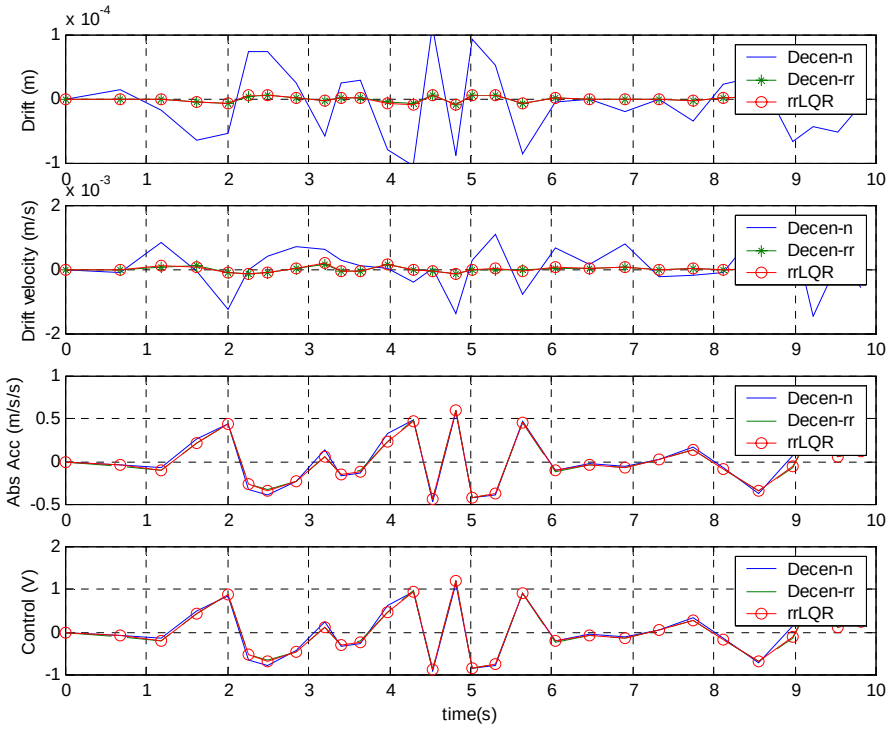

Figure 4.2: Subsystem 1 responses and controls for nominal 2DOF system

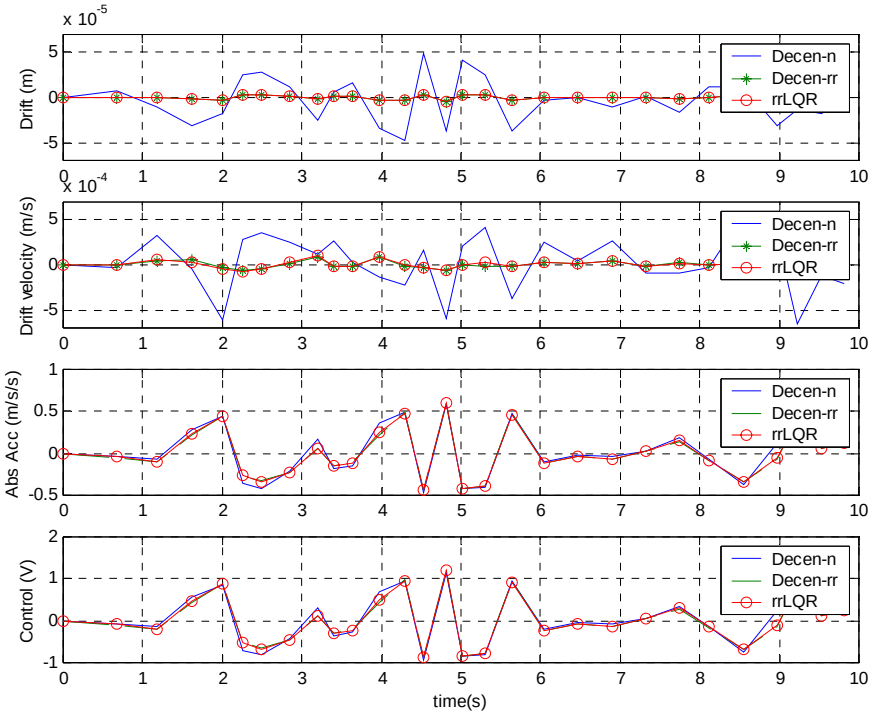

Figure 4.3: Subsystem 2 responses and controls for nominal 2DOF system

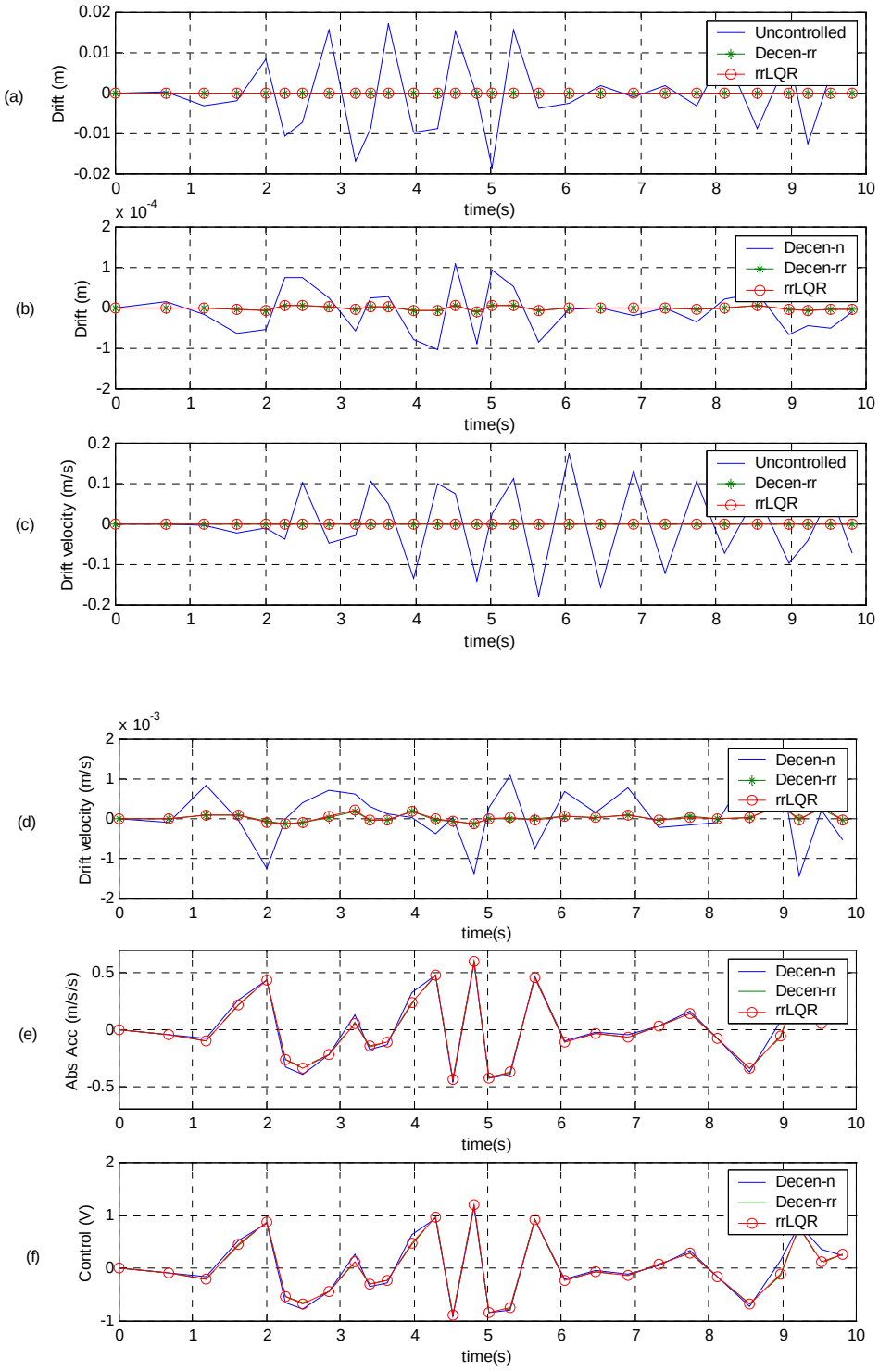

Figure 4.4: Comparisons of subsystem 1 responses under central robust reliable LQR and decentralised nominal and robust reliable controls for uncertain 2DOF system – (a) drifts including uncontrolled drifts; (b) controlled drifts; (c) velocity drifts including uncontrolled; (d) controlled velocity drifts; (e) absolute acceleration; (f) controls

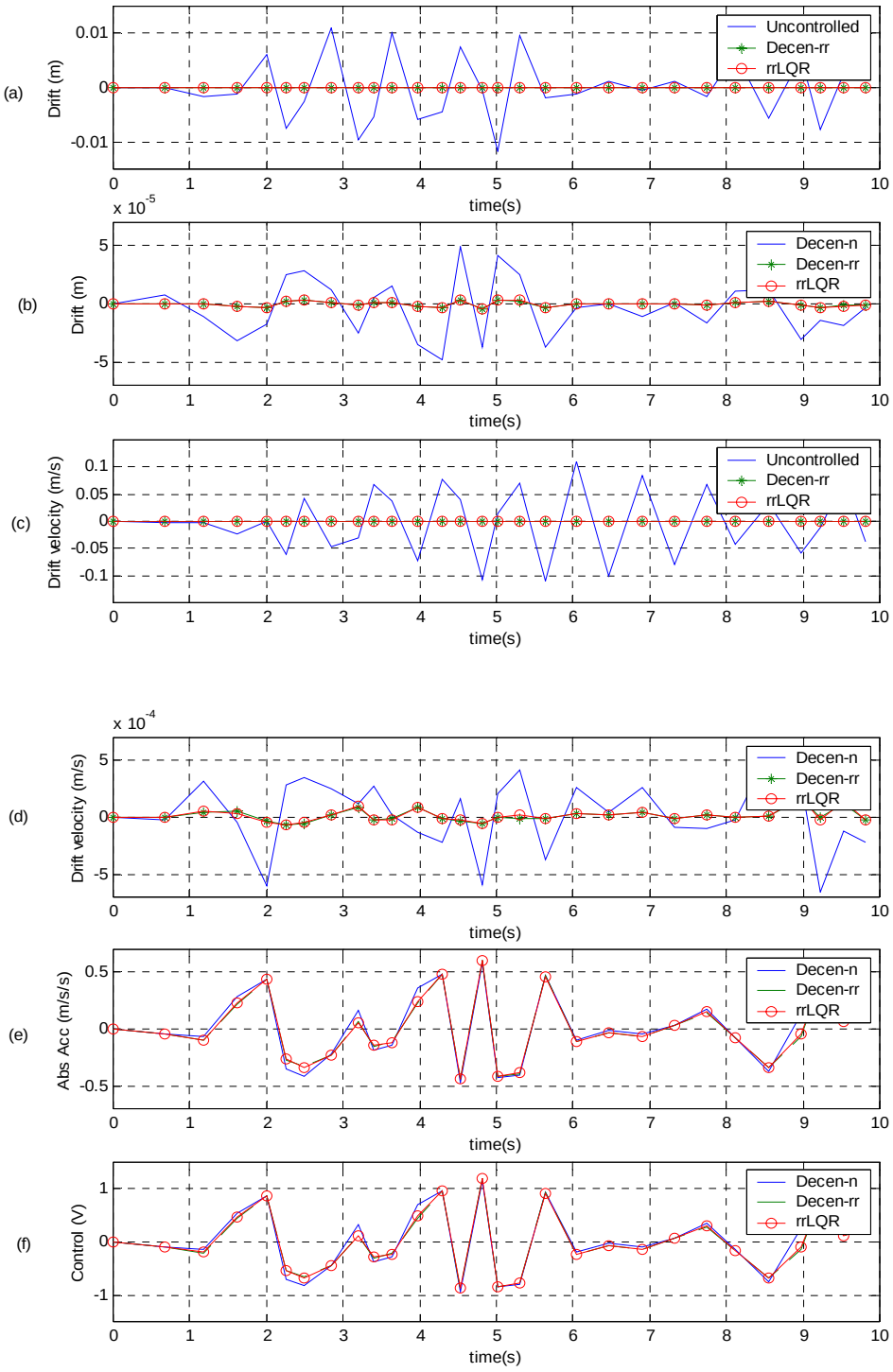

Figure 4.5: Comparisons of subsystem 2 responses under central robust reliable LQR and decentralised nominal and robust reliable controls for uncertain 2DOF system – (a) drifts including uncontrolled drifts; (b) controlled drifts; (c) velocity drifts including uncontrolled; (d) controlled velocity drifts; (e) absolute acceleration; (f) controls

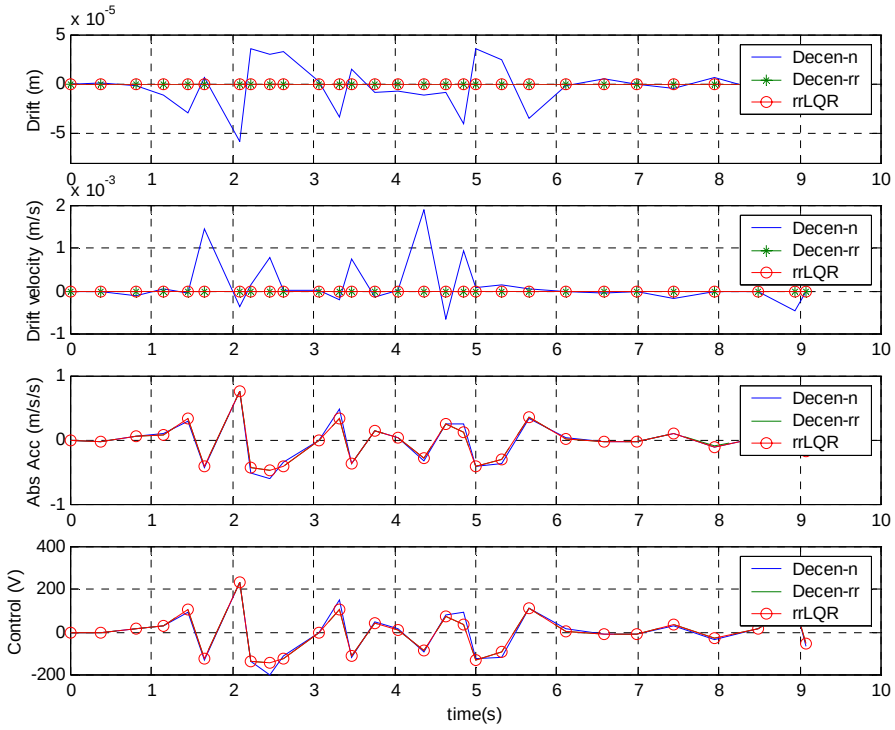

Figure 4.6: Responses and controls for 10th DOF of nominal 20DOF system

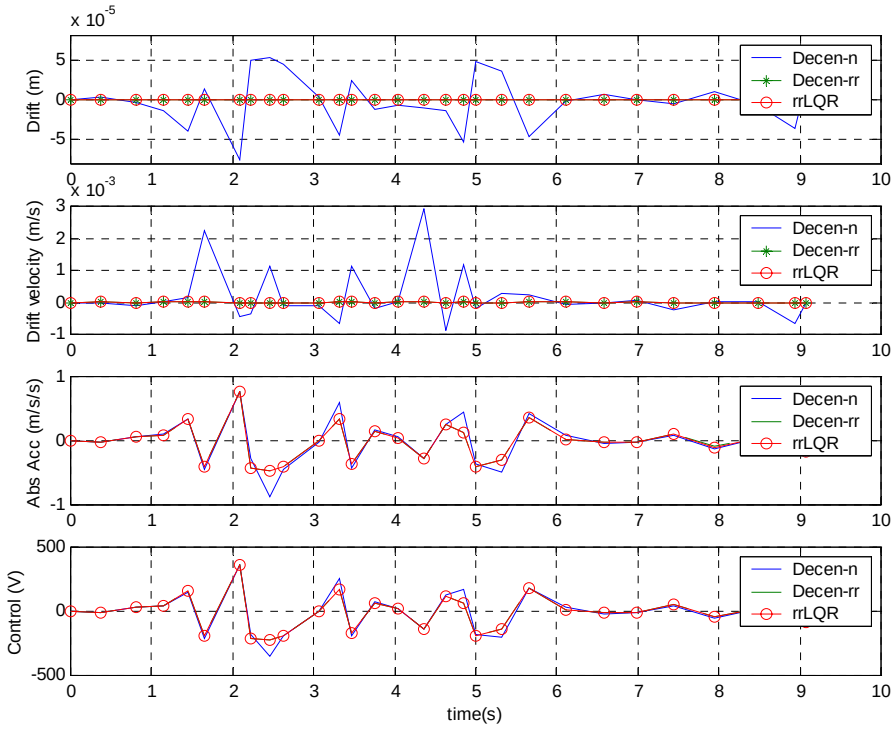

Figure 4.7: Responses and controls for 20th DOF of nominal 20DOF system

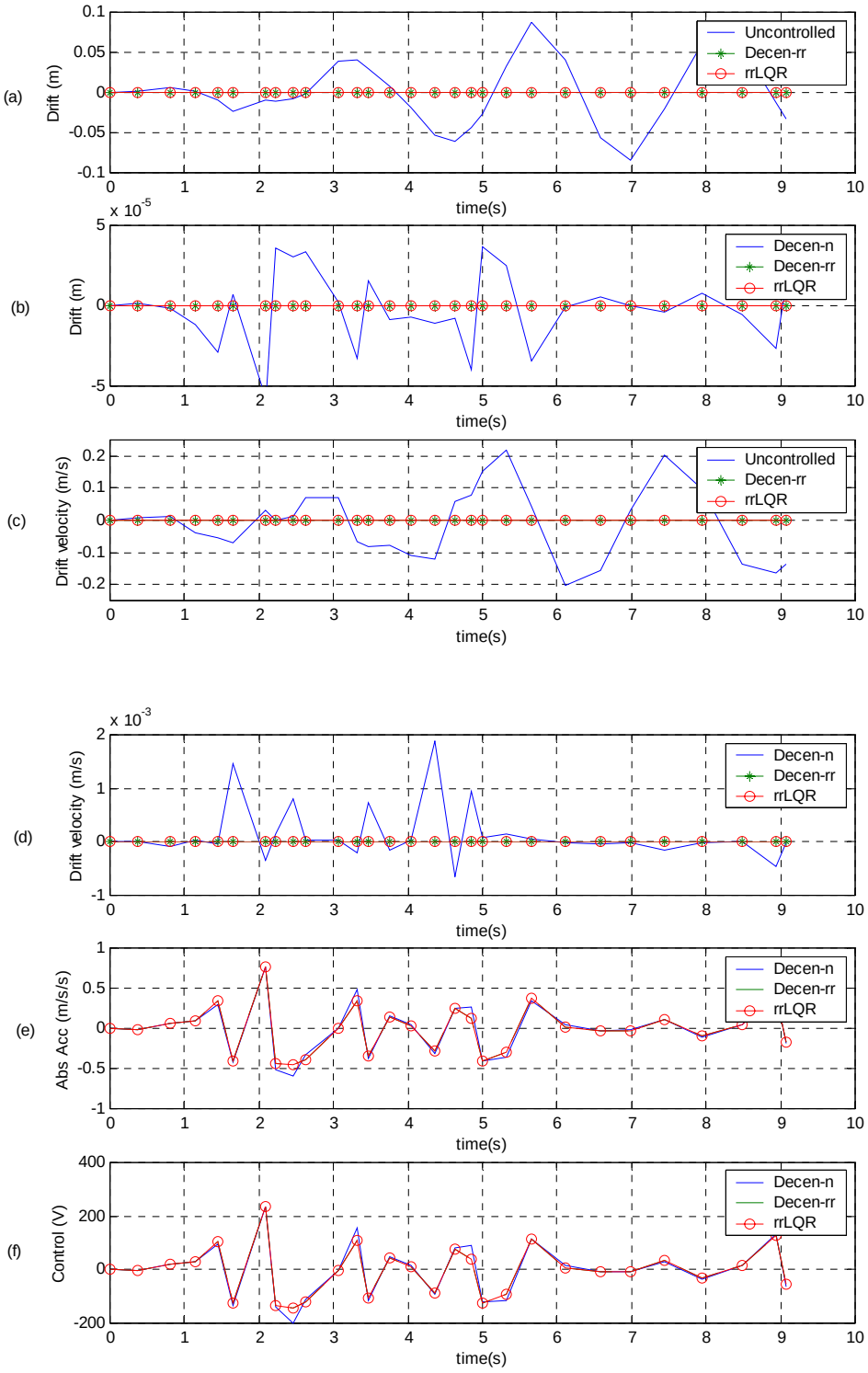

Figure 4.8: Comparisons of responses for 10th DOF of uncertain 20DOF system under central robust reliable LQR and decentralised nominal and robust reliable controls – (a) drifts including uncontrolled drifts; (b) controlled drifts; (c) velocity drifts including uncontrolled; (d) controlled velocity drifts; (e) absolute acceleration; (f) controls

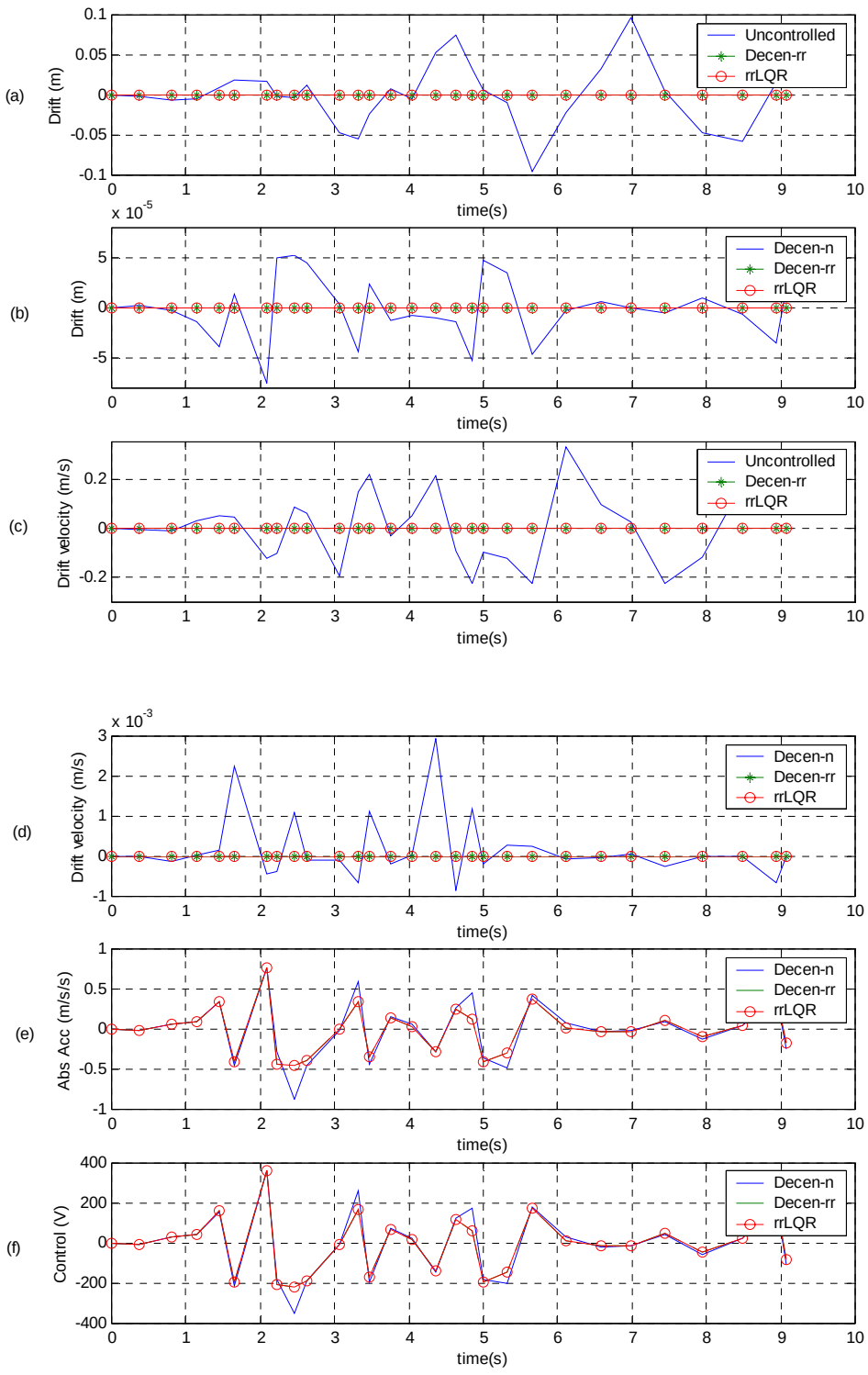

Figure 4.9: Comparisons of responses for 20th DOF of uncertain 20DOF system under central robust reliable LQR and decentralised nominal and robust reliable controls – (a) drifts including uncontrolled drifts; (b) controlled drifts; (c) velocity drifts including uncontrolled; (d) controlled velocity drifts; (e) absolute acceleration; (f) controls

CHAPTER 5

CONCLUSIONS AND FUTURE STUDIES

5.1 Conclusions

The decentralised robust reliable saturation controller is designed using the state-space Riccati-based approach to achieve closed-loop controlled system stability, robustness against system uncertainties, reliability against partial actuator failures and optimality by minimisation of user-defined performance index for the controlled linear uncertain faulty systems under seismic excitations. System uncertainties due to variations in damping and stiffness, as well as actuator failures within a predefined set are considered. Using state-space approach, the global system is state-decentralised into inter-connected local subsystems for local decentralised controls. The decentralised controllers use only local information for independent local control of subsystems. Firstly, decentralised nominal saturation controllers are designed for nominal system, followed by robust reliable controller for uncertain system, and finally combining both approaches to derive the decentralised robust reliable saturation controllers.

The decentralised nominal saturation control is designed for a nominal system. It consists of LTR-based feedback control, under noise-corrupted partial state measurements, to regulate the local ‘uncoupled’ subsystem and a saturation control to account for the coupling terms and excitations. The former uses the closed-loop state-space Riccati-based LQR control approach to derive the full state-feedback gain for the undisturbed subsystem. The latter uses Lyapunov equation to formulate the saturation control with the objective of attenuating the subsystem disturbances. The results show that for both linear nominal 2DOF system and linear nominal 20DOF

system under scaled El Centro excitation, a set of simpler decentralised nominal controllers can perform at least as good as a single global central LQR controller under similar peak control magnitude.

The central robust reliable optimal controller, consisting of closed-loop partial state-feedback LTR-based control is designed for linear uncertain faulty system to be robust against both structured and unstructured norm-bounded uncertainties as well as reliable against actuator failures confined to a predefined subset. Under the partial state-feedback control, the controlled structure is guaranteed user-defined relative stability, robust and reliable H_∞ δ-degree augmented disturbance rejection as well as H_2 control optimality. The results show that for both linear nominal and uncertain systems under scaled El Centro excitation, robust reliable optimal controls always perform better than both central nominal LQR as well as decentralised nominal saturation controls under similar peak control magnitude. In addition, robust reliable optimal control performs better under linea nominal system than linear uncertain system when system uncertainties and/or device failures do occur.

The decentralised robust reliable saturation control combines the decentralisation methodology with the robust reliable optimal control, to use only local information for independent local robust reliable control of uncertain subsystems. The results show that for both linear nominal and uncertain systems, the decentralised robust reliable controls perform much better than decentralised nominal controls, with comparable performance to central robust reliable controls, even when system uncertainties and/or device failures do occur. Robust reliable controls consistently perform better than nominal controls for both linear nominal and uncertain systems under both central and decentralised control systems.

The decentralised controls would be useful for distributed aseismic controls for large-scale uncertain linear systems under seismic excitations. The decentralised robust reliable saturation controllers can be designed specifically to cater to user-specifications and allows great design and control flexibility. This study would show a direction towards exploring further decentralised application possibilities and exploiting optimal decentralised control effectiveness and efficiency for aseismic vibration control, especially when system variations and device malfunctions do occur.

5.2 Future studies

Recommended further studies are as follows:

- Simultaneously and explicitly account for time delays, on-line detection, isolation and compensation for controller and device malfunctions for reliable control with actuator failures unconfined to predefined redundant set should be investigated.
- Coordination and applications of decentralised controllers with a variety of different sensors and actuators for a variety of 2D and 3D subsystems with different controller parameters under active, semi-active or hybrid controls need further studies.
- The GIMC (Zhou and Zhang, 2001) architecture is a very promising innovation allowing the dynamic balance of controlled performance and robustness according to the current actual system conditions. Decentralised GIMC can be designed by formulating both the decentralised nominal and robust reliable controllers into the GIMC architecture to balance controlled stability, performance, robustness and reliability.

REFERENCES

Achuthan, Ajit. Shape Control of Smart Materials. M.S. Thesis, National University of Singapore, Singapore. 1999.

Anderson, Brian D.O. and Moore, J.B. Optimal Control. Prentice Hall. 1989.

Ang K.K., Wang S.Y. and Quek S.T. Weighted energy linear quadratic regulator vibration control of piezoelectric composite plates. Smart Materials and Structures. Vol. 11. pp.98-106. 2002.

Astrom, Karl J. and Wittenmark, Bjorn. Adaptive control, 2nd edition. 574pp. USA: Addison-Wesley Publishing Company, Inc. 1995.

ATC 17-1. Proc. On Seismic Isolation, Passive Energy Dissipation, and Active Control. Appl. Tech. Council. Redwood City. California, USA. 1993.

Banks H. T., Smith R. C. and Wang Y. Smart Material Structures: Modelling, Estimation and Control. 304pp. Paris: John Wiley & Sons. 1996.

Barroso L.R., Hunt S. and Chase J.G. Application of Magneto-rheological dampers for multi-level seismic hazard mitigation of hysteretic structures. Proceedings of the 15th ASCE Engineering Mechanics Conference. June 2-5. 2002. Columbia University, New York, USA.

Brown, Aaron S. and Yang, Henry T.Y. Neural networks for multiobjective adaptive structural control. Journal of Structural Engineering. pp.203-210. Feb 2001.

Burke S E and Hubbard J E. Active vibration control of a simply-supported beam using a spatially distributed actuator. IEEE Control Systems Magazine. pp. 25-30. August 1987.

Cao, D.Q., Ko, J.M., Ni, Y.Q., and Liu, H.J. (2000), "Decentralized active tendon control and stability of cable-stayed bridges", Advances in Structural Dynamics, J.M. Ko and Y.L. Xu (eds.), Elsevier Science Ltd., Oxford, UK, Vol. II, 1257-1264.

Chandrashekhara K. and Varadarajan S. Adaptive Shape Control of Composite Beams with Piezoelectric Actuators. Journal of Intelligent Material Systems and Structures, Vol. 8. pp.112-118. Feb 1997.

Chen B.M. Robust and H control. London: Springer. 2000.

Chen B. M., Saberi A. and Sannuti P. A new stable compensator design for exact and approximate loop transfer recovery. Automatica, Vol. 27, No. 2. pp.257-280. March 1991.

Chen Chang-qing, Wang Xiao-ming and Shen Ya-peng. Finite element approach of vibration control using self-sensing piezoelectric actuators. Computers and Structures, Vol. 60, No. 3. pp.505-512. 1996.

Chiao Kuo-Ping. Least squares model reduction for non-classical damped linear systems. Journal of The Chinese Society of Mechanical Engineers. Vol. 17. No. 4. pp. 335-341. 1996.

Choi Youngjin and Chung Wan Kyun. On the stable H controller parameterization under sufficient conditions. IEEE Transactions on Automatic Control, Vol. 46, No. 10. pp.1618-1623. 2001.

Chopra, Anil K. and Goel, Rakesh K. A model pushover analysis procedure for estimating seismic demands for buildings. Earthquake engineering and structural dynamics. Vol. 31. pp.561-582. 2002.

Chopra Anil K. Dynamics of structures: theory and applications to earthquake . pp.engineering (2nd ed.). 844 pp. Upper Saddle River, New Jersey: Prentice-Hall. - 2000.

Clearwater, Scott H. Market-based control: a paradigm for distributed resource allocation. 311 pp. Singapore: World Scientific. 1996.

Cliff, Dave and Bruten, Janet. Simple Bargaining Agents for Decentralized Market-Based Control. HPL-98-17, Hewlett-Packard Company. 1998.

Collins Jr. Emmanuel G. and Song Tinglun. Robust H estimation and fault detection of uncertain dynamic systems. Journal of Guidance, Control and Dynamics, Vol. 23, No.5. pp.857-864. 2000.

Corless, M. Control of Uncertain Nonlinear Systems. Journal of Dynamic Systems, Measurements and Control, Vol. 115. pp.362-372. 1993.

Crawley E F and de Luis J. Experimental verification of distributed piezoelectric actuators for use in precision. Proc. 27th AIAA/ASME/ASCE/AHS Structures, Structural Dynamics, and Materials Conf. May 1986. San Antonio, USA.

Crawley E F and de Luis J. Use of piezo-ceramics as distributed actuators in large space structures. Proc. 26th AIAA/ASME/ASCE/AHS Structures, Structural Dynamics and Materials Conf. May 1985. San Antonio, USA.

Crawley, E.F. and K.B.Lazarus. Induced Strain Actuation of Isotropic and Anisotropic Plates. AIAA Journal, 29(6). pp.944-951. May 1985.

D'Azzo John J. and Costantine H. Houpis. Linear Control System Analysis and Design (Conventional and Modern). Singapore: McGraw-Hill Book International Company. 1981.

Delgado, D.U.C. and Zhou, K. Reconfigurable fault tolerant control using GIMC structure. MCU First Annual Report. 2002.
http://www.ece.lsu.edu/mcu/publications/year1.html

Detwiler D.T., Shen M.H.H. and Venkayya V.B. Finite element analysis of laminated composite structures containing distributed piezoelectric actuators and sensors. Finite Elements in Analysis and Design, Vol. 20. pp.87-100. 1995.

Doyle J.C. Guaranteed margins for LQG regulators. IEEE Transactions on Automatic Control, AC-23. pp.756-757. 1978.

Doyle, John. Analysis of feedback systems with structured uncertainty. IEEE Proceedings, V129, Part D, No.6. November, 1982.

Doyle, J.C., Glover, K., Khargonekar, P.P. and Francis, B.A. State-space solutions to standard H/sub 2/ and H/sub infinity / control problems. IEEE Transactions on Automatic Control, Vol. 34, No. 8. pp.831–847. 1989.

Fleming A.J. and Moheimani S.O.R. Adaptive piezo shunt damping. Smart Materials and Structures. Vol. 12. pp. 36-48. 2003.

Frank, Paul M. and Ding Xianchu. Frequency domain approach to optimally robust residual generation and evaluation for model-based fault diagnosis. Automatica, Vol. 30, No. 5. pp.789-804. 1994.

Fujino Y., Soong T.T. and Spencer B.F. Jr. Structural Control: Basic Concepts and Applications. Proc. of the 1996 ACSE Structures Congress. Chicago, Illinois. 1996.

Garg Devendra P., Zikry, Mohammed A. and Anderson Gary L. Current and potential future research activities in adaptive structures: an ARO perspective. Smart Materials and Structures, Vol. 10. pp.610-623. 2001.

Giurgiutiu, V., and C. A. Rogers. Energy-Based Comparison of Solid-State Induced-Strain Actuators. Journal of Intelligent Material Systems and Structures, Vol. 7, No.1. pp.4-14. 1996.

Goldberg D.E. Genetic Algorithms in Search, Optimization and Machine Learning. New York: Addison-Wesley Publishing Company. 1989.

Guo, Lei. Exploring the maximum capability of adaptive feedback. International Journal of adaptive control and signal processing, Vol. 16, Issue 6. pp.341-354. 2002.

Hall, A.C. The Analysis and Synthesis of Linear Servomechanisms. Cambridge, MA: The Technology Press, M.I.T. 1943.

Han M.C. and Chen Y.H. Decentralized control design: uncertain systems with strong interconnections. International Journal of Control, Vol. 61, No.6. pp.1363-1385. 1995.

Hart Gary C. and Wong Kevin. Structural Dynamics for Structural Engineers. USA: John Wiley & Sons. Chapter 10. 2000.

Holland J.H. Processing and processors for schemata. E.L. Jacks (Ed.), associaive information Processing. pp. 127-146. New York: Elsevier. 1971.

Holland J.H. Schemata and intrinsically parallel adaptation. Proc. NSF workshop of Learning systems: Theory and its Applications. 1973. Gainesville, University of Florida. pp.43-46.

Holland, J. H. Adaptation in Natural and Artificial Systems. USA: University of Michigan Press. 1975.

Hou, Z., Noori,M.N. and Shakeri,C. Smart Materials and Structures: A Review. Mechanical engineering Department, Worcestor Polytechnic Institute. 1996.

Housner G.W., Soong T.T. and Masri S.F. Second generation of active structural control in civil engineering. First World Conference on Structural Control. L.A., USA. 1994.

Housner G.W. et al. Structural control: past, present, and future. Journal of Structural Engineering, ASCE. Vol. 123. No. 9. pp. 897-971. 1997.

Hwang W S and Park H C. Finite element modeling of piezoelectric sensors and actuators. Journal of AIAA, Vol. 31. pp.930-937. 1993.

Ikeda, M., Maeda, H. and Kodama, S. Stabilization of linear systems. SIAM Journal of Control and Optimization, Vol. 10. pp. 716-729. 1972.

Jakubek S. and Jorgl H.P. Fault-dianosis and Fault-Compensation for Nonlinear Systems. 2000.

Jiang Z.P. and Mareels I. Robust Nonlinear Integral Control. IEEE Transactions on Automatic Control, Vol. 46, No. 8. August 2001.

Kalman R.E. On the general theory of control systems. Proc. First International Congress on Automatic Control. 1960. Moscow, Russia. pp.481-491.

Kalman R.E. When is a Linear Control System Optimal?. ASME Journal of Basic Engineering. pp.51-60. 1964.

Kwakernaak H. and Sivan R. Linear Optimal Control Systems. New York: John Wiley & Sons. 1972.

Kettle Paul, Murray Aengus and Holohan Anthony. Robust optimal servo motor controller design. Proc. of the International Conf. on Signal Processing Applications and Technology (ICSPAT). October 7-10, 1996. Boston, USA. pp.1196-1203.

Khargonekar P.P., Peterson I.R. and Zhou K. Robust stabilization of uncertain linear systems: quadratic stabilizability and H control theory. IEEE Transactions on Automatic Control, Vol. 35. pp.356-361. 1990.

Kim J.H. and Jabbari F. Actuator saturation and control design for buildings under seismic excitation. Journal of Engineering Mechanics, Vol. 128, No. 4. pp.403-412. 2002.

Ko J.M. and Xu Y.L. (ed). Advances in Structural Dynamics, Vol. II. pp.1257-1264. Oxford: Elsevier Science Ltd. (Cao, D.Q., Ko, J.M., Ni, Y.Q., and Liu, H.J. Decentralized active tendon control and stability of cable-stayed bridges.)

Ko J.M. and Xu Y.L. (ed). Advances in Structural Dynamics, Vol. II. pp.1405-1412. Oxford: Elsevier Science Ltd. (Wong K.K.F. and R. Yang. Optimal linear control of elastic structures with one-step time delay.)

Ko J.M. and Xu Y.L. (ed). Advances in Structural Dynamics, Vol. II. pp.1257-1264. Oxford: Elsevier Science Ltd. (Wong K.K.F. and R. Yang. Evaluation of inelastic structural energy during earthquake.)

Kobori T. The direction of earthquake resistant engineering. Journal of Architecture and Building Science. Vol. 73. pp. 5-9. 1958. (in Japanese)

Kobori T. Analytical study on active seismic response control: seismic-response-controlled structure 1. Transactions of Architectural Institute of Japan. Vol. 66. pp. 257-260. 1960. (in Japanese)

Koumboulis F.N. and Skarpetis M.G. Robust disturbance rejection and simultaneous robust input-output decoupling. Automatica, Vol. 33, No. 7. pp.1415-1421. 1997.

Krokavec, Dusan and Filasova, Anna. Unmatched Uncertainties in Robust LQ Control. IFAC Robust Control Design. Prague, Czech Republic. 2000.

Krysl, P., Lall, S. and Marsden , J.E. Dimensional model reduction in non-linear finite element dynamics of solids and structures. International Journal for Numerical Methods in Engineering. Vol. 51. pp. 479-504. 2001.

Lai W.L., Ang K.K. and Quek S.T. Layered decentralized vibration control. Proc. 2nd Int. Conf. On Structural Stability and Dynamics. 2002. Singapore. pp. 844-849.

Lam K.Y., Peng X.Q., G R Liu and Reddy J.N. A finite-element model for piezoelectric composite laminates. Smart Materials and Structures, Vol. 6. pp.583-591. 1997.

Laub A.J. A Schur Method for Solving Algebraic Riccati Equations. IEEE Transactions on Automatic Control, Vol. AC-24. pp.913-921. 1979.

Lee, C.K. Theory of Laminated Piezoelectric Plates for the Design of Distributed Sensors/Actuators. Part I: Governing Equations and Reciprocal Relationships. Journal of Acoustic Society of America, 87:114-1158. 1990.

Li Q.S., Fang J.Q., Jeary A.P. and Liu D.K. Decoupling control law for structural control implementation. International Journal of Solids and Structures, Vol. 38. pp.6147-6162. 2001.

Lin Feng and Olbrot, Andrzej W. An LQR Approach to Robust Control of Linear Systems with Uncertain Parameters. Proc. Of the 35th Conference on Decision and Control. December 1996. Kobe, Japan.

Loh Chin-Hsiung and Chung Shung-Tsair. Probabilistic assessment in seismic demand: uncertainty treatment. Proc. 15th KKCNN Symposium on Civil Engineering. 2002. Singapore. pp. S184-S191.

Loh Chin-Hsiung, Lin Chi Ying and Huang Chih Vhieh. Time domain identification of frames under earthquake loadings. Journal of Engineering Mechanics. pp.693-703. July 2000.

Lu Li-Teh, Chiang Wei-Ling and Tang Jhy-Pyng. LQG/LTR control methodology in active structural control. ASCE Journal of Engineering Mechanics, Vol. 124, No. 4. pp. 446-454. April 1998.

Lukas M. Distributed control systems: their evaluation and design. Van Nostrand Reinhold Company. New York. pp. 1-16. 1986.

Lunze J. Feedback Control of Large-Scale Systems. pp. 1-6. New York: Prentice Hall. 1992.

Lunze J. Robust Multivariable Feedback Control. 221 pp. UK: Prentice Hall. 1989.

Luo N., Rodellar J.J., de la Sen M. and Magana M.E. Decentralized Model Reference Variable Structure Control of Multi-Cable-Stayed Bridges. International Journal of Control, Vol.75, No.4. pp.285-296. 2002.

Lynch, Jerome Peter and Law, Kinocho H. A market-based control solution for semi-active structural control. Computing in civil and building engineering. Proc. of the 8th International Conference. August 14-16, 2000. Stanford, CA, USA.

Lynch, Jerome Peter and Law, Kinocho H. Formulation of a market-based approach for structural control. Proc. of the 19th International Modal Analysis Conference. Feb 5-9, 2001. Orlando, USA.

Lynch, Jerome Peter and Law, Kinocho H. Market-based control for linear structural systems. Earthquake engineering and structural dynamics, Vol. 31. pp.1855-1877. 2002.

M.C. Ray. Optimal Control of Laminated Plate with Piezoelectric sensor and Actuator Layers. AIAA Journal, 36(12):2204-2208. 1998.

Magana, Mario E. and Rodellar, Jose J. Active nonlinear robust control of cable-stayed bridges in the presence of strong vertical ground motion due to earthquakes. In Proc. of the 2nd World Conference on Structural Control, Vol. 2. 1998. Kyoto, Japan. pp. 1947-1955.

Maguire, J.R. & Wyatt, T.A. Dynamics: An Introduction for Civil and Structural Engineers (ICE Design and Practice Guide). American Society of Civil Engineers. 1999.

Maciejowski, J.M.. Multivariable Feedback Design. Addison-Wesley, 1989.

Makola M.Abdullah, Andy Richardson and Jameel Hanif. Placement of sensors/actuators on civil structures using genetic algorithms. Earthquake Engineering and Structural Dynamics, Vol. 30. pp.1167-1184. 2001.

Maxime P. Bayon de Noyer and Sathya V. Hanagud. Single Actuator and Multi-mode Acceleration Feedback Control. Georgia Institute of Technology, School of Aerospace Engineering. Atlanta, Georgia 30332-0150. 1997.

Meirovitch, Leonard. Fundamentals of Vibrations. New York: McGraw-Hill Higher Education. pp.268-273. 2000.

Michael B. McFarland and Anthony J. Calise. Adaptive nonlinear control of agile antiair missiles using neural networks. IEEE Transactions on Control Systems Technology, Vol. 8, No. 5. pp.749-756. Sep 2000.

Newton, G.C. Jr., Gould, L.A. and Kaiser, J.F. Analytical Design of Linear Feedback Controls. New York: John Wiley & Sons. 1957.

Nicholson, Walter. Intermediate microeconomics and its applications, 7th edition. 573 pp. USA: The Dryden Press. 1997.

Nishitani, Akira, Nitta,Yoshiro and Yamada,Seiji. Model reduction for active-controlled building structures. Proc. of the 2nd World Conference on Structural Control, Vol. 2. 1998. Kyoto, Japan. pp.2231-2240.

Nishitani, A. and Inoue, Y. Overview of the application of active/semiactive control to building structures in Japan. Earthquake Engineering and Structural Dynamics. Vol. 30. pp. 1565-1574. 2001.

Ogata Katushiko. Designing linear control systems with Matlab. International Edition. pp.185-209. Prentice Hall. 1994.

Ogata Katushiko. Modern Control Engineering (3rd Edition). 997 pp. Prentice Hall. 1996.

Ohtori, Y., Spencer, B.F., Christenson, R.E. and Dyke, S.J. Next generation benchmark control problem for seismically excited buildings. http://www.nd.edu/~quake. 1998.

Ohtori., Y. and Spencer, B.F., Jr. A Matlab-based tool for nonlinear structural analysis. In the Proceedings of the 13th ASCE Engineering Mechanics Division Specialty Conference. June 13-16, 1999. John Hopkins University, Baltimore.

Osama J. Aldraihem, Robert C. Wetherhold and Tarunraj Singh. Distributed Control of Laminated Beams: Timoshenko Theory vs. Euler-Bernoulli Theory. Journal of Intelligent Material Systems and Structures, Vol. 8. pp.149-156. Feb 1997.

Ozbay, Hitay. Introduction to Feedback Control Theory. CRC Press. 2000.

Rao, G Venkateswara and Gajbir Singh. A Smart structures concept for the buckling load enhancement of columns. Smart Materials and Structures, Vol. 10. pp.843-845. 2001.

Richter, C. F. An instrumental earthquake scale. Bulletin of the Seismological Society of America. No. 25. pp. 1-32. 1935

Rune Brincker, Lingmi Zhang and Palle Andersen. Modal identification of output-only systems using frequency domain decomposition. Smart Materials and Structures, Vol. 10. pp.441-445. 2001.

Schetter, Thomas, Campbell, Mark and Surka, DDDerek. Comparison of Multiple Agent-Based Organisations for Satellite Constellations (TechSat21). American Association for Artificial Intelligence. 2000.

Sestieri A. Structural dynamic modification. , Vol. 25, Part 3. pp.247-259. June 2000.

Seo Chang-Jun, Kim Byung Kook. Robust and Reliable H Control for Linear Systems with Parameter Uncertainty and Actuator Failure. Automatica, Vol.32, No.3. pp.465-467. 1996.

Siljak D.D. Decentralized control of complex systems. Academic Press: Boston. 1991. pp. 1-65.

Siljak D.D. and Stipanovic D. M. Organically-Structured Control. American Control Conference. June 25-27, 2001. Arlington, Virginia USA.

Smith, A. An Inquiry into the nature and cause of the wealth of nations. Rowman and Littlefield: Maryland. 1992.

Sohn, Hoon and Law, Kincho H. Extraction of Ritz vectors from vibration test data. Mechanical Systems and Signal Processing. Vol. 15, No. 1. pp. 213-226. 2001.

Sontag, E.D. On the input-to-state stability property. Euro. J. Control, Vol. 1. pp.24-36. 1995.

Soong, T.T. Active Structural Control: Theory and Practice. Essex, England: Longman Scientific and Technical. 1990.

Soong, T.T. and Spencer Jr. B.F. Supplemental energy dissipation: state-of-the-art and state-of-the-practice. Engineering Structures. Vol. 24. pp. 243-259. 2002.

Spencer Jr. B.F. and Sain M.K. Controlling buildings: A new frontier in feedback. IEEE Control Systems. Vol.17. pp. 19-35. 1997.

Stone, Peter. Layered Learning in Multi-Agent Systems: A Winning Approach to Robotic Soccer. MIT Press. 2000.

Stricker, Andrew and Shea, Elizabeth. White Paper: Distributed Intelligent Agents. Cognition and Instructional Technologies Laboratories. 1999.

akayoshi, Kamada; Takafumi Fujita, Takayoshi Hatayama, Takeo Arikabe, Nobuyoshi Murai, Satoru Aizawa and Kohtaro Tohyama. Active vibration control of frame structures with smart structures using piezoelectric actuators. Smart Materials and Structures, Vol. 6. pp.448-456. 1997.

Takayoshi, Kamada; Takafumi Fujita, Takayoshi Hatayama, Takeo Arikabe, Nobuyoshi Murai, Satoru Aizawa and Kohtaro Tohyama. Active vibration control of flexural-shear type frame structures with smart structures using piezoelectric actuators. Smart Materials and Structures, Vol. 7. pp.479-488. 1998.

Takewaki, Izuru. Seismic critical exciation method for robust design: a review. Journal of Structural Engineering. Vol. 128, No. 5. pp. 665-672. 2002.

Tao, Gang, Chen Shuhao & Joshi Suresh M. Adaptive state feedback and tracking control of systems with actuator failures. IEEE Transactions on Automatic Control, Vol. 46, No. 1. pp.78-95. 2001.

Tao Gang, Chen Shuhao and Joshi S.M. An adaptive control scheme for systems with unknown actuator failures. Automatica, Vol. 38. pp.1027-1034. 2002.

Tiersten, H.F. Linear Piezoelectric Plate Vibration. Plenum Press. 1969.

Timoshenko, S. Theory of Plates and Shells. 492 pp. New York and London: McGraw-Hill Book Company, Inc. 1940.

Tzou H S and Tseng C I. Distributed piezoelectric sensor/actuator design for dynamic measurement/control of distributed parametric systems: a piezoelectric finite element approach. Journal of Sound and Vibration, Vol. 138. pp.17-34. 1990.

Utku, S. Theory of adaptive structures: incorporating intelligence into engineered products. Boca Raton. CRC Press. 1998.

Vaughn D.R. A Nonrecursive Algebraic Solution for the Discrete Riccati Equation. IEEE Transactions on Automatic Control, Vol. AC-15. pp.597-599. 1970.

Veillette, R.J., J.V. Medanic and W.R. Perkins. Design of reliable control systems. IEEE Trans. Autom. Control, AC-37. pp.290-304. 1992.

Wang Sheng Guo, Yeh Y.H. and Roschke Paul N. Robust control for structural systems with parametric and unstructured uncertainties. Proc. of the American Control Conference. June 25-27, 2001. Arlington, VA.

Wang S Y, Quek S T and Ang K K. Vibration control of smart piezoelectric composite plates. Smart Materials and Structures, Vol. 10. pp.637-644. 2001.

Wang Zidong, Huang Biao and Unbehauen H. Robust reliable control for a class of uncertain nonlinear state-delayed systems. Automatica, Vol. 35. pp.955-963. 1999.

Wang Zidong and Unbehauen H. Robust H2/H -state estimation for systems with error variance constraints: the continuous-time case. IEEE Transactions on Automatic Control, Vol. 44, No. 5. pp.1061-1065. 1999.

Wang Zidong, Huang Biao and Unbehauen. Robust reliable control for a class of uncertain nonlinear state-delayed systems. Automatica. Vol.35. pp.955-963. 1999.

Wiener N. Extrapolation, Interpolation, and Smoothing of Stationary Time Series. Cambridge, MA: MIT Press. 1949.

Wong K.K.F and Wang Y. Probabilistic structural damage assessment and control based on energy approach. The Structural Design of Tall Buildings. pp.283-308. 2001.

Wong K.K.F and Wang Y. Seismic energy dissipation in structures using active control. Proc. 2nd Int. Conf. On Structural Stability and Dynamics. 2002. Singapore. pp. 850-855.

Wood, H.O., and Neumann F. Modified Mercalli Intensity Scale of 1931. Bulletin of the Seismological Society of America. No. 21. pp. 277-283. 1931.

Wooldridge, Michael. An introduction to MultiAgent Systems. 348pp. England: John Wiley & Sons Ltd. 2002.

Xie, L. and C.E. de Souza. Robust H control for linear systems with norm-bounded time-varying uncertainty. IEEE Transactions on Automatic Control, AC-37. pp.1188-1191. 1992.

Yang Guang-Hong, Wang Jian Liang, Soh Yeng Chai. Reliable H controller design for linear systems. Automatica, Vol. 37, No. 5. pp.717-725. 2001.

Yao J.T.P. Concept of Structural Control. J. Struct. Div., ASCE, Vol. 98. pp.1567-1574. 1972.

Yao Jinyi, Chen Jiang, Cai Yunpang and Li Shi. Architecture of TsinghuAeolus. http://www.lits.tsinghua.edu.cn/RoboCup/robo_ENG/software/software_client.html. 2001.

Zames G. Feedback and optimal sensitivity: Model reference transformations, multiplicative seminorms, and approximate inverses. IEEE Transactions on Automatic Control, AC-26. pp.301-320. 1981.

Zeren, M. and Ozbay, H. On the strong stabilization and stable H controller design problems for MIMO systems. IEEE Transactions on Automatic Control, vol.36. pp.1675-1684. November 2000.

Zhou, K. and Chen X.J. Are the tradeoffs between performance and robustness intrinsic for feedback systems? MCU First Annual Report. 2002. http://www.ece.lsu.edu/mcu/publications/year1.html

Zhou, K., Doyle J.C. and Glover H. Robust and Optimal Control. Prentice Hall. Upper Saddle River. N.J. 1996.

Zhou Kemin and Zhang Ren. A new controller architecture for high performance, robust, and fault-tolerant control. IEEE Transactions on Automatic Control, Vol. 46, No. 10. pp.1613-1618. 2001.

Zhou Qin. Dynamic Response of Frame-Core Wall Tall Buildings to Wind Load. M.Eng Thesis. National University of Singapore. 1994.

APPENDIX: MATLAB PROGRAMS

Chapter 2

```
% Model reduction: Chopra 1995
% vq68.m, nbeta8.m, test.m, nishitani.m
%

% Actual FOM:
m1=1e6;  % kg
m2=7e5;
c=0;
k1=1.47e9;  % N/m
k3=1.372e9;
k5=1.274e9;
k7=1.176e9;
k9=1.078e9;
k11=0.98e9;
k13=0.931e9;
k14=0.882e9;
k15=0.833e9;
k16=0.784e9;
k17=0.735e9;
k18=0.686e9;
k19=0.637e9;
k20=0.588e9;



% discrete MDOF:
md=[m1 m1 m1 m1 m1 m1 m1 m1 m1 m1 m1 m1 m1 m1 m1 m1 m1 m1 m1 m2];
kd=[k1 k1 k3 k3 k5 k5 k7 k7 k9 k9 k11 k11 k13 k14 k15 k16 k17 k18 k19
k20];
%md=[m1 m1 ];
%kd=[k1 k1 ];
%cd=zeros(1,length(md));
cd=kd/100;
%
M=zeros(length(md));
K=zeros(length(md));
Cd=zeros(length(md));
for i=1:length(md)
   M(i,i)=M(i,i)+md(i);
   if i==1
      K(i,i)=K(i,i)+kd(i);
      Cd(i,i)=Cd(i,i)+cd(i);
   else
      K(i-1,i-1)=K(i-1,i-1)+kd(i);
      K(i-1,i)=K(i-1,i)-kd(i);
      K(i,i-1)=K(i,i-1)-kd(i);
      K(i,i)=K(i,i)+kd(i);
      Cd(i-1,i-1)=Cd(i-1,i-1)+cd(i);
      Cd(i-1,i)=Cd(i-1,i)-cd(i);
      Cd(i,i-1)=Cd(i,i-1)-cd(i);
      Cd(i,i)=Cd(i,i)+cd(i);
   end
end

disp('Model Reduction retaining modal characteristics');
[ev,w,ms0]=vtb4_1(M,K);
```

```
disp('Mode shape 1: ');
%ms0(:,1)/ms0(20,1)
%pause
disp('Mode shape 2: ');
%ms0(:,2)/ms0(8,2)
%pause
disp('Mode shape 3: ');
%ms0(:,3)/ms0(5,3)
%pause
f=w/2/pi;   % natural freq (Hz)

%=====================================================================
% Chopra: Rayleigh-Ritz generalisation of froce dependent vectors:
%=====================================================================
S=-M*ones(length(md),1);
dmodes=input('Enter the max mode to be included: ');
a=zeros(dmodes);
y=zeros(length(md),1,dmodes);
ms=zeros(length(md),1,dmodes);
msc=zeros(length(md),1,dmodes);
msb=[];
for i=1:dmodes
   if i==1
      y(:,:,i)=K\S;
      ms(:,:,i)=y(:,:,i)/sqrt(y(:,:,i)'*M*y(:,:,i));

   else
      y(:,:,i)=K\M*ms(:,:,i-1);
      a(i-1,i)=ms(:,:,i-1)'*M*y(:,:,i);
      msc(:,:,i)=y(:,:,i);
      for j=1:i-1
         msc(:,:,i)=msc(:,i) - a(j,i)*ms(:,:,j);
      end
      y(:,:,i)=msc(:,:,i);
      ms(:,:,i)=y(:,:,i)/sqrt(y(:,:,i)'*M*y(:,:,i));

   end
   msb=cat(2,msb,ms(:,:,i));

end

Mb=msb'*M*msb;
Cb=msb'*Cd*msb;
Kb=msb'*K*msb;
%Fb=msb'*F;
Hb=msb'*S;
[evb,wb,ms0b]=vtb4_1(Mb,Kb);
w(1:dmodes)
wb

%==========================
% Uncertainties: dM, dC, dK
% Sestieri
%==========================
disp('Uncoupled Ritz ROM: ');
Mbr=ms0b'*Mb*ms0b;
Cbr=ms0b'*Cb*ms0b;
Kbr=ms0b'*Kb*ms0b;
%Fbr=ms0b'*Fb;

dM=0.1*M;
```

```
dC=0.1*Cd;
dK=0.1*K;

M1b=Mb+msb'*dM*msb;
C1b=Cb+msb'*dC*msb;
K1b=Kb+msb'*dK*msb;

disp('Ritz vectors on uncertainties');
[ev1b,w1b,ms1b]=vtb4_1(M1b,K1b);
S1=msb'*S;
a=zeros(dmodes);
y=zeros(dmodes,1,dmodes);
ms=zeros(dmodes,1,dmodes);
msc=zeros(dmodes,1,dmodes);
ms1b=[];
for i=1:dmodes
   if i==1
      y(:,:,i)=K1b\S1;
      ms(:,:,i)=y(:,:,i)/sqrt(y(:,:,i)'*M1b*y(:,:,i));

   else
      y(:,:,i)=K1b\M1b*ms(:,:,i-1);
      a(i-1,i)=ms(:,:,i-1)'*M1b*y(:,:,i);
      msc(:,:,i)=y(:,:,i);
      for j=1:i-1
         msc(:,:,i)=msc(:,i) - a(j,i)*ms(:,:,j);
      end
      y(:,:,i)=msc(:,:,i);
      ms(:,:,i)=y(:,:,i)/sqrt(y(:,:,i)'*M1b*y(:,:,i));

   end
   ms1b=cat(2,ms1b,ms(:,:,i));

end


% Actual Ritz vector characteristics
w2b=w1b;
ms2b=msb*ms1b;
disp('ms2b(t)*(M+dM)*ms2b = I');
M2b=ms2b'*(M+dM)*ms2b;
C2b=ms2b'*(Cd+dC)*ms2b;
K2b=ms2b'*(K+dK)*ms2b;
%F2b=ms2b'*F;
H2b=ms2b'*S;
[evb3,w3b,ms3b]=vtb4_1(M2b,K2b);

%===================================
% Control devices:
% Source: Benchmark sample controls
% ctrlr_20.m
%===================================
%ndev_flr= [4 2 2 ones(1,17)];      % number of actuators on each
floor
ndev_flr= [10 zeros(1,9) 10 zeros(1,9)];
%K1      = diag(ndev_flr); % multiple actuators per floor
K1=zeros(length(md),2);
K1(1,1)=5;
K1(length(md)/2+1,2)=5;
K2 = eye(length(md));      % each actuator is connected between 2
floors
```

```
K2(1:(length(md)-1),2:length(md)) = K2(1:(length(md)-
1),2:length(md))-eye((length(md)-1));  % force is = and opposite
%K2=[1 -1; 0 1];
Max_frc = 700e3;     % Maximum Force of Devices
Max_voltd = 10;      % Maximum Voltage of Control Signal
gain_ctr = Max_frc/Max_voltd; % Gain
Bu      = K2*K1*gain_ctr;  % output force gain matrix

Bub=msb'*Bu;
Bu2b=ms2b'*Bu;

Max_voltd = 200;
% Decentralised Nominal Controls
% magana.m
%
m=1;

Af=[zeros(dmodes) eye(dmodes);-Mb\Kb -Mb\Cb];
xdof=dmodes;
Bf=[zeros(dmodes); Mb\Bub];
Hf=[zeros(dmodes,1); Mb\Hb];
Cf=Af(xdof+1:2*xdof,:);%[zeros(2) eye(2)];
dAf=0*Af;
dBf=-0*Bf;
dHf=0*Hf;

disp('Subsystem decentralized: ');
% address each of 4 quadrants:
A1=Af(1:xdof,1:xdof);
A2=Af(1:xdof,xdof+1:2*xdof);
A3=Af(xdof+1:2*xdof,1:xdof);
A4=Af(xdof+1:2*xdof,xdof+1:2*xdof);
for i=1:xdof
   for j=1:xdof
      if i==j
         Aii(1,1,i)=A1(i,j);
         Aii(1,2,i)=A2(i,j);
         Aii(2,1,i)=A3(i,j);
         Aii(2,2,i)=A4(i,j);
      else
         Aij(1,1,i)=A1(i,j);
         Aij(1,2,i)=A2(i,j);
         Aij(2,1,i)=A3(i,j);
         Aij(2,2,i)=A4(i,j);
      end
   end
   B(:,:,i)=[Bf(i,i);Bf(i+xdof,i)];
   C(:,:,i)=Aii(2,:,i);
   Cij(:,:,i)=Aij(2,:,i);
   H(:,:,i)=[Hf(i);Hf(i+xdof)];
end

dA=0*Aii;
dAij=0*Aij;
dB=-0*B;
dH=0*H;

% Classical LTR for K:
q2=[500 1e3 1e4];   % square of q
for i=1:dmodes
   sys=ss(Aii(:,:,i),B(:,:,i),C(:,:,i),0);
```

```
   Lp=tf(sys); % plant tf
   if zero(sys)>0
      error('Unstable zeros => non-minimum phase');
   else
      disp('Stable invariant zeros => minimum phase');
   end
   Ps=tf(sys);
   disp('Test for invertible plant:');
   Psi=inv(Ps);
   w=Psi*Ps
   [num,den] = TFDATA(w,'v');
   if residue(num,den)==0
      disp('plant invertible');
   else
      error('plant Not invertible');
   end
   disp('Verify invertible');
   disp('LTR recoverable');

   for k=1:length(q2)
      Qe=q2(k)^2*B(:,:,i)*B(:,:,i)';
      Re=eye(size(C(:,:,i)',2));
      [Kt(:,:,k),Pt,E] = LQR(Aii(:,:,i)',C(:,:,i)',Qe,Re);
      KK(:,:,k)=Kt(:,:,k)';
   end
   Kf(:,:,i)=KK(:,:,1);

   disp('Simple LQR');
   Q(:,:,i)=C(:,:,i)'*100*C(:,:,i);   % control acceleration:
minimised
   R(:,:,i)=1e-2;
   Kc(:,:,i)=lqr(Aii(:,:,i),B(:,:,i),Q(:,:,i),R(:,:,i));

   % Decentralized nonlinear control: Magana & Rondellar
   Fi(:,:,i)=Aii(:,:,i)-B(:,:,i)*Kc(:,:,i);
   Pi(:,:,i)=lyap(Fi(:,:,i),[1 0;0 100]);
   d(i)=7.68;
   e(i)=8;
end


disp('Simulink subsystems');
[EQ,T]=elcent3;

disp('Simple LQR');
Qf=Cf'*100*eye(2)*Cf;   % control acceleration: minimised
Rf=1e-2*eye(2);
Kcf=lqr(Af,Bf,Qf,Rf);

% Classical LTR for K:
for k=1:length(q2)
   Qef=q2(k)^2*Bf*Bf';
   Ref=1e-2*eye(size(Cf',2));
   [Ktf(:,:,k),Pt,E] = LQR(Af',Cf',Qef,Ref);
   Ktt(:,:,k)=Ktf(:,:,k)';
end
Kff=Ktt(:,:,1);
disp('Simulink FOM system');
%maganaSf310303
maganaSf310303b
```

```
choice=input('Press Enter to plot graphs: ');
xdof=length(Af)/2;
dt=0.02;
%Fsf=expm(Af*dt);  % Uncon
%Hdf=Af\(Fsf-eye(2*xdof));
%Gf=Af\(Fsf-eye(2*xdof))*Bf;
%Hdsf=Hdf*Hf;

% Evaluation in discrete time
%z0=zeros(2*xdof,1);
Tb=T;
%tspan=[0 Tb(length(Tb))];
%zuf=zeros(2*xdof,length(Tb));
%for i=1:length(Tb)
%    if i==1
%       zuf(:,i)=z0;
%    else
%      zuf(:,i)=Fsf*zuf(:,i-1)+Hdsf*EQ(i);
%    end
%end

% Actual:
Trange=[Tb(1) Tb(length(Tb))];
dt=0.02;
s=zeros(length(md),1);
v=s;a=s;
delta=0.5;  % gamma
beta=0.25;
%Fb=-Mb*ones(2,1)*EQ;
Fs=-M*ones(length(md),1)*EQ;
[t,zuf(1:length(md),:),zuf(length(md)+1:(2*length(md)),:),ddx]=nbeta8
(M,Cd,K,Fs,dt,Trange,s,v,a,delta,beta);

% Original DOF
xdof=length(md);

% Transmitted acceleration
zauf=[zuf(xdof+1:2*xdof,:);ddx];%Fsf*zuf+Hdsf*EQ;

% For absolute acceleration:
zauf(xdof+1:2*xdof,:)=zauf(xdof+1:2*xdof,:)+ones(xdof,1)*EQ;

% Interpolate
for i=1:xdof
   zu1f(:,i) = INTERP1(Tb,zuf(i,:),simoutfd(:,1));
   zu2f(:,i) = INTERP1(Tb,zuf(xdof+i,:),simoutfd(:,1));
   zu3f(:,i) = INTERP1(Tb,zauf(xdof+i,:),simoutfd(:,1));
end

disp('For Absolute acceleration: ');
EQff = INTERP1(Tb,EQ,simoutff(:,1));
EQfd = INTERP1(Tb,EQ,simoutfd(:,1));

accf(:,1:xdof)=(msb*simoutff(:,8:9)')'+EQfd*ones(1,xdof);
accd(:,1:xdof)=(msb*simoutfd(:,8:9)')'+EQfd*ones(1,xdof);

dispff=(msb*simoutff(:,2:dmodes+1)')';
velff=(msb*simoutff(:,dmodes+2:2*dmodes+1)')';

dispfd=(msb*simoutfd(:,2:dmodes+1)')';
velfd=(msb*simoutfd(:,dmodes+2:2*dmodes+1)')';
```

```
% Drifts:
for i=1:xdof
   if i==1
      % Inter-story drift
      driftu(:,i)=zu1f(:,i);
      driftff(:,i)=dispff(:,i+1);
      driftfd(:,i)=dispfd(:,i+1);

      % Inter-story velocity drift
      dvelu(:,i)=zu2f(:,i);
      dvelff(:,i)=velff(:,i);
      dvelfd(:,i)=velfd(:,i);

   else
      % Inter-story drift
      driftu(:,i)=zu1f(:,i)-zu1f(:,i-1);
      driftff(:,i)=dispff(:,i)-dispff(:,i-1);
      driftfd(:,i)=dispfd(:,i)-dispfd(:,i-1);

      % Inter-story velocity drift
      dvelu(:,i)=zu2f(:,i)-zu2f(:,i-1);
      dvelff(:,i)=velff(:,i)-velff(:,i-1);
      dvelfd(:,i)=velfd(:,i)-velfd(:,i-1);
   end
end

nos30=0.9*length(velfd);
loc=1;
while loc~=0
   loc=input('Enter storey location or 0 to end: ');
   if loc==0 & length(loc)==1 ,break,end
   %choice=input('Compare inter-story drifts & abs acc');
   disp('1st subsystem: ');
   disp('No control: (drift, drift vel., abs acc)');
   max(abs(driftu(:,loc)))
   max(abs(dvelu(:,loc)))
   max(abs(zu3f(:,loc)))
   disp('LQR control: (drift, drift vel., abs acc, control)');
   max(abs(driftff(:,loc)))
   max(abs(dvelff(:,loc)))
   max(abs(accf(:,loc)))
   %max(abs(simoutfd(:,10)))
   disp('Nominal control: (drift, drift vel., abs acc, control)');
   max(abs(driftfd(:,loc)))
   max(abs(dvelfd(:,loc)))
   max(abs(accd(:,loc)))
   %max(abs(simoutfd(:,10)))

   if loc==10
      disp('10th DOF of 20DOF System');
      figure;
      subplot(411);plot(simoutfd(1:nos30,1),driftu(1:nos30,loc),'-
',simoutfd(1:nos30,1),driftfd(1:nos30,loc),'-
*',simoutff(1:nos30,1),driftff(1:nos30,loc),'-
o');grid;legend('Uncontrolled','Decen','FOM-LQR');
      title('');xlabel('');ylabel('Drift (m)');
      subplot(412);plot(simoutfd(1:nos30,1),dvelu(1:nos30,loc),'-
',simoutfd(1:nos30,1),dvelfd(1:nos30,loc),'-
*',simoutff(1:nos30,1),dvelff(1:nos30,loc),'-
o');grid;legend('Uncontrolled','Decen','FOM-LQR');
```

```
      title('');xlabel('');ylabel('Velocity drift (m/s)');
      subplot(413);plot(simoutfd(1:nos30,1),zu3f(1:nos30,1),'-
',simoutfd(1:nos30,1),accd(1:nos30,loc),'--
',simoutff(1:nos30,1),accf(1:nos30,loc),'-
.');grid;legend('Uncontrolled','Decen','FOM-LQR');
      title('');xlabel('');ylabel('Abs Acc (m/s/s)');

subplot(414);plot(simoutfd(1:nos30,1),simoutfd(1:nos30,4*dmodes+2),'-
',simoutff(1:nos30,1),simoutff(1:nos30,4*dmodes+2),'--
');grid;legend('Decen','FOM-LQR');
      title('');xlabel('time(s)');ylabel('Control (V)');

   elseif loc==20
      disp('20th DOF of 20DOF System');
      figure;
      subplot(411);plot(simoutfd(1:nos30,1),driftu(1:nos30,loc),'-
',simoutfd(1:nos30,1),driftfd(1:nos30,loc),'-
*',simoutff(1:nos30,1),driftff(1:nos30,loc),'-
o');grid;legend('Uncontrolled','Decen','FOM-LQR');
      title('');xlabel('');ylabel('Drift (m)');
      subplot(412);plot(simoutfd(1:nos30,1),dvelu(1:nos30,loc),'-
',simoutfd(1:nos30,1),dvelfd(1:nos30,loc),'-
*',simoutff(1:nos30,1),dvelff(1:nos30,loc),'-
o');grid;legend('Uncontrolled','Decen','FOM-LQR');
      title('');xlabel('');ylabel('Velocity drift (m/s)');
      subplot(413);plot(simoutfd(1:nos30,1),zu3f(1:nos30,1),'-
',simoutfd(1:nos30,1),accd(1:nos30,loc),'--
',simoutff(1:nos30,1),accf(1:nos30,loc),'-
.');grid;legend('Uncontrolled','Decen','FOM-LQR');
      title('');xlabel('');ylabel('Abs Acc (m/s/s)');

subplot(414);plot(simoutfd(1:nos30,1),simoutfd(1:nos30,4*dmodes+3),'-
',simoutff(1:nos30,1),simoutff(1:nos30,4*dmodes+3),'--
');grid;legend('Decen','FOM-LQR');
      title('');xlabel('time(s)');ylabel('Control (V)');

   end

   % plot only 1st 10s:
   nos30=nos30/2;

   figure;

subplot(311);plot(simoutfd(1:700:nos30,1),driftu(1:700:nos30,loc),'-
',simoutfd(1:700:nos30,1),driftfd(1:700:nos30,loc),'-
*',simoutff(1:700:nos30,1),driftff(1:700:nos30,loc),'-
o');grid;legend('Uncontrolled','Decen-n','LQR');
   title('');xlabel('');ylabel('Drift (m)');

subplot(312);plot(simoutfd(1:700:nos30,1),dvelu(1:700:nos30,loc),'-
',simoutfd(1:700:nos30,1),dvelfd(1:700:nos30,loc),'-
*',simoutff(1:700:nos30,1),dvelff(1:700:nos30,loc),'-
o');grid;legend('Uncontrolled','Decen-n','LQR');
   title('');xlabel('');ylabel('Velocity drift (m/s)');
   subplot(313);plot(simoutfd(1:700:nos30,1),zu3f(1:700:nos30,1),'-
',simoutfd(1:700:nos30,1),accd(1:700:nos30,loc),'-
*',simoutff(1:700:nos30,1),accf(1:700:nos30,loc),'-
o');grid;legend('Uncontrolled','Decen-n','LQR');
   title('');xlabel('time(s)');ylabel('Abs Acc (m/s/s)');

   figure;
```

```
subplot(211);plot(simoutfd(1:700:nos30,1),simoutfd(1:700:nos30,4*xdof
+2),'-',simoutff(1:700:nos30,1),simoutff(1:700:nos30,4*dmodes+2),'--
');grid;legend('Decen','FOM-LQR');
   title('');xlabel('time(s)');ylabel('Control (V)');

subplot(212);plot(simoutfd(1:700:nos30,1),simoutfd(1:700:nos30,4*xdof
+3),'-',simoutff(1:700:nos30,1),simoutff(1:700:nos30,4*dmodes+3),'--
');grid;legend('Decen','FOM-LQR');
   title('');xlabel('time(s)');ylabel('Control (V)');

   figure;

subplot(311);plot(simoutfd(1:700:nos30,1),driftfd(1:700:nos30,loc),'-
o',simoutff(1:700:nos30,1),driftff(1:700:nos30,loc),'-
');grid;legend('Decen-n','LQR');
   title('');xlabel('');ylabel('Drift (m)');ylim([-1.4e-5 9e-6])

subplot(312);plot(simoutfd(1:600:nos30,1),dvelfd(1:600:nos30,loc),'-
o',simoutff(1:600:nos30,1),dvelff(1:600:nos30,loc),'-
');grid;legend('Decen-n','LQR');
   title('');xlabel('');ylabel('Velocity drift (m/s)');ylim([-1e-4
2e-4])
   subplot(313);plot(simoutfd(1:700:nos30,1),accd(1:700:nos30,loc),'-
o',simoutff(1:700:nos30,1),accf(1:700:nos30,loc),'-
');grid;legend('Decen-n','LQR');
   title('');xlabel('time(s)');ylabel('Abs Acc (m/s/s)');

   figure;
   subplot(311);plot(simoutfd(1:nos30,1),driftfd(1:nos30,loc),'-
o',simoutff(1:nos30,1),driftff(1:nos30,loc),'-');grid;legend('Decen-
n','LQR');
   title('');xlabel('');ylabel('Drift (m)');ylim([-2e-5 9e-6])
   subplot(312);plot(simoutfd(1:nos30,1),dvelfd(1:nos30,loc),'-
o',simoutff(1:nos30,1),dvelff(1:nos30,loc),'-');grid;legend('Decen-
n','LQR');
   title('');xlabel('');ylabel('Velocity drift (m/s)');ylim([-1e-4
2e-4])
   subplot(313);plot(simoutfd(1:nos30,1),accd(1:nos30,loc),'-
o',simoutff(1:nos30,1),accf(1:nos30,loc),'-');grid;legend('Decen-
n','LQR');
   title('');xlabel('time(s)');ylabel('Abs Acc (m/s/s)');

end
```

Chapter 3

```
% Magana decentralized control
% u(t) = LQRy + v(t): nonlinear controls
% ICSSD
% jm130403a.m
%=======================================

uncertain=0.1;
failure=0.5;
n=1;
m=1;
Ms=[1 0;0 1];
Ks=-[-7.2980 2.7761; 2.7761 -62.8417];
Cs=-[-0.0730 0.0278; 0.0278 -0.6284];
An=[zeros(2) eye(2);-Ms\Ks -Ms\Cs];
```

```
xdof=length(An)/2;
Bn=[zeros(2);  -12.1596 -8.9808; 53.0676 -27.8441];   %[zeros(2);
eye(2)];
Hn=[0;0;4022;-1530];
Cn=An(xdof+1:2*xdof,:);%[zeros(2) eye(2)];
Dn=eye(2);


disp('Subsystem decentralized: ');
% address each of 4 quadrants:
A1=An(1:xdof,1:xdof);
A2=An(1:xdof,xdof+1:2*xdof);
A3=An(xdof+1:2*xdof,1:xdof);
A4=An(xdof+1:2*xdof,xdof+1:2*xdof);
for i=1:xdof
   for j=1:xdof
      if i==j
         Aii(1,1,i)=A1(i,j);
         Aii(1,2,i)=A2(i,j);
         Aii(2,1,i)=A3(i,j);
         Aii(2,2,i)=A4(i,j);
      else
         Aij(1,1,i)=A1(i,j);
         Aij(1,2,i)=A2(i,j);
         Aij(2,1,i)=A3(i,j);
         Aij(2,2,i)=A4(i,j);
      end
   end
   B(:,:,i)=[Bn(i,i);Bn(i+xdof,i)];
   C(:,:,i)=Aii(2,:,i);
   Cij(:,:,i)=Aij(2,:,i);
   H(:,:,i)=[Hn(i);Hn(i+xdof)];
end

dA=-uncertain*Aii;
dAij=-uncertain*Aij;
dB=-0*B;
dH=0*H;

% Classical LTR for K:
q2=[500 1e3 1e4];   % square of q
for i=1:2
   sys=ss(Aii(:,:,i),B(:,:,i),C(:,:,i),0);
   Lp=tf(sys); % plant tf
   if zero(sys)>0
      error('Unstable zeros => non-minimum phase');
   else
      disp('Stable invariant zeros => minimum phase');
   end
   Ps=tf(sys);
   disp('Test for invertible plant:');
   Psi=inv(Ps);
   w=Psi*Ps
   [num,den] = TFDATA(w,'v');
   if residue(num,den)==0
      disp('plant invertible');
   else
      error('plant Not invertible');
   end
   disp('Verify invertible');
   disp('LTR recoverable');
```

```
   for k=1:length(q2)
      Qe=q2(k)^2*B(:,:,i)*B(:,:,i)';
      Re=eye(size(C(:,:,i)',2));
      [Kt(:,:,k),Pt,Et] = LQR(Aii(:,:,i)',C(:,:,i)',Qe,Re);
      K(:,:,k)=Kt(:,:,k)';
   end
   Kf(:,:,i)=K(:,:,1);

   % Decentralised Nominal Controls:
   for k=1:length(q2)
      Qe=4*q2(k)^2*B(:,:,i)*B(:,:,i)';
      Re=eye(size(C(:,:,i)',2));
      [Kt(:,:,k),Pt,Ee] = LQR(Aii(:,:,i)',C(:,:,i)',Qe,Re);
      K(:,:,k)=Kt(:,:,k)';
   end
   Kfn(:,:,i)=K(:,:,1);

   disp('Simple LQR');
   Q(:,:,i)=C(:,:,i)'*100*C(:,:,i);   % control acceleration:
minimised
   Rn(:,:,i)=1e-2;
   Kcn(:,:,i)=lqr(Aii(:,:,i),B(:,:,i),Q(:,:,i),Rn(:,:,i));

   % Decentralized nonlinear control: Magana & Rondellar
   Fi(:,:,i)=Aii(:,:,i)-B(:,:,i)*Kcn(:,:,i);
   Pi(:,:,i)=lyap(Fi(:,:,i),[1 0;0 100]);
   d(i)=7.68;
   e(i)=8;

end


disp('Simulink subsystems');
[EQ,T]=elcent3;

disp('Simple LQR');
Qf=Cn'*100*eye(2)*Cn;   % control acceleration: minimised
Rf=1e-2*eye(2);
Kcf=lqr(An,Bn,Qf,Rf);

% Classical LTR for K:
for k=1:length(q2)
   Qef=q2(k)^2*Bn*Bn';
   Ref=1e-2*eye(size(Cn',2));
   [Ktf(:,:,k),Pt,ef] = LQR(An',Cn',Qef,Ref);
   Ktt(:,:,k)=Ktf(:,:,k)';
end
Kff=Ktt(:,:,1);

disp('Robust Reliable LQR');
% Uncertain:
%Af=[zeros(2) eye(2);-Ms\Ks -Ms\Cs];
disp('Uncertainties: general');
dK=-uncertain*Ks;
[Dk,Ek]=lu(dK);
dC=-uncertain*Cs;
[Dc,Ec]=lu(dC);
dAf=[zeros(xdof,2*xdof); -dK -dC];
D=[zeros(xdof,2*xdof);Dk Dc];
E=[Ek zeros(xdof); zeros(xdof) Ec];
```

```
Ta=D*D';
Ua=E'*E;

Af=An+dAf;
xdof=length(Af)/2;
Bf=(1-failure)*Bn;   %[zeros(2); eye(2)];
Hf=Hn;   %[0;0;-1;-1];
Cf=Af(xdof+1:2*xdof,:);%[zeros(2) eye(2)];

%Bob=[0 0;1 0];
Bob=(1-failure)*Bn;
Bo=Bn-Bob;
disp('One actuator failure');
Bw=Bo;
Bwb=Bob;
Df=Bwb(xdof+1:2*xdof,:);
Gf=ss(Af+dAf,Bwb,Cf,Df);
Gftf=tf(Gf);
[numGf,denGf]=tfdata(Gftf);


alpha=0.5;
beta=1;
delta=0.01;
dc=0;
dh=0;
ep=1e-10;   % critical: small
ep1=1e-2;
ep2=1e-2;
ep3=1e-2;
%ep4=1e-2;
Q=0.01*eye(2*xdof);

Qb=Ua/ep1 + [(1+ep2)*Cf'*Cf + (1+1/ep2)*dc^2*eye(2*xdof)]/ep/delta+Q;
eig(Qb);
if eig(Qb)>=0
else
   error('Eig(Qb)<=0');
end
%R=Bob*Bob'-ep1*B*Ta*B'-
[Bo*Bo'+(1+ep3)*H*H'+(1+1/ep3)*dh^2*eye(2)]*ep/delta;
R=Bob*Bob'/beta-ep1*Ta-
[Bo*Bo'+(1+ep3)*Hf*Hf'+(1+1/ep3)*dh^2*eye(2*xdof)]*ep/delta;
if eig(R)>=0
else
   error('Eig(R)<=0');
end
P = are(Af+alpha*eye(2*xdof), R, Qb);
Kcrr=Bwb'*P/2/beta;

Ac=Af+dAf-Bwb*Kcrr;
if eig(Ac)<-alpha
else
   error('eig(Ac)>=-alpha');
end
Bc=cat(2,Hf,Bwb);
Cc=Cf;
Tzwinf=normhinf(Ac,Bc,Cc,zeros(size(Cc,1),size(Bc,2)));
if Tzwinf<=delta
else
   error('Tzwinf>delta');
```

```
end

disp('H2 optimality');
H2=2*alpha*P + P*[-
Bob*Bob'+ep/delta*(Bo*Bo'+(1+ep3)*Hf*Hf'+(1+1/ep3)*dh^2*eye(2*xdof))+
3/2/beta*Bwb*Bwb']*P + [(1+ep2)*Cf'*Cf +
(1+1/ep2)*dc^2*eye(2*xdof)]/ep/delta+Q;
if eig(H2)<0
   disp('No H2-optimality');
else
   disp('H2-optimality condition satisfied');
end

% Classical LTR for K:
q2=[1e5 1e8 1e10];   % square of q
for k=1:length(q2)
   Qe=q2(k)^2*Bf*Bf';
   Re=eye(size(Cf',2));
   [Kt1(:,:,k),Pt1,E1] = LQR(Af',Cf',Qe,Re);
   K1(:,:,k)=Kt1(:,:,k)';
end
Kfrr=K1(:,:,1);

disp('Simulink FOM system');
maganaSf130403a

%===============================================
% ritz310303.m:
% Model reduction: Chopra 1995
% vq68.m, nbeta8.m, test.m, nishitani.m
%

% Actual FOM:
m1=1e6;  % kg
m2=7e5;
c=0;
k1=1.47e9;  % N/m
k3=1.372e9;
k5=1.274e9;
k7=1.176e9;
k9=1.078e9;
k11=0.98e9;
k13=0.931e9;
k14=0.882e9;
k15=0.833e9;
k16=0.784e9;
k17=0.735e9;
k18=0.686e9;
k19=0.637e9;
k20=0.588e9;



% discrete MDOF:
md=[m1 m1 m1 m1 m1 m1 m1 m1 m1 m1 m1 m1 m1 m1 m1 m1 m1 m1 m1 m2];
kd=[k1 k1 k3 k3 k5 k5 k7 k7 k9 k9 k11 k11 k13 k14 k15 k16 k17 k18 k19
k20];
%md=[m1 m1 ];
%kd=[k1 k1 ];
%cd=zeros(1,length(md));
cd=kd/100;
```

```
%
M=zeros(length(md));
K=zeros(length(md));
Cd=zeros(length(md));
for i=1:length(md)
   M(i,i)=M(i,i)+md(i);
   if i==1
      K(i,i)=K(i,i)+kd(i);
      Cd(i,i)=Cd(i,i)+cd(i);
   else
      K(i-1,i-1)=K(i-1,i-1)+kd(i);
      K(i-1,i)=K(i-1,i)-kd(i);
      K(i,i-1)=K(i,i-1)-kd(i);
      K(i,i)=K(i,i)+kd(i);
      Cd(i-1,i-1)=Cd(i-1,i-1)+cd(i);
      Cd(i-1,i)=Cd(i-1,i)-cd(i);
      Cd(i,i-1)=Cd(i,i-1)-cd(i);
      Cd(i,i)=Cd(i,i)+cd(i);
   end
end

disp('Model Reduction retaining modal characteristics');
[ev,w,ms0]=vtb4_1(M,K);
disp('Mode shape 1: ');
%ms0(:,1)/ms0(20,1)
%pause
disp('Mode shape 2: ');
%ms0(:,2)/ms0(8,2)
%pause
disp('Mode shape 3: ');
%ms0(:,3)/ms0(5,3)
%pause
f=w/2/pi;   % natural freq (Hz)

%=====================================================================
% Chopra: Rayleigh-Ritz generalisation of froce dependent vectors:
%=====================================================================
S=-M*ones(length(md),1);
dmodes=2;   %input('Enter the max mode to be included: ');
a=zeros(dmodes);
y=zeros(length(md),1,dmodes);
ms=zeros(length(md),1,dmodes);
msc=zeros(length(md),1,dmodes);
msb=[];
for i=1:dmodes
   if i==1
      y(:,:,i)=K\S;
      ms(:,:,i)=y(:,:,i)/sqrt(y(:,:,i)'*M*y(:,:,i));

   else
      y(:,:,i)=K\M*ms(:,:,i-1);
      a(i-1,i)=ms(:,:,i-1)'*M*y(:,:,i);
      msc(:,:,i)=y(:,:,i);
      for j=1:i-1
         msc(:,:,i)=msc(:,i) - a(j,i)*ms(:,:,j);
      end
      y(:,:,i)=msc(:,:,i);
      ms(:,:,i)=y(:,:,i)/sqrt(y(:,:,i)'*M*y(:,:,i));

   end
   msb=cat(2,msb,ms(:,:,i));
```

```
end

Mb=msb'*M*msb;
Cb=msb'*Cd*msb;
Kb=msb'*K*msb;
%Fb=msb'*F;
Hb=msb'*S;
[evb,wb,ms0b]=vtb4_1(Mb,Kb);
w(1:dmodes)
wb

%==========================
% Uncertainties: dM, dC, dK
% Sestieri
%==========================
disp('Uncoupled Ritz ROM: ');
Mbr=ms0b'*Mb*ms0b;
Cbr=ms0b'*Cb*ms0b;
Kbr=ms0b'*Kb*ms0b;
%Fbr=ms0b'*Fb;

dM=0.1*M;
dC=0.1*Cd;
dK=0.1*K;

M1b=Mb+msb'*dM*msb;
C1b=Cb+msb'*dC*msb;
K1b=Kb+msb'*dK*msb;

disp('Ritz vectors on uncertainties');
[ev1b,w1b,ms1b]=vtb4_1(M1b,K1b);
S1=msb'*S;
a=zeros(dmodes);
y=zeros(dmodes,1,dmodes);
ms=zeros(dmodes,1,dmodes);
msc=zeros(dmodes,1,dmodes);
ms1b=[];
for i=1:dmodes
   if i==1
      y(:,:,i)=K1b\S1;
      ms(:,:,i)=y(:,:,i)/sqrt(y(:,:,i)'*M1b*y(:,:,i));

   else
      y(:,:,i)=K1b\M1b*ms(:,:,i-1);
      a(i-1,i)=ms(:,:,i-1)'*M1b*y(:,:,i);
      msc(:,:,i)=y(:,:,i);
      for j=1:i-1
         msc(:,:,i)=msc(:,i) - a(j,i)*ms(:,:,j);
      end
      y(:,:,i)=msc(:,:,i);
      ms(:,:,i)=y(:,:,i)/sqrt(y(:,:,i)'*M1b*y(:,:,i));

   end
   ms1b=cat(2,ms1b,ms(:,:,i));

end


% Actual Ritz vector characteristics
w2b=w1b;
```

```
ms2b=msb*ms1b;
disp('ms2b(t)*(M+dM)*ms2b = I');
M2b=ms2b'*(M+dM)*ms2b;
C2b=ms2b'*(Cd+dC)*ms2b;
K2b=ms2b'*(K+dK)*ms2b;
%F2b=ms2b'*F;
H2b=ms2b'*S;
[evb3,w3b,ms3b]=vtb4_1(M2b,K2b);


%===========================================

choice=input('Press Enter to plot graphs: ');
xdof=length(Af)/2;
dt=0.02;
%Fsf=expm(Af*dt);  % Uncon
%Hdf=Af\(Fsf-eye(2*xdof));
%Gf=Af\(Fsf-eye(2*xdof))*Bf;
%Hdsf=Hdf*Hf;

% Evaluation in discrete time
%z0=zeros(2*xdof,1);
Tb=T;
%tspan=[0 Tb(length(Tb))];
%zuf=zeros(2*xdof,length(Tb));
%for i=1:length(Tb)
%    if i==1
%       zuf(:,i)=z0;
%    else
%      zuf(:,i)=Fsf*zuf(:,i-1)+Hdsf*EQ(i);
%    end
%end

% Actual:
Trange=[Tb(1) Tb(length(Tb))];
dt=0.02;
s=zeros(2,1);
v=s;a=s;
delta=0.5;  % gamma
beta=0.25;
Fs=-Ms*ones(2,1)*EQ;
[t,zuf(1:2,:),zuf(3:4,:),ddx]=nbeta8(Ms,(1-uncertain)*Cs,(1-
uncertain)*Ks,Fs,dt,Trange,s,v,a,delta,beta);

% Transmitted acceleration
zauf=[zuf(3:4,:);ddx];%Fsf*zuf+Hdsf*EQ;

% For absolute acceleration:
zauf(xdof+1:2*xdof,:)=zauf(xdof+1:2*xdof,:)+ones(2,1)*EQ;

% Interpolate
for i=1:xdof
   zu1f(:,i) = INTERP1(Tb,zuf(i,:),simoutfd(:,1));
   zu2f(:,i) = INTERP1(Tb,zuf(xdof+i,:),simoutfd(:,1));
   zu3f(:,i) = INTERP1(Tb,zauf(xdof+i,:),simoutfd(:,1));
end

disp('Pick out DOFs = 10, 20');
DOFchoice=zeros(dmodes,20);
DOFchoice(1,10)=1;
DOFchoice(2,20)=1;
```

```
disp('Convert ROM responses to Actual responses:');
% Actual relative acc:
simoutff(:,8:9)=(DOFchoice*msb*simoutff(:,8:9)')';
simoutfd(:,8:9)=(DOFchoice*msb*simoutfd(:,8:9)')';
simoutfdn(:,8:9)=(DOFchoice*msb*simoutfdn(:,8:9)')';
simoutfn(:,8:9)=(DOFchoice*msb*simoutfn(:,8:9)')';
simoutfnd(:,8:9)=(DOFchoice*msb*simoutfnd(:,8:9)')';
simoutfndn(:,8:9)=(DOFchoice*msb*simoutfndn(:,8:9)')';
% Actual relative vel:
simoutff(:,dmodes+2:2*dmodes+1)=(DOFchoice*msb*simoutff(:,dmodes+2:2*
dmodes+1)')';
simoutfd(:,dmodes+2:2*dmodes+1)=(DOFchoice*msb*simoutfd(:,dmodes+2:2*
dmodes+1)')';
simoutfdn(:,dmodes+2:2*dmodes+1)=(DOFchoice*msb*simoutfdn(:,dmodes+2:
2*dmodes+1)')';
simoutfn(:,dmodes+2:2*dmodes+1)=(DOFchoice*msb*simoutfn(:,dmodes+2:2*
dmodes+1)')';
simoutfnd(:,dmodes+2:2*dmodes+1)=(DOFchoice*msb*simoutfnd(:,dmodes+2:
2*dmodes+1)')';
simoutfndn(:,dmodes+2:2*dmodes+1)=(DOFchoice*msb*simoutfndn(:,dmodes+
2:2*dmodes+1)')';
% Actual relative displ:
simoutff(:,2:dmodes+1)=(DOFchoice*msb*simoutff(:,2:dmodes+1)')';
simoutfd(:,2:dmodes+1)=(DOFchoice*msb*simoutfd(:,2:dmodes+1)')';
simoutfdn(:,2:dmodes+1)=(DOFchoice*msb*simoutfdn(:,2:dmodes+1)')';
simoutfn(:,2:dmodes+1)=(DOFchoice*msb*simoutfn(:,2:dmodes+1)')';
simoutfnd(:,2:dmodes+1)=(DOFchoice*msb*simoutfnd(:,2:dmodes+1)')';
simoutfndn(:,2:dmodes+1)=(DOFchoice*msb*simoutfndn(:,2:dmodes+1)')';


disp('For Absolute acceleration: ');
% uncertain FOM:
EQff = INTERP1(Tb,EQ,simoutff(:,1));
EQfd = INTERP1(Tb,EQ,simoutfd(:,1));
EQfdn = INTERP1(Tb,EQ,simoutfdn(:,1));
simoutff(:,8:9)=simoutff(:,8:9)+EQff*ones(1,2);
simoutfd(:,8:9)=simoutfd(:,8:9)+EQfd*ones(1,2);
simoutfdn(:,8:9)=simoutfdn(:,8:9)+EQfdn*ones(1,2);
% nominal FOM:
EQfn = INTERP1(Tb,EQ,simoutfn(:,1));
EQfnd = INTERP1(Tb,EQ,simoutfnd(:,1));
EQfndn = INTERP1(Tb,EQ,simoutfndn(:,1));
simoutfn(:,8:9)=simoutfn(:,8:9)+EQfn*ones(1,2);
simoutfnd(:,8:9)=simoutfnd(:,8:9)+EQfnd*ones(1,2);
simoutfndn(:,8:9)=simoutfndn(:,8:9)+EQfndn*ones(1,2);


% Drifts:
for i=1:2
   if i==1
      % Inter-story drift
      driftu(:,i)=zu1f(:,i);
      driftff(:,i)=simoutff(:,i+1);
      driftfd(:,i)=simoutfd(:,i+1);
      driftfdn(:,i)=simoutfdn(:,i+1);
      driftfn(:,i)=simoutfn(:,i+1);
      driftfnd(:,i)=simoutfnd(:,i+1);
      driftfndn(:,i)=simoutfndn(:,i+1);

      % Inter-story velocity drift
```

```
      driftu(:,i+2)=zu2f(:,i);
      driftff(:,i+2)=simoutff(:,i+3);
      driftfd(:,i+2)=simoutfd(:,i+3);
      driftfdn(:,i+2)=simoutfdn(:,i+3);
      driftfn(:,i+2)=simoutfn(:,i+3);
      driftfnd(:,i+2)=simoutfnd(:,i+3);
      driftfndn(:,i+2)=simoutfndn(:,i+3);

   else
      % Inter-story drift
      driftu(:,i)=zu1f(:,i)-zu1f(:,i-1);
      driftff(:,i)=simoutff(:,i+1)-simoutff(:,i);
      driftfd(:,i)=simoutfd(:,i+1)-simoutfd(:,i);
      driftfdn(:,i)=simoutfdn(:,i+1)-simoutfdn(:,i);
      driftfn(:,i)=simoutfn(:,i+1)-simoutfn(:,i);
      driftfnd(:,i)=simoutfnd(:,i+1)-simoutfnd(:,i);
      driftfndn(:,i)=simoutfndn(:,i+1)-simoutfndn(:,i);

      % Inter-story velocity drift
      driftu(:,i+2)=zu2f(:,i)-zu2f(:,i-1);
      driftff(:,i+2)=simoutff(:,i+3)-simoutff(:,i+2);
      driftfd(:,i+2)=simoutfd(:,i+3)-simoutfd(:,i+2);
      driftfdn(:,i+2)=simoutfdn(:,i+3)-simoutfdn(:,i+2);
      driftfn(:,i+2)=simoutfn(:,i+3)-simoutfn(:,i+2);
      driftfnd(:,i+2)=simoutfnd(:,i+3)-simoutfnd(:,i+2);
      driftfndn(:,i+2)=simoutfndn(:,i+3)-simoutfndn(:,i+2);
   end
end

no30=0.9*length(simoutfd);

choice=1;
while choice~=0
   disp('(1) Subsystem 1: Quek-Compare inter-story drifts & abs
acc');
   disp('(2) Subsystem 2: Quek-Compare inter-story drifts & abs
acc');
   choice=input('Choose (1-4) to plot or (0) to end: ');

   switch choice
   case 1
      %choice=input('Compare inter-story drifts & abs acc');
      disp('1st subsystem: ');
      disp('No control: (drift, drift vel., abs acc)');
      max(abs(driftu(:,1)))
      max(abs(driftu(:,3)))
      max(abs(zu3f(:,1)))
      % Nominal:
      disp('LQR control for Nominal FOM: (drift, drift vel., abs acc,
control)');
      max(abs(driftfn(:,1)))
      max(abs(driftfn(:,3)))
      max(abs(simoutfn(:,8)))
      max(abs(simoutfn(:,10)))
      disp('Nominal control for Nominal FOM: (drift, drift vel., abs
acc, control)');
      max(abs(driftfndn(:,1)))
      max(abs(driftfndn(:,3)))
      max(abs(simoutfndn(:,8)))
      max(abs(simoutfndn(:,10)))
```

```
      disp('Robust Reliable control for Nominal FOM: (drift, drift
vel., abs acc, control)');
      max(abs(driftfnd(:,1)))
      max(abs(driftfnd(:,3)))
      max(abs(simoutfnd(:,8)))
      max(abs(simoutfnd(:,10)))
      % Uncertain:
      disp('LQR control: (drift, drift vel., abs acc, control)');
      max(abs(driftff(:,1)))
      max(abs(driftff(:,3)))
      max(abs(simoutff(:,8)))
      max(abs(simoutff(:,10)))
      disp('Nominal control: (drift, drift vel., abs acc, control)');
      max(abs(driftfdn(:,1)))
      max(abs(driftfdn(:,3)))
      max(abs(simoutfdn(:,8)))
      max(abs(simoutfdn(:,10)))
      disp('Robust Reliable control: (drift, drift vel., abs acc,
control)');
      max(abs(driftfd(:,1)))
      max(abs(driftfd(:,3)))
      max(abs(simoutfd(:,8)))
      max(abs(simoutfd(:,10)))

      no30 =1.8305e+004;

      disp('Complete for actual FOM');
      figure;

subplot(311);plot(simoutfd(1:650:no30,1),driftu(1:650:no30,1),'-
',simoutfd(1:650:no30,1),driftfd(1:650:no30,1),'-
*',simoutff(1:650:no30,1),driftff(1:650:no30,1),'-
o');grid;legend('Uncontrolled','rrLQR','LQR');
      title('');xlabel('time(s)');ylabel('Drift (m)');%ylim([-0.025
0.025])

subplot(312);plot(simoutfd(1:650:no30,1),driftfdn(1:650:no30,1),'-
',simoutfd(1:650:no30,1),driftfd(1:650:no30,1),'-
*',simoutff(1:650:no30,1),driftff(1:650:no30,1),'-
o');grid;legend('Decen-n','rrLQR','LQR');
      title('');xlabel('time(s)');ylabel('Drift (m)');ylim([-1e-4 1e-
4])

subplot(313);plot(simoutfd(1:650:no30,1),driftu(1:650:no30,3),'-
',simoutfd(1:650:no30,1),driftfd(1:650:no30,3),'-
*',simoutff(1:650:no30,1),driftff(1:650:no30,3),'-
o');grid;legend('Uncontrolled','rrLQR','LQR');
      title('');xlabel('time(s)');ylabel('Drift velocity
(m/s)');ylim([-0.25 0.25])

      figure;

subplot(311);plot(simoutfd(1:650:no30,1),driftfdn(1:650:no30,3),'-
',simoutfd(1:650:no30,1),driftfd(1:650:no30,3),'-
*',simoutff(1:650:no30,1),driftff(1:650:no30,3),'-
o');grid;legend('Decen-n','rrLQR','LQR');
      title('');xlabel('time(s)');ylabel('Drift velocity
(m/s)');ylim([-1e-3 1e-3])

subplot(312);plot(simoutfd(1:650:no30,1),simoutfdn(1:650:no30,8),'-
',simoutfd(1:650:no30,1),simoutfd(1:650:no30,8),'--
```

```
',simoutff(1:650:no30,1),simoutff(1:650:no30,8),'-
o');grid;legend('Decen-n','rrLQR','LQR');
      title('');xlabel('time(s)');ylabel('Abs Acc (m/s/s)');

subplot(313);plot(simoutfd(1:650:no30,1),simoutfdn(1:650:no30,10),'-
',simoutfd(1:650:no30,1),simoutfd(1:650:no30,10),'--
',simoutff(1:650:no30,1),simoutff(1:650:no30,10),'-
o');grid;legend('Decen-n','rrLQR','LQR');
      title('');xlabel('time(s)');ylabel('Control (V)');%ylim([-70
70])

      disp('Actual FOM');
      figure;

subplot(411);plot(simoutfd(1:650:no30,1),driftfdn(1:650:no30,1),'-
',simoutfd(1:650:no30,1),driftfd(1:650:no30,1),'-
*',simoutff(1:650:no30,1),driftff(1:650:no30,1),'-
o');grid;legend('Decen-n','rrLQR','LQR');
      title('');xlabel('');ylabel('Drift (m)');ylim([-1e-4 1e-4])

subplot(412);plot(simoutfd(1:650:no30,1),driftfdn(1:650:no30,3),'-
',simoutfd(1:650:no30,1),driftfd(1:650:no30,3),'-
*',simoutff(1:650:no30,1),driftff(1:650:no30,3),'-
o');grid;legend('Decen-n','rrLQR','LQR');
      title('');xlabel('');ylabel('Drift velocity (m/s)');ylim([-1e-3
1e-3])

subplot(413);plot(simoutfd(1:650:no30,1),simoutfdn(1:650:no30,8),'-
',simoutfd(1:650:no30,1),simoutfd(1:650:no30,8),'--
',simoutff(1:650:no30,1),simoutff(1:650:no30,8),'-
o');grid;legend('Decen-n','rrLQR','LQR');
      title('');xlabel('');ylabel('Abs Acc (m/s/s)');

subplot(414);plot(simoutfd(1:650:no30,1),simoutfdn(1:650:no30,10),'-
',simoutfd(1:650:no30,1),simoutfd(1:650:no30,10),'--
',simoutff(1:650:no30,1),simoutff(1:650:no30,10),'-
.');grid;legend('Decen-n','rrLQR','LQR');
      title('');xlabel('time(s)');ylabel('Control (V)');

      disp('Nominal FOM');
      figure;
      subplot(411);plot(simoutfd(1:no30,1),driftfndn(1:no30,1),'-
',simoutfd(1:no30,1),driftfnd(1:no30,1),'--
',simoutff(1:no30,1),driftfn(1:no30,1),'-.');grid;legend('Decen-
n','rrLQR','LQR');
      title('');xlabel('');ylabel('Drift (m)');ylim([-2e-5 1.5e-5])
      subplot(412);plot(simoutfd(1:no30,1),driftfndn(1:no30,3),'-
',simoutfd(1:no30,1),driftfnd(1:no30,3),'--
',simoutff(1:no30,1),driftfn(1:no30,3),'-.');grid;legend('Decen-
n','rrLQR','LQR');
      title('');xlabel('');ylabel('Velocity drift (m/s)');ylim([-
0.5e-3 1e-3])
      subplot(413);plot(simoutfd(1:no30,1),simoutfndn(1:no30,8),'-
',simoutfd(1:no30,1),simoutfnd(1:no30,8),'--
',simoutff(1:no30,1),simoutfn(1:no30,8),'-.');grid;legend('Decen-
n','rrLQR','LQR');
      title('');xlabel('');ylabel('Abs Acc (m/s/s)');
      subplot(414);plot(simoutfd(1:no30,1),simoutfndn(1:no30,10),'-
',simoutfd(1:no30,1),simoutfnd(1:no30,10),'--
',simoutff(1:no30,1),simoutfn(1:no30,10),'-.');grid;legend('Decen-
n','rrLQR','LQR');
```

```
      title('');xlabel('time(s)');ylabel('Control (V)');

      case 2
      disp('2nd subsystem: ');
      disp('No control: (drift, drift vel., abs acc)');
      max(abs(driftu(:,2)))
      max(abs(driftu(:,4)))
      max(abs(zu3f(:,2)))
      % Nominal:
      disp('LQR control for Nominal FOM: (drift, drift vel., abs acc,
control)');
      max(abs(driftfn(:,2)))
      max(abs(driftfn(:,4)))
      max(abs(simoutfn(:,9)))
      max(abs(simoutfn(:,11)))
      disp('Nominal control for Nominal FOM: (drift, drift vel., abs
acc, control)');
      max(abs(driftfndn(:,2)))
      max(abs(driftfndn(:,4)))
      max(abs(simoutfndn(:,9)))
      max(abs(simoutfndn(:,11)))
      disp('Robust Reliable control for Nominal FOM: (drift, drift
vel., abs acc, control)');
      max(abs(driftfnd(:,2)))
      max(abs(driftfnd(:,4)))
      max(abs(simoutfnd(:,9)))
      max(abs(simoutfnd(:,11)))
      % Uncertain:
      disp('LQR control: (drift, drift vel., abs acc, control)');
      max(abs(driftff(:,2)))
      max(abs(driftff(:,4)))
      max(abs(simoutff(:,9)))
      max(abs(simoutff(:,11)))
      disp('Nominal control: (drift, drift vel., abs acc, control)');
      max(abs(driftfdn(:,2)))
      max(abs(driftfdn(:,4)))
      max(abs(simoutfdn(:,9)))
      max(abs(simoutfdn(:,11)))
      disp('Robust Reliable control: (drift, drift vel., abs acc,
control)');
      max(abs(driftfd(:,2)))
      max(abs(driftfd(:,4)))
      max(abs(simoutfd(:,9)))
      max(abs(simoutfd(:,11)))

      no30 =1.8305e+004;

      disp('Complete for actual FOM');
      figure;

subplot(311);plot(simoutfd(1:650:no30,1),driftu(1:650:no30,2),'-
',simoutfd(1:650:no30,1),driftfd(1:650:no30,2),'-
*',simoutff(1:650:no30,1),driftff(1:650:no30,2),'-
o');grid;legend('Uncontrolled','rrLQR','LQR');
      title('');xlabel('time(s)');ylabel('Drift (m)');ylim([-0.1
0.1])

subplot(312);plot(simoutfd(1:650:no30,1),driftfdn(1:650:no30,2),'-
',simoutfd(1:650:no30,1),driftfd(1:650:no30,2),'-
*',simoutff(1:650:no30,1),driftff(1:650:no30,2),'-
o');grid;legend('Decen-n','rrLQR','LQR');
```

```
      title('');xlabel('time(s)');ylabel('Drift (m)');ylim([-7e-5 6e-
5])

subplot(313);plot(simoutfd(1:650:no30,1),driftu(1:650:no30,4),'-
',simoutfd(1:650:no30,1),driftfd(1:650:no30,4),'-
*',simoutff(1:650:no30,1),driftff(1:650:no30,4),'-
o');grid;legend('Uncontrolled','rrLQR','LQR');
      title('');xlabel('time(s)');ylabel('Drift velocity (m/s)');

      figure;

subplot(311);plot(simoutfd(1:650:no30,1),driftfdn(1:650:no30,4),'-
',simoutfd(1:650:no30,1),driftfd(1:650:no30,4),'-
*',simoutff(1:650:no30,1),driftff(1:650:no30,4),'-
o');grid;legend('Decen-n','rrLQR','LQR');
      title('');xlabel('time(s)');ylabel('Drift velocity
(m/s)');ylim([-1e-3 1e-3])

subplot(312);plot(simoutfd(1:650:no30,1),simoutfdn(1:650:no30,9),'-
',simoutfd(1:650:no30,1),simoutfd(1:650:no30,9),'--
',simoutff(1:650:no30,1),simoutff(1:650:no30,9),'-
o');grid;legend('Decen-n','rrLQR','LQR');
      title('');xlabel('time(s)');ylabel('Abs Acc (m/s/s)');ylim([-1
1])

subplot(313);plot(simoutfd(1:650:no30,1),simoutfdn(1:650:no30,11),'-
',simoutfd(1:650:no30,1),simoutfd(1:650:no30,11),'--
',simoutff(1:650:no30,1),simoutff(1:650:no30,11),'-
o');grid;legend('Decen-n','rrLQR','LQR');
      title('');xlabel('time(s)');ylabel('Control (V)');%ylim([-100
100])

      disp('Actual FOM');
      figure;

subplot(411);plot(simoutfd(1:650:no30,1),driftfdn(1:650:no30,2),'-
',simoutfd(1:650:no30,1),driftfd(1:650:no30,2),'-
*',simoutff(1:650:no30,1),driftff(1:650:no30,2),'-
o');grid;legend('Decen-n','rrLQR','LQR');
      title('');xlabel('');ylabel('Drift (m)');ylim([-1e-4 1e-4])

subplot(412);plot(simoutfd(1:650:no30,1),driftfdn(1:650:no30,4),'-
',simoutfd(1:650:no30,1),driftfd(1:650:no30,4),'-
*',simoutff(1:650:no30,1),driftff(1:650:no30,4),'-
o');grid;legend('Decen-n','rrLQR','LQR');
      title('');xlabel('');ylabel('Drift velocity (m/s)');ylim([-1e-3
1e-3])

subplot(413);plot(simoutfd(1:650:no30,1),simoutfdn(1:650:no30,9),'-
',simoutfd(1:650:no30,1),simoutfd(1:650:no30,9),'--
',simoutff(1:650:no30,1),simoutff(1:650:no30,9),'-
o');grid;legend('Decen-n','rrLQR','LQR');
      title('');xlabel('');ylabel('Abs Acc (m/s/s)');

subplot(414);plot(simoutfd(1:650:no30,1),simoutfdn(1:650:no30,11),'-
',simoutfd(1:650:no30,1),simoutfd(1:650:no30,11),'--
',simoutff(1:650:no30,1),simoutff(1:650:no30,11),'-
o');grid;legend('Decen-n','rrLQR','LQR');
      title('');xlabel('time(s)');ylabel('Control (V)');%ylim([-1 1])

      disp('Nominal FOM');
```

```
      figure;
      subplot(411);plot(simoutfd(1:no30,1),driftfndn(1:no30,2),'-
',simoutfd(1:no30,1),driftfnd(1:no30,2),'--
',simoutff(1:no30,1),driftfn(1:no30,2),'-.');grid;legend('Decen-
n','rrLQR','LQR');
      title('');xlabel('');ylabel('Drift (m)');ylim([-1e-5 1e-5])
      subplot(412);plot(simoutfd(1:no30,1),driftfndn(1:no30,4),'-
',simoutfd(1:no30,1),driftfnd(1:no30,4),'--
',simoutff(1:no30,1),driftfn(1:no30,4),'-.');grid;legend('Decen-
n','rrLQR','LQR');
      title('');xlabel('');ylabel('Velocity drift (m/s)');ylim([-2e-4
5e-4])
      subplot(413);plot(simoutfd(1:no30,1),simoutfndn(1:no30,9),'-
',simoutfd(1:no30,1),simoutfnd(1:no30,9),'--
',simoutff(1:no30,1),simoutfn(1:no30,9),'-.');grid;legend('Decen-
n','rrLQR','LQR');
      title('');xlabel('');ylabel('Abs Acc (m/s/s)');ylim([-1 1])
      subplot(414);plot(simoutfd(1:no30,1),simoutfndn(1:no30,11),'-
',simoutfd(1:no30,1),simoutfnd(1:no30,11),'--
',simoutff(1:no30,1),simoutfn(1:no30,11),'-.');grid;legend('Decen-
n','rrLQR','LQR');
      title('');xlabel('time(s)');ylabel('Control (V)');ylim([-50
50])

   end
end
```

Chapter 4

```
% Magana decentralized control
% u(t) = LQRy + v(t): nonlinear controls
% ICSSD
% jm200303.m, jm130403.m, jm150403a.m
% Aim: rrLQR, Decen-n, Decen-rr
%=======================================

uncertain=0.1;
failure=0.5;
n=1;
m=1;
Ms=[1 0;0 1];
Ks=-[-7.2980 2.7761; 2.7761 -62.8417];
Cs=-[-0.0730 0.0278; 0.0278 -0.6284];
An=[zeros(2) eye(2);-Ms\Ks -Ms\Cs];
xdof=length(An)/2;
Bn=[zeros(2);  -12.1596 -8.9808; 53.0676 -27.8441];   %[zeros(2);
eye(2)];
Hn=[0;0;4022;-1530];
Cn=An(xdof+1:2*xdof,:);%[zeros(2) eye(2)];
Dn=eye(2);
dAf=-uncertain*[zeros(xdof,2*xdof); An(xdof+1:2*xdof,:)];
Bf=(1-failure)*Bn;
dBf=-failure*Bn;

disp('Subsystem decentralized: ');
% address each of 4 quadrants:
A1=An(1:xdof,1:xdof);
A2=An(1:xdof,xdof+1:2*xdof);
A3=An(xdof+1:2*xdof,1:xdof);
A4=An(xdof+1:2*xdof,xdof+1:2*xdof);
```

```
for i=1:xdof
   for j=1:xdof
      if i==j
         Aii(1,1,i)=A1(i,j);
         Aii(1,2,i)=A2(i,j);
         Aii(2,1,i)=A3(i,j);
         Aii(2,2,i)=A4(i,j);
      else
         Aij(1,1,i)=A1(i,j);
         Aij(1,2,i)=A2(i,j);
         Aij(2,1,i)=A3(i,j);
         Aij(2,2,i)=A4(i,j);
      end
   end
   B(:,:,i)=[Bn(i,i);Bn(i+xdof,i)];
   C(:,:,i)=Aii(2,:,i);
   Cij(:,:,i)=Aij(2,:,i);
   H(:,:,i)=[Hn(i);Hn(i+xdof)];
end

dA=-uncertain*Aii;
dAij=-uncertain*Aij;
dB=-0*B;
dH=0*H;

% Classical LTR for K:
q2=[500 1e3 1e4];   % square of q
for i=1:2
   sys=ss(Aii(:,:,i),B(:,:,i),C(:,:,i),0);
   Lp=tf(sys); % plant tf
   if zero(sys)>0
      error('Unstable zeros => non-minimum phase');
   else
      disp('Stable invariant zeros => minimum phase');
   end
   Ps=tf(sys);
   disp('Test for invertible plant:');
   Psi=inv(Ps);
   w=Psi*Ps
   [num,den] = TFDATA(w,'v');
   if residue(num,den)==0
      disp('plant invertible');
   else
      error('plant Not invertible');
   end
   disp('Verify invertible');
   disp('LTR recoverable');

   for k=1:length(q2)
      Qe=q2(k)^2*B(:,:,i)*B(:,:,i)';
      Re=eye(size(C(:,:,i)',2));
      [Kt(:,:,k),Pt,Et] = LQR(Aii(:,:,i)',C(:,:,i)',Qe,Re);
      K(:,:,k)=Kt(:,:,k)';
   end
   Kf(:,:,i)=K(:,:,1);

   disp('Robust Reliable LQR');
   disp('Uncertainties: general');
   dK(:,:,i)=-uncertain*Ks(i,i);
   [Dk(:,:,i),Ek(:,:,i)]=lu(dK(:,:,i));
   dC(:,:,i)=-uncertain*Cs(i,i);
```

```
   [Dc(:,:,i),Ec(:,:,i)]=lu(dC(:,:,i));
   D(:,:,i)=[0 0;Dk(:,:,i) Dc(:,:,i)];
   E(:,:,i)=[Ek(:,:,i) 0; 0 Ec(:,:,i)];
   Ta(:,:,i)=D(:,:,i)*D(:,:,i)';
   Ua(:,:,i)=E(:,:,i)'*E(:,:,i);
   dA(:,:,i)=[zeros(n,2*n); dK(:,:,i) dC(:,:,i)];

   Bob(:,:,i)=(1-failure)*B(:,:,i); %[0; 0.5];
   Bo(:,:,i)=B(:,:,i)-Bob(:,:,i);
   disp('One actuator failure');
   Bw(:,:,i)=Bo(:,:,i);
   Bwb(:,:,i)=Bob(:,:,i);
   %dB(:,:,i)=Bwb(:,:,i);

   alpha=0.5;
   beta=1;
   delta=0.01;
   dc=0;
   dh=0;
   ep=1e-10;   % critical: small
   ep1=1e-2;
   ep2=1e-2;
   ep3=1e-2;
   ep4=1e-2;
   Q=0.01*eye(2);

   Qb(:,:,i)=Ua(:,:,i)/ep1 + [(1+ep2)*C(:,:,i)'*C(:,:,i) +
(1+1/ep2)*dc^2*eye(2)]/ep/delta+Q;
   eig(Qb(:,:,i));
   if eig(Qb(:,:,i))>=0
   else
      error('Eig(Qb)<=0');
   end
   R(:,:,i)=Bob(:,:,i)*Bob(:,:,i)'/beta-ep1*Ta(:,:,i)-
[Bo(:,:,i)*Bo(:,:,i)'+(1+ep3)*H(:,:,i)*H(:,:,i)'+(1+1/ep3)*dh^2*eye(2
)]*ep/delta;
   if eig(R(:,:,i))>=0
   else
      error('Eig(R)<=0');
   end
   P(:,:,i) = are(Aii(:,:,i)+alpha*eye(2), R(:,:,i), Qb(:,:,i));
   Kc(:,:,i)=Bwb(:,:,i)'*P(:,:,i)/2/beta;

   Ac(:,:,i)=Aii(:,:,i)+dA(:,:,i)-Bwb(:,:,i)*Kc(:,:,i);
   if eig(Ac(:,:,i))<-alpha
   else
      error('eig(Ac)>=-alpha');
   end
   Bc(:,:,i)=cat(2,H(:,:,i),Bw(:,:,i));
   Cc(:,:,i)=C(:,:,i);

Tzwinf(:,i)=normhinf(Ac(:,:,i),Bc(:,:,i),Cc(:,:,i),zeros(size(Cc(:,:,
i),1),size(Bc(:,:,i),2)));
   if Tzwinf(:,i)<=delta
   else
      error('Tzwinf>delta');
   end

   disp('H2 optimality');
   H2(:,:,i)=2*alpha*P(:,:,i) + P(:,:,i)*[-
Bob(:,:,i)*Bob(:,:,i)'+ep/delta*(Bo(:,:,i)*Bo(:,:,i)'+(1+ep3)*H(:,:,i
```

```
)*H(:,:,i)'+(1+1/ep3)*dh^2*eye(2))+3/2/beta*Bwb(:,:,i)*Bwb(:,:,i)']*P
(:,:,i) + [(1+ep2)*C(:,:,i)'*C(:,:,i) +
(1+1/ep2)*dc^2*eye(2)]/ep/delta+Q;
   if eig(H2(:,:,i))<0
      disp('No H2-optimality');
   else
      disp('H2-optimality condition satisfied');
   end

   % Decentralized nonlinear control: Magana & Rondellar
   Fi(:,:,i)=Aii(:,:,i)-B(:,:,i)*Kc(:,:,i);
   Pi(:,:,i)=lyap(Fi(:,:,i),[1 0;0 100]);
   d(i)=7.68;
   e(i)=8;

   % Decentralised Nominal Controls:
   for k=1:length(q2)
      Qe=4*q2(k)^2*Bwb(:,:,i)*Bwb(:,:,i)';
      Re=eye(size(C(:,:,i)',2));
      [Kt(:,:,k),Pt,Ee] = LQR(Aii(:,:,i)',C(:,:,i)',Qe,Re);
      K(:,:,k)=Kt(:,:,k)';
   end
   Kfn(:,:,i)=K(:,:,1);

   disp('Simple LQR');
   Q(:,:,i)=C(:,:,i)'*100*C(:,:,i);   % control acceleration:
minimised
   Rn(:,:,i)=1e-2;
   Kcn(:,:,i)=lqr(Aii(:,:,i),Bwb(:,:,i)/failure,Q(:,:,i),Rn(:,:,i));

end


disp('Simulink subsystems');
[EQ,T]=elcent3;

disp('Simple LQR');
Qf=Cn'*100*eye(2)*Cn;   % control acceleration: minimised
Rf=1e-2*eye(2);
Kcf=lqr(An,Bn,Qf,Rf);

% Classical LTR for K:
for k=1:length(q2)
   Qef=q2(k)^2*Bn*Bn';
   Ref=1e-2*eye(size(Cn',2));
   [Ktf(:,:,k),Pt,ef] = LQR(An',Cn',Qef,Ref);
   Ktt(:,:,k)=Ktf(:,:,k)';
end
Kff=Ktt(:,:,1);

disp('Robust Reliable LQR');
% Uncertain:
%Af=[zeros(2) eye(2);-Ms\Ks -Ms\Cs];
disp('Uncertainties: general');
dK=-uncertain*Ks;
[Dk,Ek]=lu(dK);
dC=-uncertain*Cs;
[Dc,Ec]=lu(dC);
dAf=[zeros(xdof,2*xdof); -dK -dC];
D=[zeros(xdof,2*xdof);Dk Dc];
E=[Ek zeros(xdof); zeros(xdof) Ec];
```

```
Ta=D*D';
Ua=E'*E;

Af=An+dAf;
xdof=length(Af)/2;
%Bf=Bn;  %[zeros(2); eye(2)];
Hf=Hn;   %[0;0;-1;-1];
Cf=Af(xdof+1:2*xdof,:);%[zeros(2) eye(2)];

%Bob=[0 0;1 0];
Bob=(1-failure)*Bn;
Bo=Bn-Bob;
disp('One actuator failure');
Bw=Bo;
Bwbf=Bob;
Df=Bwbf(xdof+1:2*xdof,:);
Gf=ss(Af+dAf,Bwbf,Cf,Df);
Gftf=tf(Gf);
[numGf,denGf]=tfdata(Gftf);


alpha=0.5;
beta=1;
delta=0.01;
dc=0;
dh=0;
ep=1e-10;   % critical: small
ep1=1e-2;
ep2=1e-2;
ep3=1e-2;
%ep4=1e-2;
Q=0.01*eye(2*xdof);

Qb=Ua/ep1 + [(1+ep2)*Cf'*Cf + (1+1/ep2)*dc^2*eye(2*xdof)]/ep/delta+Q;
eig(Qb);
if eig(Qb)>=0
else
   error('Eig(Qb)<=0');
end
%R=Bob*Bob'-ep1*B*Ta*B'-
[Bo*Bo'+(1+ep3)*H*H'+(1+1/ep3)*dh^2*eye(2)]*ep/delta;
R=Bob*Bob'/beta-ep1*Ta-
[Bo*Bo'+(1+ep3)*Hf*Hf'+(1+1/ep3)*dh^2*eye(2*xdof)]*ep/delta;
if eig(R)>=0
else
   error('Eig(R)<=0');
end
P = are(Af+alpha*eye(2*xdof), R, Qb);
Kcrr=Bwbf'*P/2/beta;

Ac=Af+dAf-Bwbf*Kcrr;
if eig(Ac)<-alpha
else
   error('eig(Ac)>=-alpha');
end
Bc=cat(2,Hf,Bwbf);
Cc=Cf;
Tzwinf=normhinf(Ac,Bc,Cc,zeros(size(Cc,1),size(Bc,2)));
if Tzwinf<=delta
else
   error('Tzwinf>delta');
```

```
end

disp('H2 optimality');
H2=2*alpha*P + P*[-
Bob*Bob'+ep/delta*(Bo*Bo'+(1+ep3)*Hf*Hf'+(1+1/ep3)*dh^2*eye(2*xdof))+
3/2/beta*Bwbf*Bwbf']*P + [(1+ep2)*Cf'*Cf +
(1+1/ep2)*dc^2*eye(2*xdof)]/ep/delta+Q;
if eig(H2)<0
   disp('No H2-optimality');
else
   disp('H2-optimality condition satisfied');
end

% Classical LTR for K:
q2=[1e5 1e8 1e10];   % square of q
for k=1:length(q2)
   Qe=q2(k)^2*Bf*Bf';
   Re=eye(size(Cf',2));
   [Kt1(:,:,k),Pt1,E1] = LQR(Af',Cf',Qe,Re);
   K1(:,:,k)=Kt1(:,:,k)';
end
Kfrr=K1(:,:,1);

disp('Simulink FOM system');
maganaSf150403a

%===========================================
% ritz310303.m:
% Model reduction: Chopra 1995
% vq68.m, nbeta8.m, test.m, nishitani.m
%

% Actual FOM:
m1=1e6;  % kg
m2=7e5;
c=0;
k1=1.47e9;  % N/m
k3=1.372e9;
k5=1.274e9;
k7=1.176e9;
k9=1.078e9;
k11=0.98e9;
k13=0.931e9;
k14=0.882e9;
k15=0.833e9;
k16=0.784e9;
k17=0.735e9;
k18=0.686e9;
k19=0.637e9;
k20=0.588e9;



% discrete MDOF:
md=[m1 m1 m1 m1 m1 m1 m1 m1 m1 m1 m1 m1 m1 m1 m1 m1 m1 m1 m1 m2];
kd=[k1 k1 k3 k3 k5 k5 k7 k7 k9 k9 k11 k11 k13 k14 k15 k16 k17 k18 k19
k20];
%md=[m1 m1 ];
%kd=[k1 k1 ];
%cd=zeros(1,length(md));
cd=kd/100;
```

```
%
M=zeros(length(md));
K=zeros(length(md));
Cd=zeros(length(md));
for i=1:length(md)
   M(i,i)=M(i,i)+md(i);
   if i==1
      K(i,i)=K(i,i)+kd(i);
      Cd(i,i)=Cd(i,i)+cd(i);
   else
      K(i-1,i-1)=K(i-1,i-1)+kd(i);
      K(i-1,i)=K(i-1,i)-kd(i);
      K(i,i-1)=K(i,i-1)-kd(i);
      K(i,i)=K(i,i)+kd(i);
      Cd(i-1,i-1)=Cd(i-1,i-1)+cd(i);
      Cd(i-1,i)=Cd(i-1,i)-cd(i);
      Cd(i,i-1)=Cd(i,i-1)-cd(i);
      Cd(i,i)=Cd(i,i)+cd(i);
   end
end

disp('Model Reduction retaining modal characteristics');
[ev,w,ms0]=vtb4_1(M,K);
disp('Mode shape 1: ');
%ms0(:,1)/ms0(20,1)
%pause
disp('Mode shape 2: ');
%ms0(:,2)/ms0(8,2)
%pause
disp('Mode shape 3: ');
%ms0(:,3)/ms0(5,3)
%pause
f=w/2/pi;   % natural freq (Hz)

%=====================================================================
% Chopra: Rayleigh-Ritz generalisation of froce dependent vectors:
%=====================================================================
S=-M*ones(length(md),1);
dmodes=2;   %input('Enter the max mode to be included: ');
a=zeros(dmodes);
y=zeros(length(md),1,dmodes);
ms=zeros(length(md),1,dmodes);
msc=zeros(length(md),1,dmodes);
msb=[];
for i=1:dmodes
   if i==1
      y(:,:,i)=K\S;
      ms(:,:,i)=y(:,:,i)/sqrt(y(:,:,i)'*M*y(:,:,i));

   else
      y(:,:,i)=K\M*ms(:,:,i-1);
      a(i-1,i)=ms(:,:,i-1)'*M*y(:,:,i);
      msc(:,:,i)=y(:,:,i);
      for j=1:i-1
         msc(:,:,i)=msc(:,i) - a(j,i)*ms(:,:,j);
      end
      y(:,:,i)=msc(:,:,i);
      ms(:,:,i)=y(:,:,i)/sqrt(y(:,:,i)'*M*y(:,:,i));

   end
   msb=cat(2,msb,ms(:,:,i));
```

```
end

Mb=msb'*M*msb;
Cb=msb'*Cd*msb;
Kb=msb'*K*msb;
%Fb=msb'*F;
Hb=msb'*S;
[evb,wb,ms0b]=vtb4_1(Mb,Kb);
w(1:dmodes)
wb

%==========================
% Uncertainties: dM, dC, dK
% Sestieri
%==========================
disp('Uncoupled Ritz ROM: ');
Mbr=ms0b'*Mb*ms0b;
Cbr=ms0b'*Cb*ms0b;
Kbr=ms0b'*Kb*ms0b;
%Fbr=ms0b'*Fb;

dM=0.1*M;
dC=0.1*Cd;
dK=0.1*K;

M1b=Mb+msb'*dM*msb;
C1b=Cb+msb'*dC*msb;
K1b=Kb+msb'*dK*msb;

disp('Ritz vectors on uncertainties');
[ev1b,w1b,ms1b]=vtb4_1(M1b,K1b);
S1=msb'*S;
a=zeros(dmodes);
y=zeros(dmodes,1,dmodes);
ms=zeros(dmodes,1,dmodes);
msc=zeros(dmodes,1,dmodes);
ms1b=[];
for i=1:dmodes
   if i==1
      y(:,:,i)=K1b\S1;
      ms(:,:,i)=y(:,:,i)/sqrt(y(:,:,i)'*M1b*y(:,:,i));

   else
      y(:,:,i)=K1b\M1b*ms(:,:,i-1);
      a(i-1,i)=ms(:,:,i-1)'*M1b*y(:,:,i);
      msc(:,:,i)=y(:,:,i);
      for j=1:i-1
         msc(:,:,i)=msc(:,i) - a(j,i)*ms(:,:,j);
      end
      y(:,:,i)=msc(:,:,i);
      ms(:,:,i)=y(:,:,i)/sqrt(y(:,:,i)'*M1b*y(:,:,i));

   end
   ms1b=cat(2,ms1b,ms(:,:,i));

end


% Actual Ritz vector characteristics
w2b=w1b;
```

```
ms2b=msb*ms1b;
disp('ms2b(t)*(M+dM)*ms2b = I');
M2b=ms2b'*(M+dM)*ms2b;
C2b=ms2b'*(Cd+dC)*ms2b;
K2b=ms2b'*(K+dK)*ms2b;
%F2b=ms2b'*F;
H2b=ms2b'*S;
[evb3,w3b,ms3b]=vtb4_1(M2b,K2b);


%===========================================


choice=input('Press Enter to plot graphs: ');
xdof=length(Af)/2;
dt=0.02;
%Fsf=expm(Af*dt);  % Uncon
%Hdf=Af\(Fsf-eye(2*xdof));
%Gf=Af\(Fsf-eye(2*xdof))*Bf;
%Hdsf=Hdf*Hf;

% Evaluation in discrete time
%z0=zeros(2*xdof,1);
Tb=T;
%tspan=[0 Tb(length(Tb))];
%zuf=zeros(2*xdof,length(Tb));
%for i=1:length(Tb)
%    if i==1
%       zuf(:,i)=z0;
%    else
%      zuf(:,i)=Fsf*zuf(:,i-1)+Hdsf*EQ(i);
%    end
%end

% Actual:
Trange=[Tb(1) Tb(length(Tb))];
dt=0.02;
s=zeros(2,1);
v=s;a=s;
delta=0.5;  % gamma
beta=0.25;
Fs=-Ms*ones(2,1)*EQ;
[t,zuf(1:2,:),zuf(3:4,:),ddx]=nbeta8(Ms,(1-uncertain)*Cs,(1-
uncertain)*Ks,Fs,dt,Trange,s,v,a,delta,beta);

% Transmitted acceleration
zauf=[zuf(3:4,:);ddx];%Fsf*zuf+Hdsf*EQ;

% For absolute acceleration:
zauf(xdof+1:2*xdof,:)=zauf(xdof+1:2*xdof,:)+ones(2,1)*EQ;

% Interpolate
for i=1:xdof
   zu1f(:,i) = INTERP1(Tb,zuf(i,:),simoutfd(:,1));
   zu2f(:,i) = INTERP1(Tb,zuf(xdof+i,:),simoutfd(:,1));
   zu3f(:,i) = INTERP1(Tb,zauf(xdof+i,:),simoutfd(:,1));
end

disp('Pick out DOFs = 10, 20');
DOFchoice=zeros(dmodes,20);
DOFchoice(1,10)=1;
```

```
DOFchoice(2,20)=1;

disp('Convert ROM responses to Actual responses:');
% Actual relative acc:
simoutff(:,8:9)=(DOFchoice*msb*simoutff(:,8:9)')';
simoutfd(:,8:9)=(DOFchoice*msb*simoutfd(:,8:9)')';
simoutfdn(:,8:9)=(DOFchoice*msb*simoutfdn(:,8:9)')';
simoutfn(:,8:9)=(DOFchoice*msb*simoutfn(:,8:9)')';
simoutfnd(:,8:9)=(DOFchoice*msb*simoutfnd(:,8:9)')';
simoutfndn(:,8:9)=(DOFchoice*msb*simoutfndn(:,8:9)')';
% Actual relative vel:
simoutff(:,dmodes+2:2*dmodes+1)=(DOFchoice*msb*simoutff(:,dmodes+2:2*
dmodes+1)')';
simoutfd(:,dmodes+2:2*dmodes+1)=(DOFchoice*msb*simoutfd(:,dmodes+2:2*
dmodes+1)')';
simoutfdn(:,dmodes+2:2*dmodes+1)=(DOFchoice*msb*simoutfdn(:,dmodes+2:
2*dmodes+1)')';
simoutfn(:,dmodes+2:2*dmodes+1)=(DOFchoice*msb*simoutfn(:,dmodes+2:2*
dmodes+1)')';
simoutfnd(:,dmodes+2:2*dmodes+1)=(DOFchoice*msb*simoutfnd(:,dmodes+2:
2*dmodes+1)')';
simoutfndn(:,dmodes+2:2*dmodes+1)=(DOFchoice*msb*simoutfndn(:,dmodes+
2:2*dmodes+1)')';
% Actual relative displ:
simoutff(:,2:dmodes+1)=(DOFchoice*msb*simoutff(:,2:dmodes+1)')';
simoutfd(:,2:dmodes+1)=(DOFchoice*msb*simoutfd(:,2:dmodes+1)')';
simoutfdn(:,2:dmodes+1)=(DOFchoice*msb*simoutfdn(:,2:dmodes+1)')';
simoutfn(:,2:dmodes+1)=(DOFchoice*msb*simoutfn(:,2:dmodes+1)')';
simoutfnd(:,2:dmodes+1)=(DOFchoice*msb*simoutfnd(:,2:dmodes+1)')';
simoutfndn(:,2:dmodes+1)=(DOFchoice*msb*simoutfndn(:,2:dmodes+1)')';


disp('For Absolute acceleration: ');
% uncertain FOM:
EQff = INTERP1(Tb,EQ,simoutff(:,1));
EQfd = INTERP1(Tb,EQ,simoutfd(:,1));
EQfdn = INTERP1(Tb,EQ,simoutfdn(:,1));
simoutff(:,8:9)=simoutff(:,8:9)+EQff*ones(1,2);
simoutfd(:,8:9)=simoutfd(:,8:9)+EQfd*ones(1,2);
simoutfdn(:,8:9)=simoutfdn(:,8:9)+EQfdn*ones(1,2);
% nominal FOM:
EQfn = INTERP1(Tb,EQ,simoutfn(:,1));
EQfnd = INTERP1(Tb,EQ,simoutfnd(:,1));
EQfndn = INTERP1(Tb,EQ,simoutfndn(:,1));
simoutfn(:,8:9)=simoutfn(:,8:9)+EQfn*ones(1,2);
simoutfnd(:,8:9)=simoutfnd(:,8:9)+EQfnd*ones(1,2);
simoutfndn(:,8:9)=simoutfndn(:,8:9)+EQfndn*ones(1,2);


% Drifts:
for i=1:2
   if i==1
      % Inter-story drift
      driftu(:,i)=zu1f(:,i);
      driftff(:,i)=simoutff(:,i+1);
      driftfd(:,i)=simoutfd(:,i+1);
      driftfdn(:,i)=simoutfdn(:,i+1);
      driftfn(:,i)=simoutfn(:,i+1);
      driftfnd(:,i)=simoutfnd(:,i+1);
      driftfndn(:,i)=simoutfndn(:,i+1);
```

```
      % Inter-story Drift velocity
      driftu(:,i+2)=zu2f(:,i);
      driftff(:,i+2)=simoutff(:,i+3);
      driftfd(:,i+2)=simoutfd(:,i+3);
      driftfdn(:,i+2)=simoutfdn(:,i+3);
      driftfn(:,i+2)=simoutfn(:,i+3);
      driftfnd(:,i+2)=simoutfnd(:,i+3);
      driftfndn(:,i+2)=simoutfndn(:,i+3);

   else
      % Inter-story drift
      driftu(:,i)=zu1f(:,i)-zu1f(:,i-1);
      driftff(:,i)=simoutff(:,i+1)-simoutff(:,i);
      driftfd(:,i)=simoutfd(:,i+1)-simoutfd(:,i);
      driftfdn(:,i)=simoutfdn(:,i+1)-simoutfdn(:,i);
      driftfn(:,i)=simoutfn(:,i+1)-simoutfn(:,i);
      driftfnd(:,i)=simoutfnd(:,i+1)-simoutfnd(:,i);
      driftfndn(:,i)=simoutfndn(:,i+1)-simoutfndn(:,i);

      % Inter-story Drift velocity
      driftu(:,i+2)=zu2f(:,i)-zu2f(:,i-1);
      driftff(:,i+2)=simoutff(:,i+3)-simoutff(:,i+2);
      driftfd(:,i+2)=simoutfd(:,i+3)-simoutfd(:,i+2);
      driftfdn(:,i+2)=simoutfdn(:,i+3)-simoutfdn(:,i+2);
      driftfn(:,i+2)=simoutfn(:,i+3)-simoutfn(:,i+2);
      driftfnd(:,i+2)=simoutfnd(:,i+3)-simoutfnd(:,i+2);
      driftfndn(:,i+2)=simoutfndn(:,i+3)-simoutfndn(:,i+2);
   end
end

no30=0.8*length(simoutfd);

choice=1;
while choice~=0
   disp('(1) Subsystem 1: Quek-Compare inter-story drifts & abs
acc');
   disp('(2) Subsystem 2: Quek-Compare inter-story drifts & abs
acc');
   choice=input('Choose (1-4) to plot or (0) to end: ');

   switch choice
      case 1
      %choice=input('Compare inter-story drifts & abs acc');
      disp('1st subsystem: ');
      disp('No control: (drift, drift vel., abs acc)');
      max(abs(driftu(:,1)))
      max(abs(driftu(:,3)))
      max(abs(zu3f(:,1)))
      % Nominal:
      disp('Robust Reliable control for Nominal FOM: (drift, drift
vel., abs acc, control)');
      max(abs(driftfn(:,1)))
      max(abs(driftfn(:,3)))
      max(abs(simoutfn(:,8)))
      max(abs(simoutfn(:,10)))
      disp('Nominal control for Nominal FOM: (drift, drift vel., abs
acc, control)');
      max(abs(driftfndn(:,1)))
      max(abs(driftfndn(:,3)))
      max(abs(simoutfndn(:,8)))
      max(abs(simoutfndn(:,10)))
```

```
      disp('Decen-rr control for Nominal FOM: (drift, drift vel., abs
acc, control)');
      max(abs(driftfnd(:,1)))
      max(abs(driftfnd(:,3)))
      max(abs(simoutfnd(:,8)))
      max(abs(simoutfnd(:,10)))
      % Uncertain:
      disp('Robust Reliable control: (drift, drift vel., abs acc,
control)');
      max(abs(driftff(:,1)))
      max(abs(driftff(:,3)))
      max(abs(simoutff(:,8)))
      max(abs(simoutff(:,10)))
      disp('Nominal control: (drift, drift vel., abs acc, control)');
      max(abs(driftfdn(:,1)))
      max(abs(driftfdn(:,3)))
      max(abs(simoutfdn(:,8)))
      max(abs(simoutfdn(:,10)))
      disp('Decen-rr control: (drift, drift vel., abs acc,
control)');
      max(abs(driftfd(:,1)))
      max(abs(driftfd(:,3)))
      max(abs(simoutfd(:,8)))
      max(abs(simoutfd(:,10)))

      disp('Complete for actual FOM');
      figure;
      subplot(311);plot(simoutfd(1:no30,1),driftu(1:no30,1),'-
',simoutfd(1:no30,1),driftfd(1:no30,1),'-
*',simoutff(1:no30,1),driftff(1:no30,1),'-
o');grid;legend('Uncontrolled','Decen-rr','rrLQR');
      title('');xlabel('time(s)');ylabel('Drift (m)');ylim([-0.025
0.025])
      subplot(312);plot(simoutfd(1:no30,1),driftfdn(1:no30,1),'-
',simoutfd(1:no30,1),driftfd(1:no30,1),'-
*',simoutff(1:no30,1),driftff(1:no30,1),'-o');grid;legend('Decen-
n','Decen-rr','rrLQR');
      title('');xlabel('time(s)');ylabel('Drift (m)');ylim([-2e-4 2e-
4])
      subplot(313);plot(simoutfd(1:no30,1),driftu(1:no30,3),'-
',simoutfd(1:no30,1),driftfd(1:no30,3),'-
*',simoutff(1:no30,1),driftff(1:no30,3),'-
o');grid;legend('Uncontrolled','Decen-rr','rrLQR');
      title('');xlabel('time(s)');ylabel('Drift velocity (m/s)');

      figure;
      subplot(311);plot(simoutfd(1:no30,1),driftfdn(1:no30,3),'-
',simoutfd(1:no30,1),driftfd(1:no30,3),'-
*',simoutff(1:no30,1),driftff(1:no30,3),'-o');grid;legend('Decen-
n','Decen-rr','rrLQR');
      title('');xlabel('time(s)');ylabel('Drift velocity
(m/s)');ylim([-1e-3 3e-3])
      subplot(312);plot(simoutfd(1:no30,1),simoutfdn(1:no30,8),'-
',simoutfd(1:no30,1),simoutfd(1:no30,8),'--
',simoutff(1:no30,1),simoutff(1:no30,8),'-o');grid;legend('Decen-
n','Decen-rr','rrLQR');
      title('');xlabel('time(s)');ylabel('Abs Acc (m/s/s)');
      subplot(313);plot(simoutfd(1:no30,1),simoutfdn(1:no30,10),'-
',simoutfd(1:no30,1),simoutfd(1:no30,10),'--
',simoutff(1:no30,1),simoutff(1:no30,10),'-o');grid;legend('Decen-
n','Decen-rr','rrLQR');
```

```
      title('');xlabel('time(s)');ylabel('Control (V)');

      disp('Actual FOM');
      figure;
      subplot(411);plot(simoutfd(1:no30,1),driftfdn(1:no30,1),'-
',simoutfd(1:no30,1),driftfd(1:no30,1),'-
*',simoutff(1:no30,1),driftff(1:no30,1),'-o');grid;legend('Decen-
n','Decen-rr','rrLQR');
      title('');xlabel('');ylabel('Drift (m)');ylim([-0.8e-4 0.5e-4])
      subplot(412);plot(simoutfd(1:no30,1),driftfdn(1:no30,3),'-
',simoutfd(1:no30,1),driftfd(1:no30,3),'-
*',simoutff(1:no30,1),driftff(1:no30,3),'-o');grid;legend('Decen-
n','Decen-rr','rrLQR');
      title('');xlabel('');ylabel('Drift velocity (m/s)');ylim([-1e-3
3e-3])
      subplot(413);plot(simoutfd(1:no30,1),simoutfdn(1:no30,8),'-
',simoutfd(1:no30,1),simoutfd(1:no30,8),'--
',simoutff(1:no30,1),simoutff(1:no30,8),'-o');grid;legend('Decen-
n','Decen-rr','rrLQR');
      title('');xlabel('');ylabel('Abs Acc (m/s/s)');
      subplot(414);plot(simoutfd(1:no30,1),simoutfdn(1:no30,10),'-
',simoutfd(1:no30,1),simoutfd(1:no30,10),'--
',simoutff(1:no30,1),simoutff(1:no30,10),'-o');grid;legend('Decen-
n','Decen-rr','rrLQR');
      title('');xlabel('time(s)');ylabel('Control (V)');

      disp('Nominal FOM');
      figure;
      subplot(411);plot(simoutfd(1:no30,1),driftfndn(1:no30,1),'-
',simoutfd(1:no30,1),driftfnd(1:no30,1),'--
',simoutff(1:no30,1),driftfn(1:no30,1),'-.');grid;legend('Decen-
n','Decen-rr','rrLQR');
      title('');xlabel('');ylabel('Drift (m)');ylim([-1e-4 1e-4])
      subplot(412);plot(simoutfd(1:no30,1),driftfndn(1:no30,3),'-
',simoutfd(1:no30,1),driftfnd(1:no30,3),'--
',simoutff(1:no30,1),driftfn(1:no30,3),'-.');grid;legend('Decen-
n','Decen-rr','rrLQR');
      title('');xlabel('');ylabel('Drift velocity (m/s)');ylim([-1e-3
3e-3])
      subplot(413);plot(simoutfd(1:no30,1),simoutfndn(1:no30,8),'-
',simoutfd(1:no30,1),simoutfnd(1:no30,8),'--
',simoutff(1:no30,1),simoutfn(1:no30,8),'-.');grid;legend('Decen-
n','Decen-rr','rrLQR');
      title('');xlabel('');ylabel('Abs Acc (m/s/s)');
      subplot(414);plot(simoutfd(1:no30,1),simoutfndn(1:no30,10),'-
',simoutfd(1:no30,1),simoutfnd(1:no30,10),'--
',simoutff(1:no30,1),simoutfn(1:no30,10),'-.');grid;legend('Decen-
n','Decen-rr','rrLQR');
      title('');xlabel('time(s)');ylabel('Control (V)');

      case 2
      disp('2nd subsystem: ');
      disp('No control: (drift, drift vel., abs acc)');
      max(abs(driftu(:,2)))
      max(abs(driftu(:,4)))
      max(abs(zu3f(:,2)))
      % Nominal:
      disp('Robust Reliable control for Nominal FOM: (drift, drift
vel., abs acc, control)');
      max(abs(driftfn(:,2)))
      max(abs(driftfn(:,4)))
```

```
      max(abs(simoutfn(:,9)))
      max(abs(simoutfn(:,11)))
      disp('Nominal control for Nominal FOM: (drift, drift vel., abs
acc, control)');
      max(abs(driftfndn(:,2)))
      max(abs(driftfndn(:,4)))
      max(abs(simoutfndn(:,9)))
      max(abs(simoutfndn(:,11)))
      disp('Decen-rr control for Nominal FOM: (drift, drift vel., abs
acc, control)');
      max(abs(driftfnd(:,2)))
      max(abs(driftfnd(:,4)))
      max(abs(simoutfnd(:,9)))
      max(abs(simoutfnd(:,11)))
      % Uncertain:
      disp('Robust Reliable control: (drift, drift vel., abs acc,
control)');
      max(abs(driftff(:,2)))
      max(abs(driftff(:,4)))
      max(abs(simoutff(:,9)))
      max(abs(simoutff(:,11)))
      disp('Nominal control: (drift, drift vel., abs acc, control)');
      max(abs(driftfdn(:,2)))
      max(abs(driftfdn(:,4)))
      max(abs(simoutfdn(:,9)))
      max(abs(simoutfdn(:,11)))
      disp('Decen-rr control: (drift, drift vel., abs acc,
control)');
      max(abs(driftfd(:,2)))
      max(abs(driftfd(:,4)))
      max(abs(simoutfd(:,9)))
      max(abs(simoutfd(:,11)))

      disp('Complete for actual FOM');
      figure;
      subplot(311);plot(simoutfd(1:no30,1),driftu(1:no30,2),'-
',simoutfd(1:no30,1),driftfd(1:no30,2),'-
*',simoutff(1:no30,1),driftff(1:no30,2),'-
o');grid;legend('Uncontrolled','Decen-rr','rrLQR');
      title('');xlabel('time(s)');ylabel('Drift (m)');
      subplot(312);plot(simoutfd(1:no30,1),driftfdn(1:no30,2),'-
',simoutfd(1:no30,1),driftfd(1:no30,2),'-
*',simoutff(1:no30,1),driftff(1:no30,2),'-o');grid;legend('Decen-
n','Decen-rr','rrLQR');
      title('');xlabel('time(s)');ylabel('Drift (m)');ylim([-1e-4 1e-
4])
      subplot(313);plot(simoutfd(1:no30,1),driftu(1:no30,4),'-
',simoutfd(1:no30,1),driftfd(1:no30,4),'-
*',simoutff(1:no30,1),driftff(1:no30,4),'-
o');grid;legend('Uncontrolled','Decen-rr','rrLQR');
      title('');xlabel('time(s)');ylabel('Drift velocity
(m/s)');ylim([-0.4 0.4])

      figure;
      subplot(311);plot(simoutfd(1:no30,1),driftfdn(1:no30,4),'-
',simoutfd(1:no30,1),driftfd(1:no30,4),'-
*',simoutff(1:no30,1),driftff(1:no30,4),'-o');grid;legend('Decen-
n','Decen-rr','rrLQR');
      title('');xlabel('time(s)');ylabel('Drift velocity
(m/s)');ylim([-1e-3 2e-3])
```

```
      subplot(312);plot(simoutfd(1:no30,1),simoutfdn(1:no30,9),'-
',simoutfd(1:no30,1),simoutfd(1:no30,9),'--
',simoutff(1:no30,1),simoutff(1:no30,9),'-o');grid;legend('Decen-
n','Decen-rr','rrLQR');
      title('');xlabel('time(s)');ylabel('Abs Acc (m/s/s)');
      subplot(313);plot(simoutfd(1:no30,1),simoutfdn(1:no30,11),'-
',simoutfd(1:no30,1),simoutfd(1:no30,11),'--
',simoutff(1:no30,1),simoutff(1:no30,11),'-o');grid;legend('Decen-
n','Decen-rr','rrLQR');
      title('');xlabel('time(s)');ylabel('Control (V)');%ylim([-2 2])

      disp('Actual FOM');
      figure;
      subplot(411);plot(simoutfd(1:no30,1),driftfdn(1:no30,2),'-
',simoutfd(1:no30,1),driftfd(1:no30,2),'-
*',simoutff(1:no30,1),driftff(1:no30,2),'-o');grid;legend('Decen-
n','Decen-rr','rrLQR');
      title('');xlabel('');ylabel('Drift (m)');ylim([-1.2e-4 1e-4])
      subplot(412);plot(simoutfd(1:no30,1),driftfdn(1:no30,4),'-
',simoutfd(1:no30,1),driftfd(1:no30,4),'-
*',simoutff(1:no30,1),driftff(1:no30,4),'-o');grid;legend('Decen-
n','Decen-rr','rrLQR');
      title('');xlabel('');ylabel('Drift velocity (m/s)');ylim([-1e-3
2e-3])
      subplot(413);plot(simoutfd(1:no30,1),simoutfdn(1:no30,9),'-
',simoutfd(1:no30,1),simoutfd(1:no30,9),'--
',simoutff(1:no30,1),simoutff(1:no30,9),'-o');grid;legend('Decen-
n','Decen-rr','rrLQR');
      title('');xlabel('');ylabel('Abs Acc (m/s/s)');
      subplot(414);plot(simoutfd(1:no30,1),simoutfdn(1:no30,11),'-
',simoutfd(1:no30,1),simoutfd(1:no30,11),'--
',simoutff(1:no30,1),simoutff(1:no30,11),'-o');grid;legend('Decen-
n','Decen-rr','rrLQR');
      title('');xlabel('time(s)');ylabel('Control (V)');%ylim([-1 1])

      disp('Nominal FOM');
      figure;
      subplot(411);plot(simoutfd(1:no30,1),driftfndn(1:no30,2),'-
',simoutfd(1:no30,1),driftfnd(1:no30,2),'--
',simoutff(1:no30,1),driftfn(1:no30,2),'-.');grid;legend('Decen-
n','Decen-rr','rrLQR');
      title('');xlabel('');ylabel('Drift (m)');ylim([-5e-5 5e-5])
      subplot(412);plot(simoutfd(1:no30,1),driftfndn(1:no30,4),'-
',simoutfd(1:no30,1),driftfnd(1:no30,4),'--
',simoutff(1:no30,1),driftfn(1:no30,4),'-.');grid;legend('Decen-
n','Decen-rr','rrLQR');
      title('');xlabel('');ylabel('Drift velocity (m/s)');ylim([-
0.5e-3 1e-3])
      subplot(413);plot(simoutfd(1:no30,1),simoutfndn(1:no30,9),'-
',simoutfd(1:no30,1),simoutfnd(1:no30,9),'--
',simoutff(1:no30,1),simoutfn(1:no30,9),'-.');grid;legend('Decen-
n','Decen-rr','rrLQR');
      title('');xlabel('');ylabel('Abs Acc (m/s/s)');
      subplot(414);plot(simoutfd(1:no30,1),simoutfndn(1:no30,11),'-
',simoutfd(1:no30,1),simoutfnd(1:no30,11),'--
',simoutff(1:no30,1),simoutfn(1:no30,11),'-.');grid;legend('Decen-
n','Decen-rr','rrLQR');
      title('');xlabel('time(s)');ylabel('Control (V)');%ylim([-1 1])

   end
end
```

APPENDIX: SIMULINK DIAGRAMS

Chapter 2

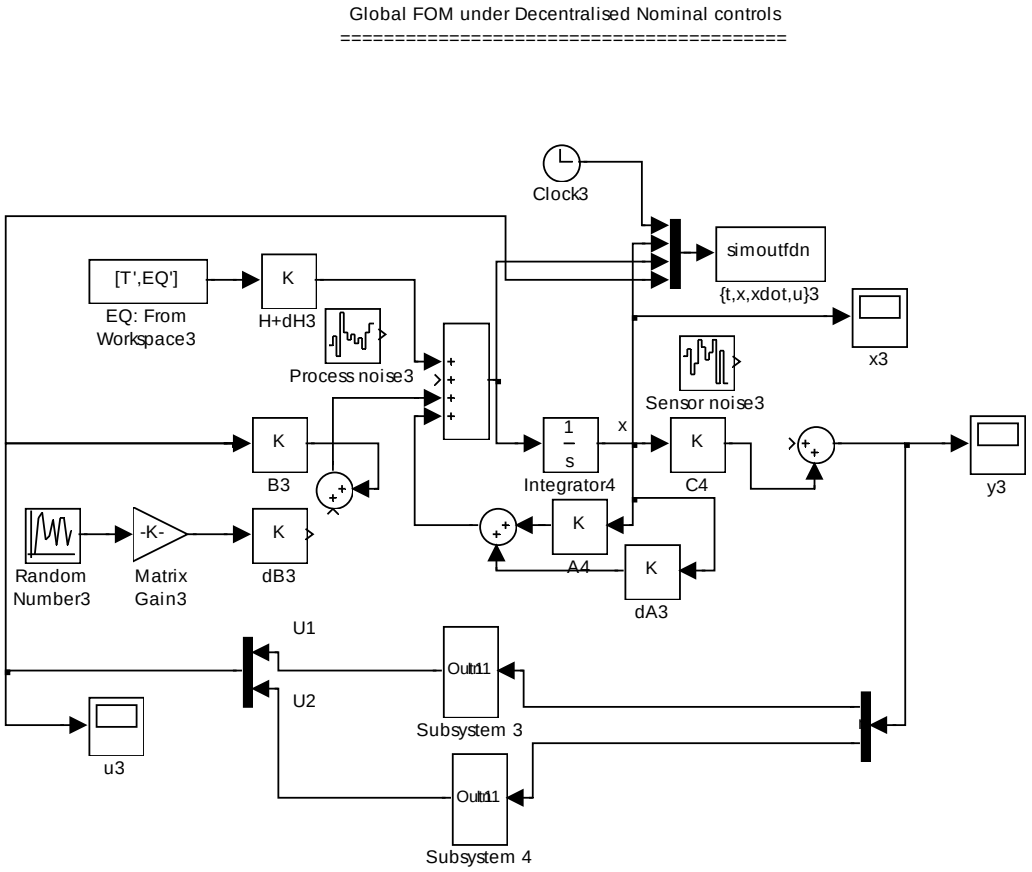

Typical Decentralised Nominal Saturation Controller:

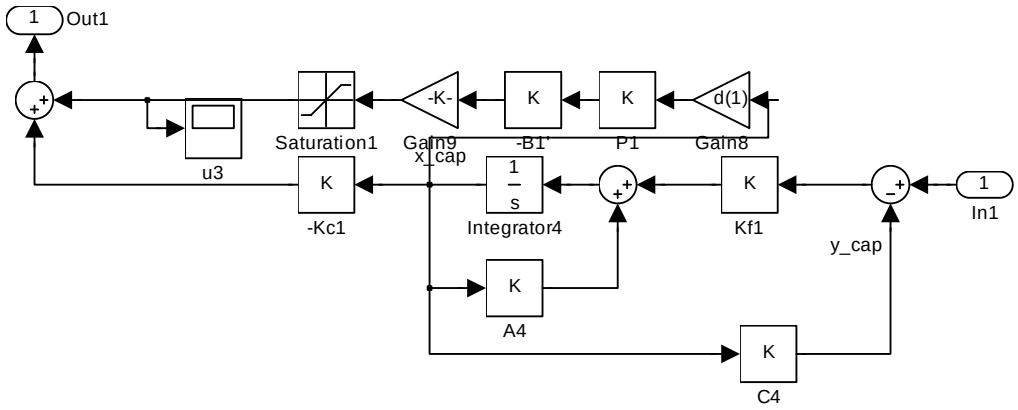

Chapter 3

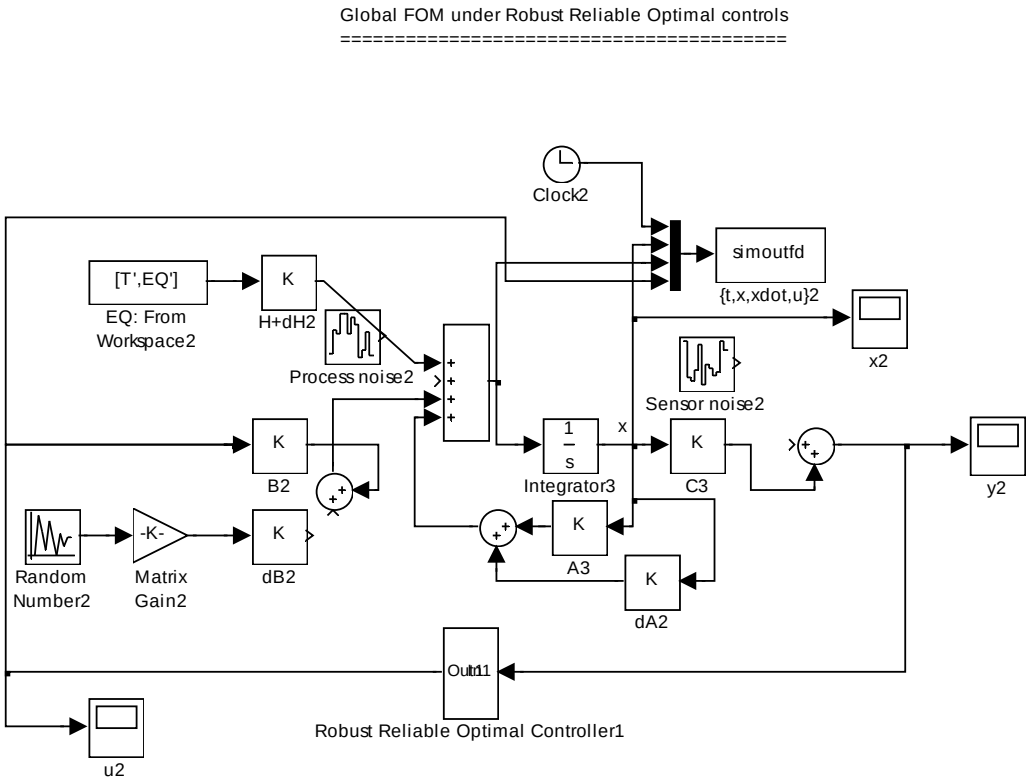

Robust Reliable Optimal Saturation Controller:

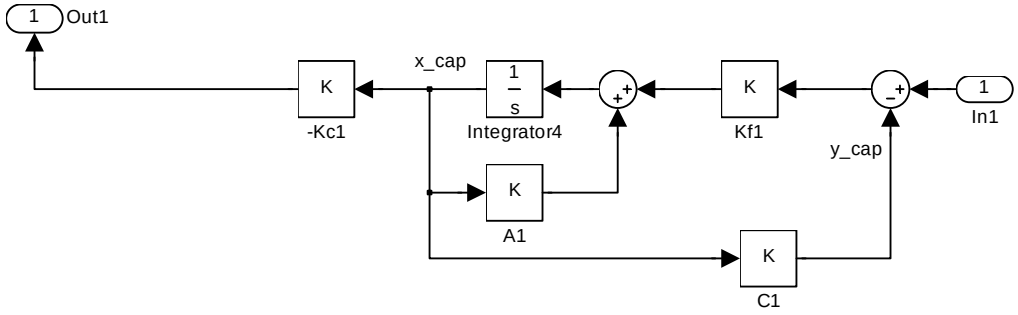

Chapter 4

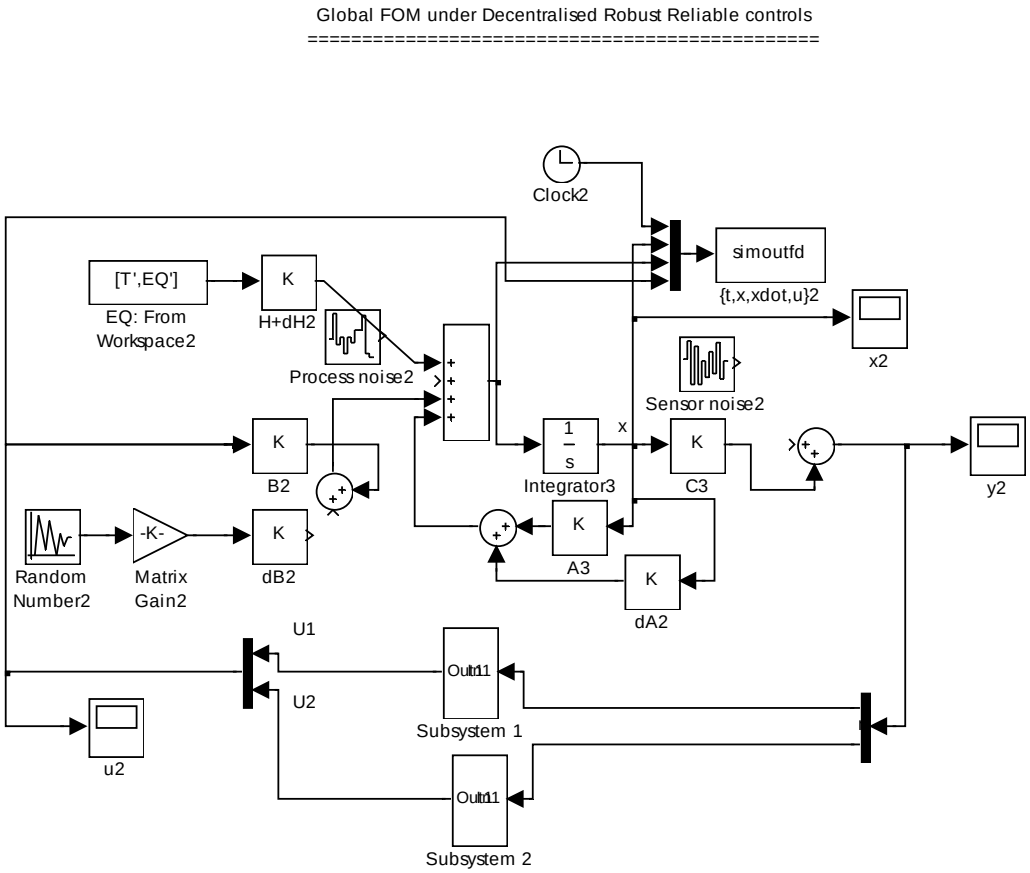

Typical Decentralised Robust Reliable Optimal Saturation Controller:

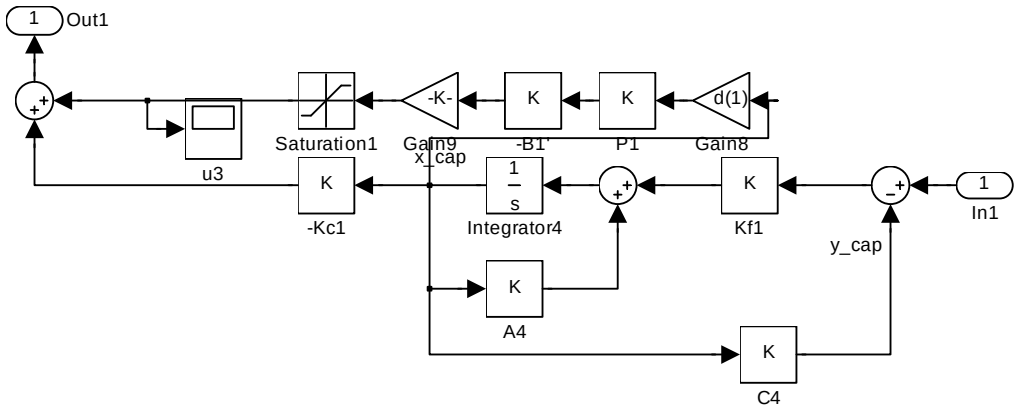

Robust Model Reduction

§Objectives

1. Derive effective reduced-order model (ROM) for desired DOFs
2. Equivalent responses at desired DOFs of ROM to actual full-order model (FOM) with system uncertainties
3. Retain modal characteristics of FOM within ROM
4. Robust input-output decoupling into equivalent subsystems with physical outputs under equivalent disturbances

§References

Chopra Anil K., Dynamics of structures: theory and applications to earthquake engineering, Prentice-Hall, Upper Saddle River, NJ, 2000 (2nd Ed.), 844 pp.

Chiao Kuo-Ping. Least squares model reduction for non-classical damped linear systems. Journal of The Chinese Society of Mechanical Engineers. Vol. 17. No. 4. pp. 335-341. 1996.

Nishitani,Akira, Nitta,Yoshiro and Yamada,Seiji, "Model reduction for active-controlled building structures", Proc. of the 2nd World Conference on Structural Control, Kyoto, Japan, Vol. 2, pp. 2231-2240.

Koumboulis F.N. and Skarpetis M.G., "Robust disturbance rejection and simultaneous robust input-output decoupling", Automatica, Vol. 33, No. 7, pp. 1415-1421.

Sestieri A., "Structural dynamic modification", *Sādhanā* , Vol. 25, Part 3, June 2000, pp. 247-259.

§Derivation of equations of motion

Using Principle of Virtual Work assuming conservation of energy,
External work done on element = Internal work done by element

subjected to the equilibrium criterion by the Theorem of Minimum Work:
Element deformation to keep strain energy minimum

Stress equations of motion:
$\sigma_{ij,i} + f_i = \rho\ddot{u}_j$ where i is the plane of orientation and j is the direction
Charge equation of electrostatics:
$D_{i,i} = 0$
where σ, f, ρ, u, D are stresses, body forces, density, displacement and electric flux density

Giving: $\int_V (\sigma_{ij,i} - \rho\ddot{u}_j)\delta u_j dV + \int_{Vp} (D_{j,j}\delta\phi)dV_p = 0$

Where ϕ is electric potential, V is the material volume and V_p is the piezoelectric volume

Applying the divergence theorem,
$$\int_V (\rho\ddot{u}_j\delta u_j)dV + \int_V (\rho_{ij}\delta u_{j,i})dV + \int_{Vp} (D_i\delta\phi_{,i})dV_p = \int_A (n_i\sigma_{ij}\delta u_j)dA + \int_{Ap} (n_i D_i\delta\phi)dA_p$$

Strain vector ε_i can be denoted by the engineering strain tensor ε_{ij} as

Substituting $\varepsilon_{ij} = \frac{1}{2}(u_{i,j} + u_{j,i})$ and $E_i = -\phi_{,i}$ gives

$$\int_V (\rho \ddot{u}_j \delta u_j) dV + \int_V (\sigma_{ij} \delta \varepsilon_{ij}) dV - \int_{Vp} (D_i \delta E_i) dV_p = \int_A (T_i \delta u_j) dA + \int_{Ap} (Q \delta \phi) dA_p$$

where T_i are the tractions applied on the surface A and Q is the electrical charge applied on the surface of the piezoelectric A_p

Nodal forces are included within the integral of external forces.

§Structural Mechanics (Meirovitch 2000)
Any continuum structural mechanics involves the formulation and solution of equilibrium equations, constitutive stress-strain relations and kinematic strain-displacement relations subjected to the constraints of boundary conditions and compatibility.

In statics, two approaches are widely-used for structural analysis - differential equation approach and variational mechanics approach. Of these, the most popular is the displacement method of FEA and its corresponding principle of minimum potential energy.

In dynamics, the dynamic forces or kinetic energy has to be accounted for. Using D'Alembert's principle, dynamic problems can be solved in Newtonian form with the addition of resultant dynamic forces to the static formulation. Hamilton's principle is applied to generalise the approach for any conservative coordinate system. In the most general form, the extended Hamilton's principle can be applied for the combination of conservative and unconservative systems.

§Fundamentals of Finite Element Method
Discretization of structure into distinct elements interconnected by nodes where compatibility is assumed and equilibrium is imposed. In this study, a regular static mesh is assumed.

Nodal-interior displacement relationship using shape function:
$\{u\} = \{N\}\{\delta\}$
where u is the elemental interior displacement, N is the interpolation shape function and δ is the nodal displacement which would be derived by controlled dynamic solution.

The elemental global coordinates are in x and y. Isoparametric element in local coordinates ξ and η is used together with the Lagrange polynomial:

$$L_l^{nodes-1} = \frac{(\xi - \xi_1)...(\xi - \xi_{l-1})(\xi - \xi_{l+1})...(\xi - \xi_n)}{(\xi_l - \xi_1)...(\xi_l - \xi_{l-1})(\xi_l - \xi_{l+1})...(\xi_l - \xi_n)}$$

where nodes is the number of nodes per element, l is the interpolation from each node of the element.

Strain-displacement relationship is
$\{\varepsilon\} = \{B\}\{\delta\}$
where B is the strain-displacement matrix derived by appropriate derivative of the shape function, assuming that δ is constant for the present time step.

The electric field across the member and into the plane is

$\{E\} = \{A\}\{\Phi\}$

where E is the electric field column vector in three orthogonal directions, A is the field-potential matrix and Φ is the electric potential.

Using extended Hamilton's variational principle,

$$\delta \int_{t1}^{t2} (T - U + W) dt = 0$$

where T is the kinetic energy scalar, U is the potential energy scalar and W is the work done by external sources.

The equilibrium equation for a piezoelectric-coupled element is:

$$\begin{bmatrix} M_{uu} & 0 \\ 0 & 0 \end{bmatrix} \begin{bmatrix} \ddot{\delta} \\ -\Phi \end{bmatrix} + \begin{bmatrix} C_{uu} & 0 \\ 0 & 0 \end{bmatrix} \begin{bmatrix} \dot{\delta} \\ -\Phi \end{bmatrix} + \begin{bmatrix} K_{uu} & K_{u\phi} \\ K_{\phi u} & K_{\phi\phi} \end{bmatrix} \begin{bmatrix} \delta \\ -\Phi \end{bmatrix} = \begin{bmatrix} F_m \\ F_q \end{bmatrix}$$

where M_{uu} is the structural element mass matrix, C_{uu} is the structural element damping matrix, K_{uu} is the structural element stiffness, $K_{u\phi}$ & $K_{\phi u}$ are the piezoelectric element coupling matrices, $K_{\phi\phi}$ is the dielectric element matrix, F_m is the mechanical nodal load vector, F_q is the electrical nodal charge vector, δ is the mechanical nodal displacement vector and ϕ is the electrical nodal potential vector.

The elemental consistent mass matrix is

$$\{M_{uu}\} = \int_V (\rho N^T N) dV$$

and the diagonal lumped mass matrix is derived by summing each row elements into each diagonal element.

The structural element stiffness matrix is

$$\{K_{uu}\} = \int_V (B^T C B) dV$$

with the orthogonal properties $\chi^T M_{uu} \chi = I$ and $\chi^T K_{uu} \chi = \Lambda$, where χ is the basis of eigenvectors and Λ is diagonal matrix of eigenvalues in the order of χ.

Rayleigh (classical) damping is assumed for structural element damping matrix to inherit orthogonality:

$\{C_{uu}\} = \alpha\{M_{uu}\} + \beta\{K_{uu}\}$

where α and β are the mass and stiffness weightings respectively.

§Equation of motion

The elemental equation of motion is

$\{M_{uu}\}\{\ddot{x}_e\} + \{C_{uu}\}\{\dot{x}_e\} + \{K_{uu}\}\{x_e\}\} = \{f_e\} + \{K_{u\phi}\}\{\Phi_a$

where x_e is the elemental nodal displacement vector, Φ_a is the elemental actuator potential and f_e is the elemental nodal load vector.

By appropriate ordering of all elements of the global structure, the structural equation of motion under ground excitations and actuated by axial and bending moment control is

$$\{M\}\{\ddot{X}\}+\{C\}\{\dot{X}\}+\{K\}\{X\}=\{F_p\}+\{M_p\}-\{M\}\begin{Bmatrix}I\\0\end{Bmatrix}\{\ddot{z}\}+\{w_f\}=\{F\}$$

where

$\{X\}=\{\{x\}\{\theta\}\}^T=\{x_1\ldots x_n\theta_1\ldots\theta_n\}^T$ is structural displacement vector in global coordinates with n global nodes

$\{M\}=\begin{bmatrix}[M_m] & 0\\ 0 & [M_I]\end{bmatrix}$ is the square composite mass matrix with M_m the global mass matrix and M_I the global moment of inertia

C is the global damping matrix

K is the global mechanical stiffness matrix

w_f is the global wind load vector, which is assumed zero

$\{\ddot{z}\}$ is the seismic ground acceleration

$\{F_p\}$ is the global shearing force applied by the stacked actuators

$\{M_p\}$ is the global moment applied by the stacked actuators

$\{F\}$ is the lumped global external force vector

§System description

Equation of motion of coupled global linear uncertain system of FOM is:

$$(M+\Delta M)\ddot{X}+(C+\Delta C)\dot{X}+(K+\Delta K)X=F$$

This represents a set of N linear coupled equations in N global degrees of freedom in the FOM which is assumed to be the exact representation of the actual structure. Note that $X(\xi,t)$ is a function of both space and time.

§Global system uncoupling for classical damping (Sestieri 2000)

Following the modal synthesis method for the direct problem (Sesteiri 2000), make this assumption:

$$X(\xi,t)=\Psi(\xi)q(t)$$

that $X(\xi,t)$ is variable separable into the linear combination of a spatial component $\Psi(\xi)$ and a time-varying component $q(t)$.

§Nominal system uncoupling

Consider the nominal system only with global equation of motion:

$$M\ddot{X}+C\dot{X}+KX=F$$

Make the following assumption: $X(\xi,t)=\phi(\xi)\hat{q}(t)$

For the undamped homogeneous problem: $M\ddot{X}+KX=0$

Solve the eigen-problem: $(K-\hat{\lambda}M)\phi=0$

To derive the natural frequencies and modeshapes: $\hat{\Lambda}=diag\{\hat{\omega}_1^{\,2},\hat{\omega}_2^{\,2},...,\hat{\omega}_N^{\,2}\}$ and $\phi=[\phi_1\phi_2...\phi_N]$

Modal orthonormal conditions transform the nominal coupled equation of motion into uncoupled system:

$$\ddot{\hat{q}}+\phi^T C\phi\dot{\hat{q}}+\hat{\Lambda}\hat{q}=\phi^T F$$

where $\phi^T C\phi=diag\{2\hat{\varsigma}_i\hat{\omega}_i\}$, $i=1,2,\ldots,N$.

Consider the full coupled uncertain system:
$(M+\Delta M)\ddot{X}+(C+\Delta C)\dot{X}+(K+\Delta K)X=F$
Applying the assumed $X(\xi,t)=\phi(\xi)\hat{q}(t)$, derive the following coupled system:
$(I+\Delta\hat{M})\ddot{\hat{q}}+(\phi^T C\phi+\Delta\hat{C})\dot{\hat{q}}+(\hat{\Lambda}+\Delta\hat{K})\hat{q}=\phi^T F$
where $\Delta\hat{M}=\phi^T\Delta M\phi$, $\Delta\hat{C}=\phi^T\Delta C\phi$ and $\Delta\hat{K}=\phi^T\Delta K\phi$ are still coupled. This implies that the time-varying component is also spatial-varying, i.e. $\hat{q}(\xi,t)$.

§System uncertainties uncoupling
Apply same modal synthesis only to the coupled system uncertainties as the nominal system. Make the following assumption:
$\hat{q}(\xi,t)=\tilde{\phi}(\xi)q(t)$
Consider the undamped homogeneous problem:
$(I+\Delta\hat{M})\ddot{\hat{q}}+(\hat{\Lambda}+\Delta\hat{K})\hat{q}=0$
Solve the eigen-problem:
$[(\hat{\Lambda}+\Delta\hat{K})-\lambda(I+\Delta\hat{M})]\tilde{\phi}=0$
Derive the natural frequencies:
$\Lambda=diag\{\omega_1{}^2,\omega_2{}^2,...,\omega_N{}^2\}$
and modeshapes:
$\tilde{\phi}=[\tilde{\phi}_1\tilde{\phi}_2...\tilde{\phi}_N]$
for uncoupling the coupled system uncertainties.
Modal orthonormal conditions transform the coupled system uncertainties into the uncoupled system:
$\ddot{q}+\tilde{C}\dot{q}+\Lambda q=\tilde{\phi}^T\phi^T F$
where $\tilde{\phi}^T(I+\Delta\hat{M})\tilde{\phi}=I$, $\tilde{C}=\tilde{\phi}^T(\phi^T C\phi+\Delta\hat{C})\tilde{\phi}$ and $\Lambda=\tilde{\phi}^T(\hat{\Lambda}+\Delta\hat{K})\tilde{\phi}$.

§Full global uncertain system uncoupling
With $(M+\Delta M)\ddot{X}+(C+\Delta C)\dot{X}+(K+\Delta K)X=F$, assume $X(\xi,t)=\Psi(\xi)q(t)$, then the uncoupled uncertain system with *N* uncoupled equations is:
$\ddot{q}+\tilde{C}\dot{q}+\Lambda q=\Psi^T F$
with natural frequencies $\Lambda=diag\{\omega_1{}^2,\omega_2{}^2,...,\omega_N{}^2\}$ and modeshapes
$\Psi(\xi)=\phi(\xi)\tilde{\phi}(\xi)$ with general element $\psi_{rs}=\sum_{l=1}^{N}\phi_{rl}\tilde{\phi}_{ls}$ as well as $\tilde{C}=diag\{2\varsigma_i\omega_i\}$, *i=1,2,…,N*.
Note that the above decoupling is exact w.r.t. the FOM and no modal truncation has occurred yet.

§Dynamic model reduction
Static reduction (Guyan 1965) enables exact model reduction in statics or zero frequency only. Errors would accumulate towards non-zero and higher frequencies. Hence, dynamic reduction techniques are required. These are comprised of modal synthesis techniques and frequency response function (FRF) approaches (Sestieri 2000). Modal synthesis has the advantages of good accuracy at lower modes and being more computationally efficient, but has the disadvantage that accuracy deteriorates towards higher and neglected modes. FRF approaches have the

advantage of better dynamic characteristics across desired frequency range than modal synthesis, but have the disadvantage of computational inefficiency. In this study, the modal synthesis method is chosen for both its simplicity and effectiveness at lower modes especially required in seismic vibration control.

The Improved Reduced System (IRS) method (O'Callahan 1989) adds an extra term to static reduction to transform the neglected inertia forces. The System Equivalent Reduction Expansion Process (SEREP) (Kammer et al 1987) is a reduction transformation based on a subset of the modes of the full-order model with the selected modes at the retained degrees of freedom. The iterated IRS (Friswell et al 1998) is an iterative scheme for improving IRS and is proved to converged into the SEREP transformation. The dynamic condensation method (Qu et al 2001) is also an iterative method for deriving the reduction factor in the transformation in relation to the physical space of the actual model. However, the above does not directly address the modal excitation influence on the reduced model and some require iterations. Hence, the model reduction technique based on new modal participation factors (Nishitani et al 1998) is used.

§Iterative dynamic condensation method (Qu 2002)

Consider the nominal system only with global equation of motion:

$M\ddot{X} + C\dot{X} + KX = F$

where C is the classical damping matrix diagonalisable by mode decomposition:

$C = \alpha M + \beta K$

In model reduction, the total DOFs in X can be split into master (retained, kept) DOFs X_m and slave (deleted) DOFs X_s:

$$\begin{bmatrix} M_{mm} & M_{ms} \\ M_{sm} & M_{ss} \end{bmatrix} \begin{Bmatrix} \ddot{X}_m \\ \ddot{X}_s \end{Bmatrix} + \begin{bmatrix} C_{mm} & C_{ms} \\ C_{sm} & C_{ss} \end{bmatrix} \begin{Bmatrix} \dot{X}_m \\ \dot{X}_s \end{Bmatrix} + \begin{bmatrix} K_{mm} & K_{ms} \\ K_{sm} & K_{ss} \end{bmatrix} \begin{Bmatrix} X_m \\ X_s \end{Bmatrix} = \begin{Bmatrix} F_m \\ F_s \end{Bmatrix}$$

It can be proven that C does not affect dynamic condensation matrix which is also independent of the external force F_s. Hence,

$$\begin{bmatrix} M_{mm} & M_{ms} \\ M_{sm} & M_{ss} \end{bmatrix} \begin{Bmatrix} \ddot{X}_m \\ \ddot{X}_s \end{Bmatrix} + \begin{bmatrix} K_{mm} & K_{ms} \\ K_{sm} & K_{ss} \end{bmatrix} \begin{Bmatrix} X_m \\ X_s \end{Bmatrix} = \begin{Bmatrix} F_m \\ 0 \end{Bmatrix}$$

Expanding the second row gives:

$X_s = -K_{ss}^{-1}\left(M_{sm}\ddot{X}_m + M_{ss}\ddot{X}_s + K_{sm}X_m\right)$

Assume:

$\ddot{X}_m = 0$ and $\ddot{X}_s = 0$

Then:

$X_s = -K_{ss}^{-1}K_{sm}X_m \equiv R^{(0)}X_m$

where $R^{(0)} = -K_{ss}^{-1}K_{sm}$ is the Guyan (1965) static condensation matrix which is exact only for static problems with heavy dependence on the selection of X_m & decreasing accuracy and increasing reduction errors as structural natural frequencies increase.

The reduced model is given by:

$M_R^{(0)}\ddot{X}_m + C_R^{(0)}\dot{X}_m + K_R^{(0)}X_m = F_R^{(0)}$

where the reduced system and excitation matrices are as follows:

$M_R^{(0)} = M_{mm} + \left[R^{(0)}\right]^T M_{sm} + M_{ms}R^{(0)} + \left[R^{(0)}\right]^T M_{ss}R^{(0)}$

$$K_R^{(0)} = K_{mm} + \left[R^{(0)}\right]^T K_{sm} + K_{ms} R^{(0)} + \left[R^{(0)}\right]^T K_{ss} R^{(0)}$$
$$C_R^{(0)} = \alpha M_R^{(0)} + \beta K_R^{(0)} = C_{mm} + \left[R^{(0)}\right]^T C_{sm} + C_{ms} R^{(0)} + \left[R^{(0)}\right]^T C_{ss} R^{(0)}$$
$$F_R^{(0)} = F_m + \left[R^{(0)}\right]^T F_s$$

In order to recover the dynamic properties lost in static condensation to improve accuracy and reduce reduction residual, the condensation matrix $R^{(i)}$, *i=0,…,N* (*N* is the desired terminal iterative step) is modified as follows:
Free vibration of the undamped reduced model is:
$M_R^{(i)} \ddot{X}_m + K_R^{(i)} X_m = 0$
Hence,
$\ddot{X}_m = -\left[M_R^{(i)}\right]^{-1} K_R^{(i)} X_m$
Differentiating twice X_s:
$\ddot{X}_s = R^{(i)} \ddot{X}_m$
$= -R^{(i)} \left[M_R^{(i)}\right]^{-1} K_R^{(i)} X_m$
Replacing the assumptions of $\ddot{X}_m = 0$ and $\ddot{X}_s = 0$ with the above into:
$X_s = -K_{ss}^{-1} \left(M_{sm} \ddot{X}_m + M_{ss} \ddot{X}_s + K_{sm} X_m \right)$
This gives:
$X_s = K_{ss}^{-1} \left\{ \left[M_{sm} + M_{ss} R^{(i)} \right] \left[M_R^{(i)}\right]^{-1} K_R^{(0)} - K_{sm} \right\} X_m$

Hence, the iterated dynamic condensation matrix $R^{(i)}$, *i=0,…,(N-1)* is as follows:
$R^{((i+1)} = K_{ss}^{-1} \left\{ \left[M_{sm} + M_{ss} R^{(i)} \right] \left[M_R^{(i)}\right]^{-1} K_R^{(0)} - K_{sm} \right\}$
Repeat iteration to desired degree of accuracy, then the dynamic reduced model is:
$M_R^{(i+1)} \ddot{X}_m + C_R^{(i+1)} \dot{X}_m + K_R^{(i+1)} X_m = F_R^{(i+1)}$
where the final reduced system and excitation matrices are derived as above.

Note that the above iterated dynamic condensation scheme (Qu 2002) is similar to the iterated LTR procedure for the recovery of LQR properties for LQG controllers. The iteration can be replaced by optimal recovery to pre-specified desired degree of accuracy using optimal control techniques (Chen et al 1991, Chen 2002 course).

§Dynamic model reduction (Nishitani et al 1998)
Consider the uncertain system with global equation of motion:
$(M + \Delta M)\ddot{X} + (C + \Delta C)\dot{X} + (K + \Delta K)X = F$

Assume that the retained master degrees of freedom is $X_r = [x_{rs}]$, *s=1,…,S*, where *S* is the maximum number of master DOFs. Assume that the lowest *S* modes are chosen to be retained.
Let $r \in R$, where *R* is the set of retained DOFs.
Let $s \in \mu$, where μ is the set of retained modes.
Partition the modeshapes of the full-order system:
$$\Psi = \begin{bmatrix} \psi_{rs} & \psi_{r\bar{s}} \\ \psi_{\bar{r}s} & \psi_{\bar{r}\bar{s}} \end{bmatrix}$$
Perform modal truncation by retaining ψ_{rs}.

Using the dynamic property for every *r*:
$\sum_s \overline{\beta}_s \psi_{rs} = 1$
Derive the new participation factors $\overline{\beta}_s$.
Use the derived β_s, find the reduced-order model modeshapes $\overline{\Psi} = \{\overline{\psi}_s\}$:
$\overline{\psi}_s = \overline{\beta}_s \psi_s$

Then, the reduced-order uncertain system is:
$M_r \ddot{X}_r + C_r \dot{X}_r + K_r X_r = F_r$
where
$M_r = \left(\overline{\Psi}^T\right)^{-1} I \left(\overline{\Psi}\right)^{-1}$
$C_r = \left(\overline{\Psi}^T\right)^{-1} \tilde{C} \left(\overline{\Psi}\right)^{-1}$
$K_r = \left(\overline{\Psi}^T\right)^{-1} \Lambda \left(\overline{\Psi}\right)^{-1}$
$F_r = \left(\overline{\Psi}^T\right)^{-1} \overline{F}$ and $\overline{F} = \tilde{\phi}^T \phi^T F = \Psi^T F$.

For a controlled uncertain system:
$(M + \Delta M)\ddot{X} + (C + \Delta C)\dot{X} + (K + \Delta K)X = (b + \Delta b)u + F$
where control input is $u \in \Re^m$, nominal control location matrix *b* and variation is Δb.

The full-order uncoupled uncertain system is:
$\ddot{q} + \tilde{C}\dot{q} + \Lambda q = \overline{F} + \Psi^T (b + \Delta b)u$

The reduced-order uncertain system is:
$M_r \ddot{X}_r + C_r \dot{X}_r + K_r X_r = F_r + b_r u$
where
$b_r = \left(\overline{\Psi}^T\right)^{-1} \Psi^T (b + \Delta b)$

§Model reduction using force-dependent Ritz vectors (Chopra 1995/2000, Soh & Law 2001)
Consider the nominal system only with global equation of motion:
$M\ddot{X} + C\dot{X} + KX = F$
where $F(t) = S\ddot{z}_0(t)$, *S* is the seismic force distribution vector and $\ddot{z}_0$ is the seismic acceleration.
Let $X(\xi, t) = \Phi(\xi)\hat{q}(t)$, where $\Phi(\xi) \in \Re^{nxr}$ is the transformed spatially-varying modeshape matrix and $\hat{q}(t)$ is the time-varying vector.

§Generation of force-dependent Ritz vectors with Gram-Schmidt orthogonalisation (Chopra 1995/2000)
Apply the following procedure to derive $\Phi(\xi)$ for the retention of the lowest *r* modes:

Determine the first Ritz mode-shape vector ϕ_1:
Derive virtual displacement vector y_1 by solving:
$Ky_1 = S$

Perform normalisation to be mass orthonormal to derive the first mode-shape vector:

$$\phi_1 = \frac{y_1}{\left(y_1{}^T M y_1\right)^{1/2}}$$

Determine the other Ritz mode-shape vectors ϕ_i, i=*2,…,r*:
Derive virtual displacement vector y_i by solving:

$$Ky_i = M\phi_{i-1}$$

The virtual displacement vector y_i is composed of a vector $\hat{\phi}_i$ to be determined and a linear combination of previous mass orthonormal Ritz vectors ϕ_j, *j=1,…,i-1*:

$$y_i = \hat{\phi}_i + \sum_{j=1}^{i-1} a_{ji}\phi$$

where a_{ji} is determined using modal orthogonality property such that:

$$a_{ji} = \phi_j{}^T M y_i$$

Then vector $\hat{\phi}_i$ is given by:

$$\hat{\phi}_i = y_i - \sum_{j=1}^{i-1} a_{ji}\phi$$

Perform normalisation to be mass orthonormal to derive the *i*th Ritz mode-shape vector:

$$\phi_i = \frac{\hat{\phi}_i}{\left(\hat{\phi}_i{}^T M \hat{\phi}_i\right)^{1/2}}$$

Assembling:

$$\Phi(\xi) = \{\phi_i\},\ i=1,\ldots,r.$$

The transformed system is:

$$\hat{M}\ddot{\hat{q}} + \hat{C}\dot{\hat{q}} + \hat{K}\hat{q} = \hat{F}$$

where

$\hat{M} = \Phi^T M \Phi$ is coupled and non-diagonal, hence apply Ritz vector generalization again for diagonal ROM mass

$\hat{C} = \Phi^T C \Phi$ is diagonal for classical damping, but non-diagonal for non-classical damping, where off-diagonal terms need to be accounted for

$\hat{K} = \Phi^T K \Phi$

$\hat{F} = \Phi^T F$

Transform $\hat{q}(t)$ into the actual reduced displacement $X_r(t)$:

$$X_r(t) = \Phi_r \hat{q}(t)$$

where Φ_r is sub-matrix of $\Phi(\xi)$ that corresponds to the reduced-order degrees of freedom.

§Uncertain systems

Consider the uncertain system with global equation of motion:

$$\left(M + \Delta M\right)\ddot{X} + \left(C + \Delta C\right)\dot{X} + \left(K + \Delta K\right)X = F$$

If the variation matrices can be measured or specified, the generalized Ritz vector method can be performed first on the nominal system, then again on the system uncertainties using the nominal transformation Ritz vectors. Since the uncertain system is still not mass normalised, perform the method again on the system uncertainties and combine accordingly as done in Sestieri 2000.

If the variation matrices are arbitrary, the nominal transformation Ritz vectors would serve as approximation and there would not be mass normalisation. However, if the variations are bounded, the sensitivity error can be minimised with approximate mass normalisation with robust transformation Ritz vectors.

Let the actual and Ritz approximated modal participation factors be Γ_n and $\hat{\Gamma}_n$ for the *n*th mode. Noting that:

$$S = \sum_{n=1}^{N} \Gamma_n M \Psi_n \approx \sum_{n=1}^{J} \hat{\Gamma}_n M \Phi_n$$

where $\hat{\Gamma}_n = \phi_n{}^T S$ and *J* Ritz vectors are included.

Define Ritz approximation error for *J* Ritz vectors as:

$$E_J = S - \sum_{n=1}^{J} \hat{\Gamma}_n M \Phi_n$$

Use the error norm as a measure of the degree of Ritz approximation:

$$e_J = \frac{S^T E_J}{S^T S}$$

§Selection of master DOFs (Qu et al 2001)

Note that the selection of the reduced degrees of freedom significantly affect the accuracy of the reduction. The retained (master) degrees of freedom must satisfy the following conditions: low stiffness-to-inertia ratios, controlled by actuators, observed by sensors and/or be of interest to active control (Qu et al 2001). The first condition shows the structure design would influence model reduction. The second and third conditions highlight the need for good or optimal placement of sensors and actuators. The last condition would relate to the active control specifications.

§Optimal Sensor and/or Actuator Selection and Placement (Roh et al 1997, Lim 1997, Abdullah et al 2001)

The problem of sensor and/or actuator selection involves determination of a suitable measure of optimality and the constraints which include the number of available sensors and actuators, the geometry and capacity as well as the feasible placements. These can be performed sequentially or simultaneously for sensors or actuators or both. Normally, the placement problem is treated together with the minimisation of the control gains.

For discrete placement of sensor/actuator pairs, assumed to be collocated – i.e. $C = B^T$, Abdullah et al 2001 has studied this with GA together with optimisation of LQR control gains. The optimality measure is the trace of LQR ARE solution. Roh et al proposed the novel modal degree of controllability (MDOC) as the optimality measure which minimises the control energy required and interpreted as the relative regulation performance for a specific mode. The above studies address the optimisation on the time domain. Lim 1997 has proposed a novel placement strategy

based on the Hankel singular value (HSV) weighted by disturbance rejection specifications associated with all combinations of sensor-actuator pairs. A placement selection table based on the HSV performance measure can be constructed and used for optimal selection of either sensors or actuators or both.